The effect of Resveratrol on the Upregulation of Ngb ©

Mohamed Rezk, B.Sc. (honours)

[Submitted in partial fulfillment of the requirements for the degree of Master of Science Biological Sciences – Cell and Molecular Biology specialization]

Department of Biological Sciences

Brock University

St. Catharines, Ontario, Canada

I-Abstract:

Apoptosis involves a series of biochemical events that leads to the eventual death of the cell. One pathway – intrinsic pathway, involves the fragmentation of mitochondria and the release of pro-apoptotic proteins, such as cytochrome c. A certain globin protein has been shown to be able to protect cells from apoptosis, called Neuroglobin (Ngb). Ngb is a globin haem protein that has been shown to reduce the ferric form of cytochrome c to inhibit apoptosis. In addition, Ngb has been shown to translocate into the mitochondria under stress, where it reacts with cytochrome c.

Estradiol (E2) has been shown to greatly upregulate the levels of Ngb and also stimulates the translocation of Ngb into the mitochondria. The upregulation of Ngb has been shown to be mediated via the ER subtype, ERβ. Even though literature covers the effects of E2 and the ERβ agonist DPN (Diartylpropiolnitrile), there is a lack of evidence on the ER agonist, Resveratrol (RES); RES is a phytoestrogen that has been shown to induce mitochondrial biogenesis and abrogate mitochondrial fragmentation, ameliorating apoptosis. The hypothesis of this study is that RES will upregulate Ngb levels as E2 does, and will translocate Ngb into the mitochondria as E2 does.

The results of this study showed that Ngb bands could not be detected via western blots, and the mRNA transcript levels in MCF-7 and DLD-1 could not be quantified. The Ngb-GFP fusion protein did not fluoresce and Ngb's translocation into the mitochondria could not be determined. Ngb overexpression did not inhibit mitochondrial fragmentation and did not induce mitochondrial fusion.

II – Keywords:

Mitochondria, cytochrome c, neuroglobin, resveratrol, cell culture, peroxidase, apoptosis, hyperfusion, mitochondrial dynamics, hypoxia, hydrogen peroxide

III – Acknowledgments:

In the name of Allah, the most Gracious, the most Merciful. All praises for this study, from thesis writing to the effort placed in the experiments are attributed to Allah, and after, I would like to thank my mother and father, my sister, my brother Ahmad, my sister Rana, my niece Cindy, my wife Nancy, my aunt Aisha, my colleagues Fereshte, Greg, Holt, João, Lucas, Marina, Matt, Sarah, Shannon, Shehab, Sherry, Ryan and Taylor, my students Brian and Navreek, my friends Adi, Cal, Jina, Julie, Parth, Rachel, Vinay and Zakia, my teachers Dr. Lepp, Dr. Waller and Dr. Lukewich, my professors Dr. Liang, Dr. Carlone and Dr. McCormick, our honoured visitor Dr. Fiocchetti, and my advisory committee: my supervisor Dr. Stuart, my co-supervisor Dr. Necakov and the head of the committee Dr. Inglis.

Table of Contents:

IV – List of Abbreviations:

AIF	apoptosis inducing factor

ANOVA	analysis of variance
BSA	bovine serum albumin
DMEM	Dulbecco's modified eagle medium
DMSO	dimethylsulfoxide
DTT	DL-dithiothreitol
FBS	fetal bovine serum
H_2O_2	hydrogen peroxide
HEPES	((4-(2-hydroxyethyl)-1-piperazineethanesulfonic acid)
OGD	oxygen glucose deprivation
PBS	phosphate buffered saline
PBS-T	phosphate buffered saline with TWEEN 20
SEM	standard error of the mean
TBS	tris buffered saline
TBS-T	tris buffered saline with TWEEN 20

V – List of Figures:

VI – Dissemination of results:

Chapter 2 – The optimization of the reaction combined with protocol provision were performed by my colleague, Lucas Maddalena. The reaction, measurements and the entire experiment were performed by me.

Chapter 3 – Cell culture work was performed by my studetns Brian, Debbie, Navreek and Rachel, under my supervision; I also performed cell culture work. RT-PCR teaching was performed by Dr. Amanda Lepp, while the experiments involving RT-PCR and western blots were performed by me. Ngb-GFP plasmid construction was taught by Dr. Aleksandar Necakov, and the PCR, plasmid extractions and purification were performed by me; plasmid transfection into cells was performed by Dr. Marco Fiocchetti.

Chapter 4 – Live imaging of cells was performed by Dr. Marco Fiocchetti and myself, with the western blots for transfection confirmation were performed by the both of us. MiNA statistical analysis was performed by me.

1.0 Introduction

Apoptosis is programmed cell death, which can occur when a cell experiences various forms of stress, such as reactive oxygen species (ROS) (Gao et al., 2008). Apoptosis involves two major pathways: extrinsic and intrinsic pathways. The former involves death ligands (such as Tumour Necrosis Factor (TNF)) binding to death receptors which would lead to the activation of caspase 8 and the eventual activation of apoptosis. The latter is mediated by the release of pro-apoptotic proteins, such as cytochrome c (cyt c) from the mitochondria into the cytoplasm. When these pro-apoptotic proteins are released, they activate a caspase cascade, which contributes to the regulated death of the cell (Figure 1.1).

Multiple factors lead to the release of pro-apoptotic proteins from the mitochondria, including the peroxidation of the mitochondrial inner membrane phospholipid cardiolipin (CL). Cytoplasmic proteins also lead to the opening of pores and channels in the mitochondrial outer membrane, to aid in the release of the pro-apoptotic proteins. Another factor that aids the release of the pro-apoptotic proteins is calcium; calcium is normally released from the smooth endoplasmic reticulum and enters the mitochondria. The accumulation of the mitochondria causes swelling, which leads to mitochondrial fragmentation; the loss of mitochondrial membrane potential due to calcium occurs, leading to the opening of the mPTP (mitochondrial Permeability Transition Pore), aiding in the release of pro-apoptotic proteins as well.

Estrogen receptors (ERs) are a group of receptors that affect the transcription of many genes (Nussey and Whitehead, 2013), when bound to their ligands. There are two different classes of ER: nuclear receptors (ERα and ERβ), and membrane receptors (mER) (Micevych and Kelly, 2012; Soltysik and Czekaj, 2013), such as ER-X, G_q-mER and GPER (GPR30) (Prossnitz et al., 2007). The ligand for these receptors is the steroid hormone estrogen, which is comprised of

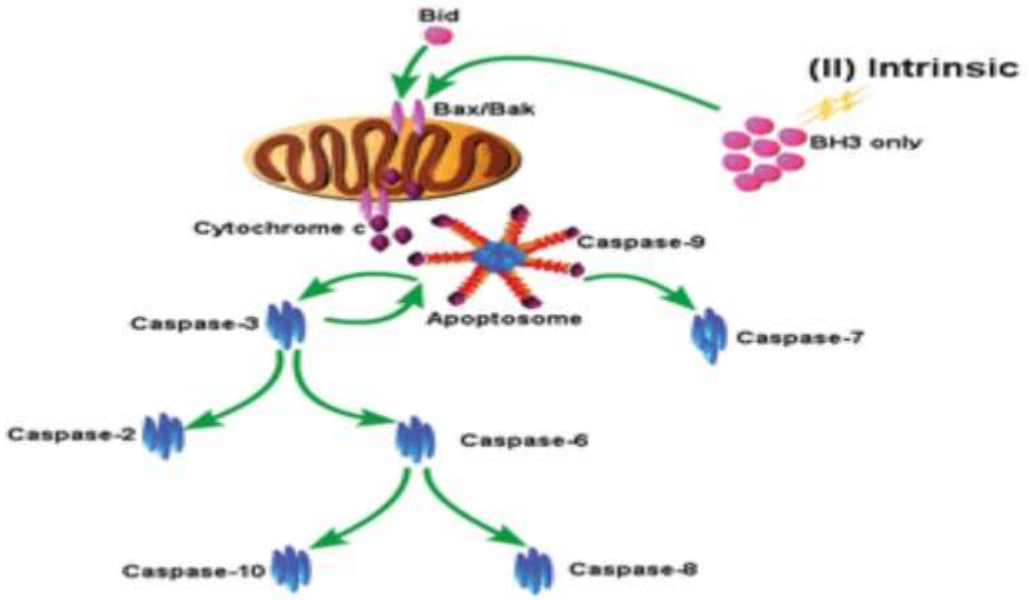

Figure 1.1 Intrinsic Apoptotic Pathway

The figure depicts the intrinsic apoptotic pathway. The release of cytochrome c from the mitochondrion into the cytosol, leads to the formation of the apoptosome. The apoptosome activates procaspase-9 into caspase-9 that activates the caspase cascade, inexorably leading to apoptosis. The image was obtained from Logue and Martin, 2008.

estrone (E1), estradiol (E2) and estradiol (E3); E2 is the most predominant estrogen out of all three types.

17β estradiol (E2) has been shown to promote antiapoptotic responses in cells (Nilsen and Brinton, 2003), and this effect is specific towards ERβ. The ERs act as receptors for exogenous ligands, in addition to the endogenous E2; a polyphenolic compound extracted from grapes, named Resveratrol (RES), has a binding affinity towards ERs, making it a phytoestrogen. Coincidentally, the effects of RES have been shown to be mediated via the ERβ (Wang et al., 2013). A key downstream protein of the ERβ-mediated antiapoptic pathway is Neuroglobin (Ngb), which is greatly upregulated by E2 once it binds to ERβ.

Neuroglobin is a globin protein found primarily in the nervous system, as well as non-neuronal tissue, and has been shown in several studies to induce protection against hypoxia-induced and oxidative stress-induced apoptosis.

Since Resveratrol has cytoprotective capabilities via ERβ binding, and that the upregulation of neuroglobin is ERβ-mediated, the hypothesis of this study is that Resveratrol would exert the same protective capabilities as E2 through neuroglobin upregulation. It is hypothesized that RES upregulates neuroglobin levels, and that this effect is ERβ-mediated.

1.1 Literature Review

1.1.1 Mitochondria

Mitochondria are organelles that are responsible for ATP production (Gao et al., 2008; Celsi et al., 2009), calcium homeostasis (Celsi et al., 2009), redox signaling, reactive oxygen species (ROS) production (Gao et al., 2008; Vosler et al., 2009), and apoptosis (Vosler et al., 2009). Mutations in mitochondrial genes have been associated with hypertension, hypercholesterolemia, hypomagnesemia (Kim et al., 2008), cardiomyopathy, liver dysfunction, neurological disorders (Sharef et al., 2013) and reduced insulin secretion (Kim et al., 2008).

1.1.2 Reactive Oxygen Species (ROS) and Reactive Nitrogen Species (RNS)

Reactive Oxygen Species (ROS) is a group of reactive molecules, compromised of oxygen (Hayyan et al., 2016). They are normally produced as a result of oxygen usage within the mitochondria. ROS is normally produced at the last stage of respiration, where a few electrons "leak" to the final electron acceptor (oxygen), as they are being transported via the respiratory complexes. The main complexes for ROS production involve complex I and complex III (Nicolson, 2007; Li et al., 2013), particularly I_F and I_Q (Brand et al., 2016) sites of complex I and III_{Qo} site if complex III (Sena et al., 2012) (Figure 1.2). In addition to complexes I and III, the II_F site of complex II is also a ROS production site. As electrons are being transported via the complexes, Oxygen will sometimes interact with the complexes prematurely, leading to the

formation of the superoxide radical anion (O2· −) (Matsuzaki et al., 2009). Superoxide radicals (O2•−) are then converted to different species, such as hydrogen peroxide (H_2O_2) and the hydroxyl radical (OH•); these different radicals are collectively known as ROS (Szeto, 2006). Another type of reactive species, in the form of the peroxynitrite anion (ONOO−), is formed either when superoxide anions react with nitric oxide (NO) (Pacher et al., 2007.) or when H_2O_2 reacts with the nitrite anion (Robinson and Beckman, 2005.) which are collectively known as reactive nitrogen species (RNS).

ROS can cause damage to DNA, proteins, and lipids due to its reactive nature (Cadenas and Davies, 2000). ROS also inhibits the electron transport chain, which is essential for production of ATP as part of the oxidative phosphorylation stage in respiration (Galkin and Moncada, 2007.). All cells have various means of detoxifying ROS to prevent excessive damage. Enzymes that protect against ROS catalyze the conversion of superoxide to H_2O_2 via manganese superoxide dismutase (MnSOD) in the matrix, and the copper/zinc superoxide dismutase (Cu/ZnSOD) in the intermembrane space; the removal of H_2O_2 is catalyzed by catalase, peroxiredoxins and glutathione peroxidase (Sivitz and Yorek, 2010). Antioxidant molecules, such as ascorbic acid (vitamin C), glutathione (GSH) and tocopherols (vitamin E), are also important contributors to limiting ROS levels in and around cells (Karihtala and Soini, 2007).

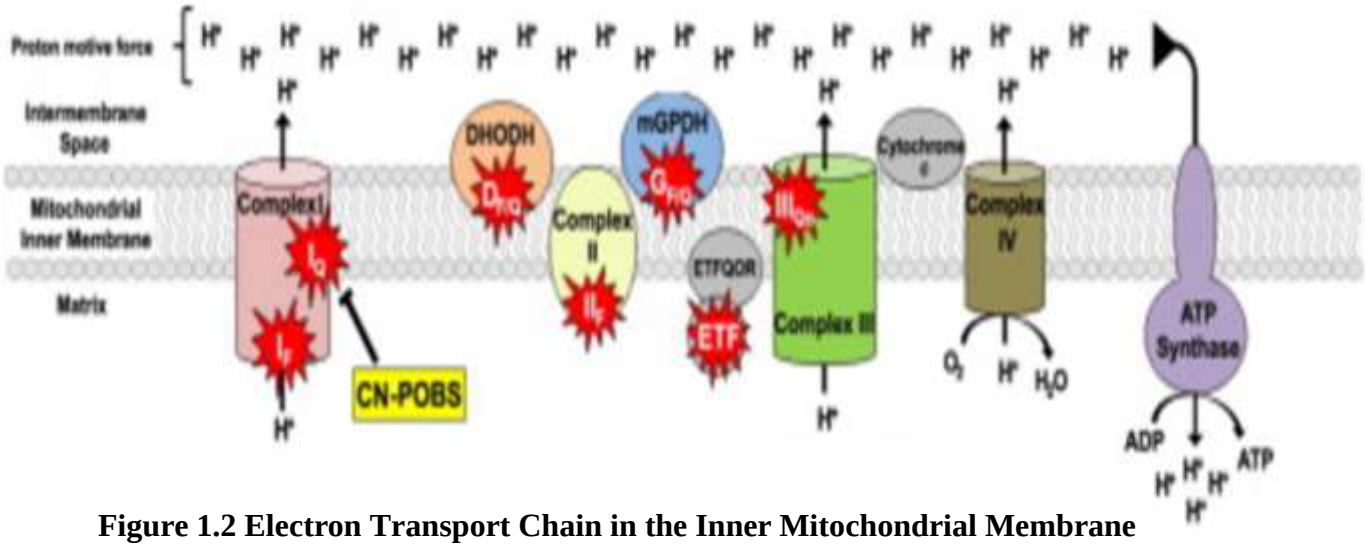

Figure 1.2 Electron Transport Chain in the Inner Mitochondrial Membrane

The figure depicts the complexes embedded within the inner mitochondrial membrane that are responsible for transport of electrons. The sites at which ROS are produced are portrayed as the red shapes. The image was obtained from Orr et al., 2013.

1.1.3 Intrinsic Apoptotic Pathway

The intrinsic apoptotic pathway involves the release of several proapoptotic proteins, such as cytochrome c (Cyt c), Apoptosis Initiation Factor (AIF) and SMAC/Diablo (Second Mitochondria-derived Activator of Caspases); the release of Cyt c and SMAC lead to the eventual activation of the proteolytic enzymes known as caspases (Kroemer and Reed, 2000). Cyt c, AIF and SMAC activate apoptosis through different mechanisms: Cyt c induces the allosteric activation of Apaf-1 (apoptosis-protease activating factor-1), which produces an apoptosome (Purring-Koch and McLendon, 2000). The apoptosome activates caspase-9, which in turn leads to the catalytic cleavage of caspase-3 and caspase 7 (Taylor et al., 2008; Ascenzi et al., 2011). However, SMAC activates the caspases by binding to and inhibiting the caspase inhibitor IAPs (Inhibitor of Apoptosis Proteins). In contrast, AIF does not activate caspases, but instead, it activates apoptosis when it moves into the nucleus from the cytoplasm to

start DNA fragmentation and chromosome condensation, initiating apoptosis (Yu et al., 2006). A member of the Bcl-2 family, Bax, aids in the release of the pro-apoptotic proteins.

Bax is believed to induce the opening of VDAC (Voltage-dependent Anion Channel) (Shi et al., 2003) and MAC (Mitochondrial Apoptosis-induced Channel) (Buytaert et al., 2006); the opening of MAC (Dejean et al., 2006) and VDAC is said to aid in the release of the proapoptotic proteins from the mitochondria, which triggers apoptosis. This effect is enhanced due to the belief that p53 helps in the integration of Bax into the membrane of the mitochondria (Toshiyuki and Reed, 1995).

The proapoptotic protein members of the Bcl-2 (B-cell/lymphoma 2) family generally induce pore openings in the membrane of the mitochondria (Green and Kroemer, 2004; Lutter et al., 2000; Kuwana et al., 2002); they regulate upstream events, relative to the mitochondria, and act based on whether cell death or survival is best, depending on the strength of the stress signal (Skommer et al., 2007); the intrinsic pathway is elucidated in Figure 1.3. The process could occur as part of embryogenesis, such as the separation of toes and fingers, but also due to cellular stress. Such stress could be caused by, for example, the accumulation of amyloid beta peptide, oxygen/glucose deprivation (OGD), increased levels of calcium, increased levels of ROS (Raha and Robinson, 2001; Galluzzi et al., 2009) or mitochondrial fragmentation; the mitochondrion is responsible for the mediation of the intrinsic apoptotic pathway (Green and Kroemer, 2004).

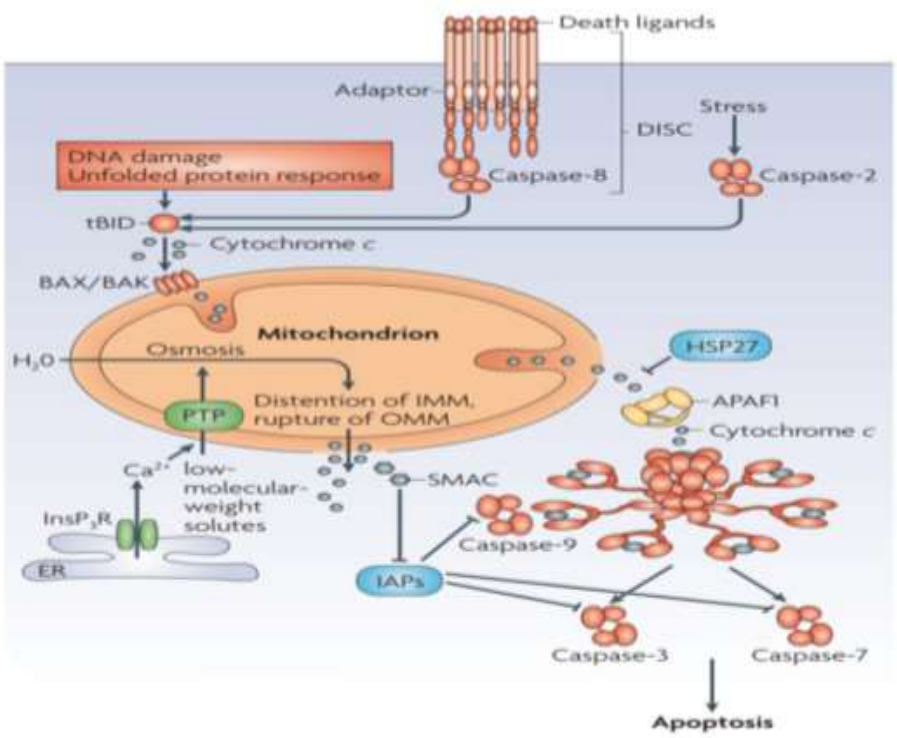

Figure 1.3 Apoptotic Signalling Pathway

The figure depicts both the extrinsic and the intrinsic apoptotic pathway. The right hand side of the figure shows the release of cytochrome c from the mitochondrion into the cytosol, forming the apoptosome. The apoptosome activates procaspase-9 into caspase-9 that will eventually lead to apoptosis. The image was obtained from Yong-ling et al., 2008.

1.1.4 Cytochrome c

Cytochrome c, a heme protein, is located between the inner and the outer membrane of the mitochondria and is responsible for transferring electrons from ubiquinone–cytochrome c reductase (Complex III) to cytochrome c oxidase (Complex IV); it is also responsible for the prevention of oxidative stress by scavenging $O2\cdot -$ and H_2O_2 (Gnaiger 2003; Min and Jiang-xing, 2007; Ow et al., 2008; Lenaz and Genova, 2010; Santucci et al., 2010; Ascenzi et al., 2011). When cytochrome c is released into the cytosol, it binds with Apaf-1 and procaspase-9; the resulting complex, the apoptosome, initiates the activation of procaspase-9 to yield caspase-

9. This, in turn, initiates the catalytic cleavage of the effector caspase – caspase-3, which initiates the apoptotic pathway (Ascenzi et al., 2011). The release of cytochrome c has been also associated with the peroxidation of cardiolipin (Ott et al., 2002; Iverson and Orrenius, 2004; Nakagawa, 2004). Cardiolipin is a phospholipid that constitutes the inner membrane of the mitochondria, and has been suggested to aid in the release of cytochrome c (Green and Kroemer, 2004).

1.1.4.1 Cytochrome c and Cardiolipin

Kagan et al., 2005 has shown that Cyt c itself catalyzes the peroxidization of CL, thereby leading to its own release. The normal tertiary structure of Cyt c has the heme iron group in the hexacoordinated configuration, which prevents access of H_2O_2 that is produced as a result of ROS catalytic enzymes, to the heme group. CL interaction with Cyt c exposes the heme iron group to H_2O_2, and once it binds to it, the peroxidase activity of Cyt c is induced (Kagan et al., 2005).

The reason Cyt c's heme iron group is not normally exposed to H_2O_2 is because all of the positions on the heme iron group are occupied when Cyt c is functioning as an electron shuttle between mitochondrial complexes III and IV. Hence, H_2O_2 cannot easily bind to it (Stellwagen, 1968). The interaction between CL and Cyt c causes an unfolding in the structure of the latter, which seems to be as a result of the loss of the bond between the heme iron group and the amino acid residue Met80 (which acts as a ligand for the heme iron group) (Bernad et al., 2004; Tuominen et al., 2002; Nantes et al., 2001; Zucchi et al., 2003). The perxodiation of CL causes the detachment of Cyt c and the eventual release of Cyt c (Ott et al., 2002).

1.1.5 Cardiolipin

Cardiolipin, a lipid that composes the inner mitochondrial membrane, has cytochrome c bound to it and allosterically changes the structure of Cyt c, changing its function from respiration to apoptosis (Ascenzi et al., 2011).

The normal distribution of CL within the inner membrane of the mitochondria, between the matrix surface and the intermembrane surface is in a ratio of 60:40 (Garcia Fernandez et al., 2002; Cossarizza et al., 2002). It has been shown however, that oxidative stress causes an increase in intermembrane surface CL distribution, and a decrease in CL distribution on the matrix surface, combined with an increase in CL distribution within the outer membrane (Kagan et al., 2005; Chu et al., 2013; De Arriba et al., 2013), hinting at the possibility of preparing for peroxidation to release Cyt c.

The change in CL distribution within the membrane has been shown to occur before the loss of the mitochondrial membrane potential and after the production of ROS (Garcia Fernandez et al., 2002). Since the MPT normally opens via various factors, such as the loss of membrane potential, with the presence of calcium, it can be assumed that MPT lacks input in Cyt c release, since CL distribution change occurs before the loss in potential (Baines et al., 2005).

1.1.6 Nuclear Estrogen Receptors

Estrogen receptors are nuclear receptor/transcription factors (Olefsky, 2001). The receptors have two subtypes: ERα (discovered in 1958) and ERβ (cloned in 1996; Kuiper et al., 1996). These two receptors differ in tissue distribution, where ERβ is present in the cardiovascular system, ovary, central nervous system, prostate, lung, bone, colon and kidney, while ERα is expressed in ovary, testis, uterus, breast, white adipose tissue, bone, liver and heart (Jia et al., 2015; Drummond and Fuller, 2010). Because ERβ is distributed more throughout the body, it tends to regulate bodily systems and processes, such as the cardiovascular system,

inflammation, and reproductive organ development (Drummond and Fuller, 2010; Emmen et al., 2005). The estrogen receptors also differ in terms of gene loci and molecular weight. ERs are normally found in the nucleus, however, they can also be found within the mitochondria (Chen et al., 2004); Pedram et al., 2006; Yang et al., 2004) and the cytosol.

The receptors are composed of five domains, with the N-terminus and C-terminus and ligand binding site composing 3 of those domains (Figure 1.4). Even though the two receptors are expressed on different chromosomes, and have differences in domain structure (Deroo and Buensuceso, 2010.), the ligand binding sites are similar (Pike et al., 1999.). ERα and ERβ receptors show similar binding affinities with endogenous and synthetic ligands (Drummond and Fuller, 2012; Katzenellenbogen, 1996; Hall and Korach, 2002), although certain ligands favour one subtype over another, such as phytoestrogens (Kuiper et al., 1997; Whitten and Naftolin, 1998) and genistein (Kupier et al., 1997; Whitten and Patisaul, 2001; Martin et al., 2004) favoring ERβ over ERα.

1.1.7 Estrogen Receptors Mechanism of Action

ERs operate in three known mechanisms of action: "classical" ligand-dependent activation, ligand-independent activation and non-genomic activation. For the ligand-dependent activation, the unbound ERs, which are present within the cytoplasm, are inactivated by forming a complex with a variety of heat shock proteins (Hsp), which has been reviewed in Sanchez, 2012. Once the ligand binds, the Hsps dissociate and binding with DNA occurs, recruiting co-regulators, such as steroid receptor coactivators (SRCs) (Xu et al., 2009); the conformation of the

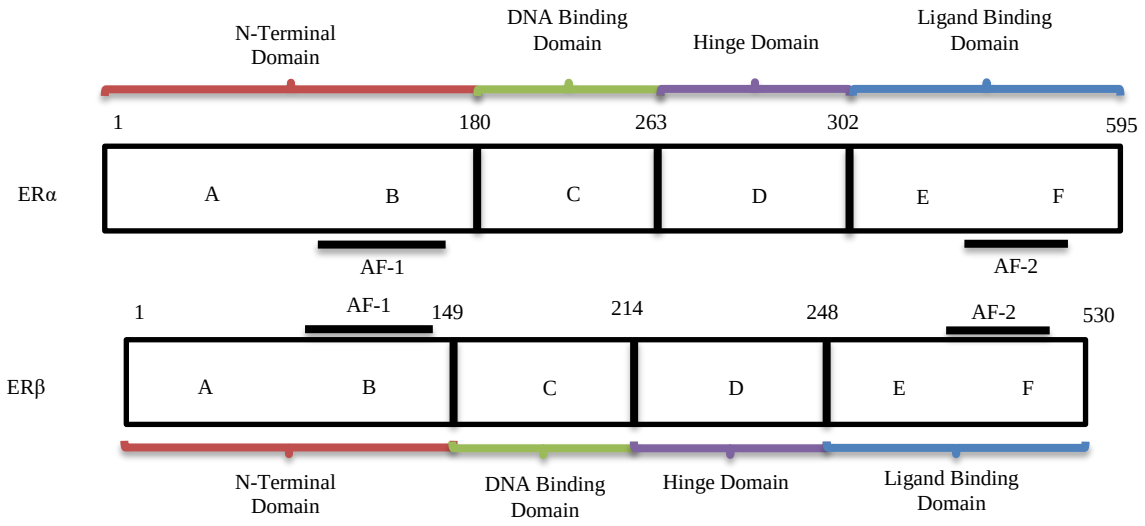

Figure 1.4 Estrogen Receptor Structure

The figure depicts the structural overview of the estrogen receptors. The top structure portrays the ERα and the bottom structure pertains to ERβ. The numbers on the structures represent the amino acid sequences, and the domains are labeled from A to F; domains A and B form the N-Terminal Domain, and E and F form the Ligand Binding Domain. AF: Activation Function

receptor towards coactivators and corepressors is affected by the nature of the ligand (Paige et al., 1999; Pike et al., 1999). Since ERs are also transcription factors, they influence the expression of genes, specifically through binding with the ERE (Estrogen Response Element) (Hall and Korach, 2002; Gruber et al., 2004; Hall et al., 2002). Chang et al., 2006 showed different genes that were regulated by ERβ specifically, including FOXM1, CDC25A, E2F1 and SURVIVIN, SDF-1, THBS1 and BMP-7 genes. Other genes regulated by ERβ include PCNA and CDC6 genes (Lobenhofer et al., 2002; Frasor et al., 2003), and CDC2 and CKS2 genes (Lin et al., 2007); however, ligand-bound ERs could activate other transcription factors that are not related to EREs (see below). For the ligand-dependent activation, the unbound ERs are activated via phosphorylation via different kinases, such as MAPK and PI3K (Miller et al., 2011; Riggio et al., 2011; McGlynn et al., 2013), Erk and Akt; a review performed by Thomas and Gustafsson,

2011 showed the essential role kinases play in the activation of ERα and its association with breast cancer. For the non-genomic mechanism, the ligands bind to ERs localized at the plasma membranes; this mechanism could justify the rapid effects of E2 treatment (Simoncini et al., 2004), including increases in ion fluxes across membranes, activation of eNOS (endothelial nictric oxide synthase) and kinases (Deroo and Buensuceso, 2010).

Depending on the situation and the accessibility of the promoter of transcription, the ERs will either induce or inhibit gene expression (Ratajczuk, 2001): transcription is activated via histone acetyltransferase (HAT), which causes a disruption in the chromatin structure via acetylation, and is then continued via RNA polymerase; transcription is inhibited through the action of HDACs (Histone deacetylases), which prevent the ERs from reaching the promoter (Leitman et al., 2012). The HAT and the HDAC are members of the coregulators, which are enzymes that either help in transcription activation (coactivator) or in transcription inhibition (corepressor) (Smith and O'Malley, 2004).

ERs that are bound to ligands could also commonly (Charn et al., 2010; Carrollet al., 2006) bind to other transcription factors that are not related to the ERE, such as NFκB, and affect the transcription of these unrelated elements (Gruber et al., 2004; Leitman et al., 2012). In addition to the ligand binding activation of ERs, it has been shown that intracellular signaling molecules, through the activation of kinases, could lead to the activation of ERs, without the need for any ligand (Weigel and Zhang, 1998). Moreover, it has been shown that ERs might not need to bind to EREs to induce a particular response; instead, it has been shown that ligands could bind to cytoplasmic ERs, and through the activation of certain processes, such as ion influx and efflux, induce a response, which is quicker (Simoncini et al., 2004) than if a ligand moved into the nucleus and bonded with the receptor there (Deroo and Buensuceso, 2010); this quick

response could be as a result of the ERs localized at the plasma membrane (Levin, 2000; Levin, 2009; Lösel and Wehling, 2003; Acconcia and Marino, 2011; Fiocchetti et al., 2014; Fiocchetti et al., 2015).

Interestingly, ERβ and ERα seem to have opposing transcriptional activations (Hall and McDonnell, 1999; Lindberg et al., 2003; Thomas and Gustfasson, 2011; Bartella et al., 2012), and since they differ in localization and distribution, it could be assumed that the effect of estrogens, or other ER agonists, depends on the levels of both subtypes. For example, ERα has been shown to activate antiapoptotic genes, whereas ERβ favours proapoptotic genes (Acconcia and Marino, 2011; Fox et al., 2009; Marino et al., 2006; Thomas and Gustafsson, 2011); this contradiction in responses has also been documented within osteosarcoma cells (Monroe et al., 2003; Stossi et al., 2004).

Although ERβ is shown to favour apoptosis, it has been shown to also protect the cell from apoptosis caused by oxidative stress by preventing Bax and Bad activation, which would lead to cytochrome c release and the eventual caspase-3 activation (Liang et al., 2015).

1.1.8 Estrogens

Estrogen is classified into estrone (E1), a weak estrogen hormone (Kuhl, 2005), 17β-estradiol (E2), the most physiologically important estrogen hormone (Ryan, 1982) and estriol (E3), another weak estrogen hormone (Kuhl, 2005). Estrogen has a multitude of functions, which include cell growth, differentiation, expression of the complex I, complex IV, and complex V/ATP synthase in the mitochondria (Rettberg et al., 2014) and cellular oxidative stress (Miro et al., 2011; Sastre-Serra et al., 2012; Sastre-Serra et al., 2010; Yao and Brinton, 2012; Simpkins and Dykens, 2008; Richardson et al., 2011; Simpkins et al., 2010). Estrogen has been associated with the inhibition of apoptosis by sequestering mitochondrial Ca2+ (Nilsen and Brinton, 2003;

Sarkar et al., 2008; Brinton, 2008) while decreasing cytoplasmic Ca2+ (Nilsen and Brinton, 2003; Simpkins et al., 2010).

1.1.9 Resveratrol

Resveratrol (RES), a phytoestrogen produced by the stilbene pathway, has been shown to confer cytoprotection in a variety of cell lines via a mechanism that requires ERβ (Wang et al., 2013). In general, many of the cellular effects of RES are quite similar to those of E2 and the ERβ-selective agonist DPN. RES has also been shown to confer neuroprotection when administered in the diet prior to an ischemic event (Fiocchetti et al., 2014).

Resveratrol has also been shown to upregulate MnSOD in the mitochondria. This upregulation was shown to inhibit cell proliferation and increase cellular threshold to stress in different cell lines, especially in SHSY5Y human neuroblastoma cells; knockdown of MnSOD expression through iRNA led to effects contrary to the ones mentioned to manifest, due to insult from H_2O_2 and paraquat. The effects of resveratrol were also observed with E2 and DPN, but were not observed with propylpyrazole triol (PPT), which is an ERα agonist, indicating that these responses are ERβ –mediated (Robb and Stuart, 2011). Moreover, the stilbenes pterostilbene and piceid, which are metabolites and structural analogues of resveratrol, have been shown to have some of these same effects by activating the same responses (Robb and Stuart, 2014.).

1.1.10 Neuroglobin

Globins are proteins characterized by having an iron-containing heme prosthetic group that conveys oxygen binding capabilities. Neuroglobin (Ngb), a monomeric globin protein recognized in 2000 (Burmester et al., 2000) and named so due to its expression in nervous tissue, as well as endocrine tissues (Burmester et al., 2000; Reuss et al., 2002). Ngb is widely

distributed amongst vertebrates, including mice and humans (Burmester et al., 2000), zebrafish, rats and pufferfish (Awenius et al., 2001; Zhang et al., 2002).

Neuroglobin has a molecular weight of 17 kDa, with a three on three globin fold (Figure 1.5), where each fold is comprised of eight α-helices, and binds to a single heme group (Vallone, et al., 2004; Pesce et al., 2003; Vallone et al., 2004). Ngb binds to oxygen reversibly, with its ligand binding capabilities being dependent on the hexacoordination (Figure 1.6) of the heme iron atom (Trent and Hargrove, 2002; Dewilde et al., 2001; Pesce et al., 2002; Hamdane et al., 2003). Ferric Ngb assumes the hexacoordinated haem, where the HisF8 residue is the fifth haem ligand, and the HisE7 residue is the sixth haem ligand. Once oxygen binds to Ngb, the HisE7 Fe ligand becomes displaced by oxygen; oxygenated Ngb assumes pentacoordinate conformation, to which oxygen has a high affinity to (Weiland et al., 2004). However, due to the competition between oxygen and the HisE7 residue over haem group coordination, the Ngb oxygen affinity is lower than expected, and is somewhat similar to myoglobin (Burmester et al., 2000; Dewilde et al., 2001; Pesce et al., 2002). The coordinate conformation of Ngb differs from those of Mb and Hb as both globins bind to their haem groups in their pentacoordinate conformation. The changes of Ngb conformation between hexacoordinate and pentacoordinate seem to be regulated post-translational; an example involves formation of disulphide linkage between Cys46 and Cys55 due to oxidation (Hamdane et al., 2003). A second example involves hypoxia and ischemia post-translational modification of Ngb. Jayaraman et al., 2011 identified that the post-translational phosphorylation of Ngb could be through two putative motifs (Figure 1.7): two 14-3-3 protein binding sites and an ERK docking domain; 14-3-3 protein interactions regulate phosphorylation (Wang et al., 2004), phosphorylation stability (Dent et al., 1995; Chiang et al., 2001; Margolis et

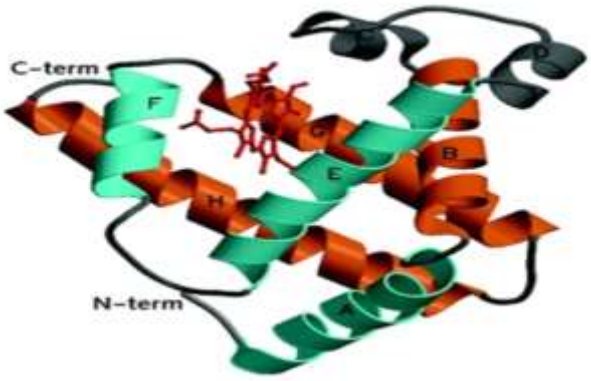

Figure 1.5 Three "Over" Three Globin Fold Structure Overview

The figure depicts the globin fold of Ngb, comprised of 8 α-helical segments labeled from A to H. The three over three fold involves 3 helices B, G and H "over" the 3 helices A, E and F. The haem group is "sandwiched" within the fold. The image was obtained from Pesce et al., 2002.

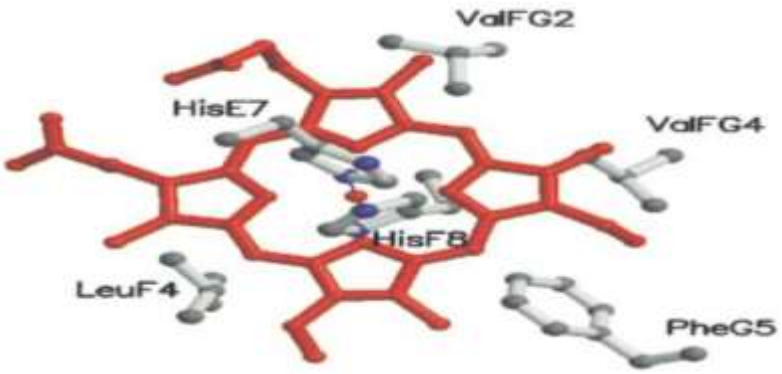

Figure 1.6 Stereo View of the Hexacoordinate Haem
The residues HisE7 (distal), HisF8, LeuF4, ValFG2, ValFG4, and PheG5 (proximal) are depicted. The HisE7 and HisF8 residues assume an orthogonal orientation. The image was obtained from Pesce et al., 2003.

Figure 1.7 Primary Structure of Ngb with ERK and 14-3-3 Binding Sites
The residues HisE7 and HisF8 that coordinate the haem group are highlighted in yellow, the residues comprising the 14-3-3 binding sites are highlighted in green and the pink highlight represents the ERK docking site. The letters in dark represent the phosphorylation of PKA and ERK.

al., 2003) and tertiary structures, while the ERK pathway is activated under hypoxic or ischemic events (Minet et al., 2000; Saurin et al., 2000). The phosphorylation due to the aforementioned sites has been shown to affect the conformation of Ngb and its ligand binding (Jayaraman et al., 2011).

Another difference between Ngb and the globin proteins is the amino acid sequence; the similarity between them is around 25% of the amino acid sequence (Figure 1.8). Phylogenetic studies of the lineage of Ngb showed that vertebrate globins and Ngb differed from one another 600 million years ago (Hankeln et al., 2005), but also shows that Ngb shares an evolutionary origin with invertebrate globins (Burmester et al., 2000; Pesce et al., 2002).

1.1.11 Neuroglobin Location and Distribution

Ngb is expressed in the central nervous system (CNS) (Burmester et al., 2000) and peripheral nervous system (PNS) (Reuss et al., 2002). These locations were established via mRNA in situ hybridization and immunostaining (Reuss et al., 2002; Mammen et al., 2002; Sun et al., 2001; Zhang et al., 2002; Wystub et al., 2003; Geuens et al., 2003). Ngb is expressed strongly in the retina (Schmidt et al., 2003), specifically in the plexiform layer and the photoreceptors, being exclusively in the mitochondria-rich apical part of the inner segments (Schmidt et al., 2003), which have a high demand for oxygen. Ngb mRNA and protein were located in neuronal perikarya and processes (Reuss et al., 2002; Mammen et al., 2002; Sun

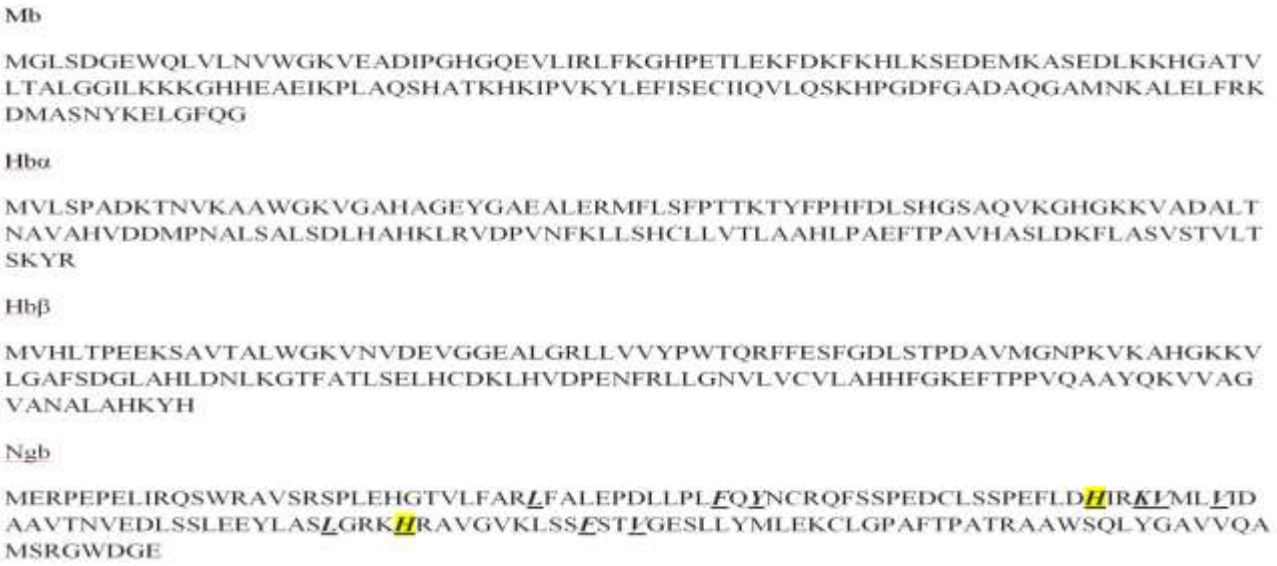

Figure 1.8 Primary Structures of the Globins Ngb, Mb and Hb
The top amino acid sequence represents myoglobin, the second and third amino acid sequences represent haemoglobin (α and β respectively) and the bottom line represents neuroglobin. The residues HisE7 and HisF8 that coordinate the haem group are highlighted in yellow on the Ngb sequence. The residues that come into contact with the haem group are italicized, underlined and in bold.

et al., 2001; Zhang et al., 2002; Wystub et al., 2003; Geuens et al., 2003), cerebral cortex, cerebellum, medulla, caudatoputamen, and substantia nigra (Burmester et al., 2000); Ngb levels were also detected in the human brain (Jin et al., 2010), hippocampus, thalamus and hypothalamus (Wystub et al., 2003.). Moreover, analysis of ischemic brain tissue showed upregulation of neuroglobin, indicating the neuroprotective capabilities of neuroglobin in ischemia/reperfusion injury (Sun et al., 2001; Sun et al., 2003). Studies have associated Ngb with neuroprotection (Szymanski et al., 2008; Chuang et al., 2010; Lin et al., 2008) further, as it has been shown that the decrease in Ngb expression is associated with an increase in the incidence of Alzheimer's disease (Szymanski et al., 2008), which is mainly characterized with neurodegeneration. However, there are studies that show Ngb expression is present in non-neuronal tissues, such as liver cancer cells (Zhang et al., 2013; Fiocchetti et al., 2014), colorectal cancer cells (Fiocchetti et al., 2015), breast cancer cells (Fiocchetti et al., 2016).

Neuroglobin was thought to be a cytoplasmic protein, which was confirmed when the transfection of *N*- and *C*-terminal gene fusion constructs between neuroglobin and a green fluorescent protein into eukaryotic cell did not show that neuroglobin was combined with or moving towards any intracellular structures (Hankeln et al., 2004). However, Ngb was later found, through immunostaining, to be expressed in the nucleus and mitochondria, in addition to the cytoplasm of SK-N-BE cell lines. These locations of neuroglobin (Hundahl et al., 2010; Hundahl, et al., 2011) along with interactions between neuroglobin and proteins within the mitochondria (Haines et al., 2012), have since been shown in other cell lines. For example, Fiocchetti et al. (2016) demonstrated the localization of Ngb in the mitochondria of MCF-7 cells.

1.1.12 Neuroglobin and Cytochrome c

The interaction between Ngb and Cyt c involves the formation of a complex between the two proteins, followed by an electron exchange (Fago et al., 2006; Bonding et al., 2008). This process is enhanced via electrostatic interactions between Ngb and Cyt c, as the former is acidic, while the latter is basic, leading to the formation of opposite charges at a neutral pH. In addition to differences in charge, it would seem that the residues Lys25 and Lys72 are important in the interaction between the two proteins. This is based on findings that have shown an interaction between Cyt c and Apaf-1 through the exact same residues (Yu et al., 2001; Abdullaev et al., 2002; Ellerby et al., 2000; Chertkova et al., 2008), which will lead to the apoptosome that activates the caspase cascade. It is interesting to note that Ngb cannot affect the apoptosome formation between Cyt c and Apaf-1, but instead undergoes a redox reaction that causes Cyt c to lose its activity (Raychaudhuri et al., 2010). This reaction ceases the formation of the apoptosome, successfully leading to the inactivation of caspase 9 (Brittain et al., 2010.; Raychaudhuri et al., 2010).This redox reaction involves ferrous Ngb binding with ferric

cytochrome c, which is the active form, reducing it to ferrous, which is the inactive form (Suto et al., 2005; Borutaite and Brown, 2007; Brown and Borutaite, 2008), oxidizing Ngb from ferrous form to ferric form.

1.1.13 Neuroglobin Upregulation

Since Ngb has oxygen binding capabilities, it would seem to have a role in ischemia and hypoxia (Kelsen et al., 2008; Wang *et al*., 2008.; Dong et al., 2010.). During hypoxia, it was shown that Ngb expression is induced (Yu et al., 2009.) as it is responsible for regulating apoptotic signals caused by hypoxia (Hota et al., 2012; Brittain et al., 2010; Brittain and Skommer, 2012.). Ngb has been shown to be upregulated during hypoxia in vitro for protection (Fordel et al., 2004; Sun et al., 2001). Ngb overexpression in cell cultures derived from hippocampal neurons was shown to protect the cells from hypoxic insult, an effect that was reversed in Ngb knockdown (Sun et al., 2001). Another study performed on mouse cortical neuron cultures with Ngb overexpression has shown neuronal protection againts hypoxic insults (Liu et al., 2009). It seems that hypoxia does not upregulate Ngb levels in vivo (Fordel et al., 2004b; Mammen et al., 2002; Sun et al., 2003). Interestingly, HIF-1 (hypoxia-inducible factor-1) expression during hypoxia was shown to regulate Ngb expression (Haines *et al*., 2012). As for ischemia, it was observed that there was an increase in Ngb expression in patients with strokes (Jin et al., 2010.). An in vivo study showed that overexpression of Ngb in transgenic mice protected them from myocardial and cerebral ischemia in comparison with wild-type mice (Khan et al., 2006), and a later study confirmed cerebral ischemic insult amelioration by Ngb overexpression in transgenic mice (Wang et al., 2008). In Ngb-null mice, it was shown that infarct sizes increase after ischemic insults (Raida et al., 2012), furthering Ngb's role in

neuroprotection. Other studies showed the effect of Ngb on an insult similar to hypoxic/ischemic insult – oxygen glucose deprivation (OGD).

OGD affects Ngb as well, as evidence showed the expression of certain hypoxia-response genes occurs during OGD as a result of Ngb (Yu et al., 2009). Ngb transcript levels as well as protein levels have been shown to be upregulated during ODG (Fordel et al., 2007). Furthermore, Ngb overexpression in mouse cortical neuron cultures was able to ameliorate neuronal death when OGD was imposed; in contrast, Ngb knockdown showed the opposite during OGD insult (Yu et al., 2013). And even though Ngb has been shown to be localized within the mitochondria, its localization seemingly increases within the mitochondria after OGD occurs (Yu et al., 2012).

1.1.13.1 Mechanisms of Neuroglobin Regulation

In addition to oxidative stress, Ngb expression (De Marinis et al., 2010) is also upregulated greatly by E2 via ERβ. E2 stimulation has been shown to upregulate Ngb expression by approximately 300%, translocate Ngb into the mitochondria and overall, exert an antiapoptotic effect through the upregulation of Ngb (De Marinis et al., 2010; De Marinis et al., 2013; Fiocchetti et al., 2013). The effect of E2 on Ngb levels appears to be dependent on the dosage and the time of treatment in MCF-7 and HepG2 cells (Fiocchetti et al., 2014) and DLD-1 cells (Fiocchetti et al., 2015). 10 nM E2 seems to induce the highest Ngb expression, which peaks between 4 and 6 hours following the onset of treatment followed by a gradual decrease for up to 24 hours in the MCF-7 and HepG2 cells (Fiocchetti et al., 2014), while the levels remained constant from 4 to 24 hours for DLD-1 cells (Fiocchetti et al., 2015). As Ngb upregulation is dependent on E2 via ERβ, and since ERβ acts as a transcription factor, the transcriptional modulation of Ngb proves insightful. The transcriptional modulation of Ngb upregulation was studied via the application of actinomycin D (Act), a transcription inhibitor, and the modulation

of E2-dependent Ngb upregulation was studied via 2-bromohexadecanoid acid (2-Br), a palmitoyl acyltransferase (PAT) inhibitor that inhibits the cell membrane localization of ERs (Acconcia and Marino, 2011; Marino et al., 2006). The impairment of Ngb upregulation with E2 stimulation by actinomycin D shows that E2-dependent upregulation of Ngb is modulated transcriptionally in MCF-7, HepG2 (Fiocchetti et al., 2014) and DLD-1 cells (Fiocchetti et al., 2015). The upregulation of Ngb with E2 stimulation by 2-bromohexadecanoid acid also shows that the modulation of E2-dependent Ngb upregulation depends on signaling pathways that begin with the plasma membrane in MCF-7, HepG2 (Fiocchetti et al., 2014) and DLD-1 cells (Fiocchetti et al., 2015). A more specific look at the signaling pathways revealed the role kinases play in E2-dependent Ngb upregulation.

Studies showed that around 10 minutes of 10 nM E2 treatment increased the phosphorylation of p38/MAPK, AKT and ERK (Acconcia et al., 2005; Galluzzo et al., 2007), which are present in the transduction cascades of ER signaling pathways (Acconcia and Marino 2011). After 24 hours of E2 stimulation, the Ngb upregulation was prevented by AKT and ERK inhibitors in MCF-7 (Fiocchetti et al., 2014) and was prevented by p38 inhibitors in HepG2 (Fiocchetti et al., 2014) and DLD-1 cells (Fiocchetti et al., 2015), confirming the role p38 plays in the upregulation of Ngb (Caiazza et al., 2007; Galluzzo et al., 2007), which might suggest cell-line specific kinase activity with respect to E2-dependent Ngb upregulation.

For mRNA levels, it was shown that 4 hours of E2 treatment showed peak mRNA transcript levels in the MCF-7 and HepG2 cells (Fiocchetti et al., 2014) but remains fairly constant between 4 and 24 hours in DLD-1 cells (Fiocchetti et al., 2015); this suggests that E2 could prevent Ngb degradation post-transcriptionally. The post-transcriptional prevention of Ngb degradation was tested via chloroquine, an inhibitor of lysosomal enzymes by altering the pH of

lysosomes and endosomes (Totta et al., 2014), and Mg-132, a 26S proteasome-mediated degradation inhibitor (Totta et al., 2014). The increase in the levels of Ngb in the presence of the inhibitors (Fiocchetti et al., 2015) would suggest that Ngb is degraded via lyososomes and proteasomes.

Even though E2 induces the translocation of Ngb into the mitochondria in neuronal cells (De Marinis et al., 2013), it was shown that E2 affects Ngb translocation in non-neuronal cells. 24 hours of 10 nM E2 stimulation was shown to increase Ngb localization in the mitochondrial subcellular compartment in MCF-7 and HepG2 cells (Fiocchetti et al., 2014) and DLD-1 (Fiocchetti et al., 2015); Ngb localization decreased in the nuclear compartment alongside the mitochondrial increase in all the cell lines. Interestingly, Ngb localization was shown to increase in the cytoplasm within HepG2 cells (Fiocchetti et al., 2014) and DLD-1 cells (Fiocchetti et al., 2015), but not for MCF-7 cells (Fiocchetti et al., 2014). As E2 stimulation is required for Ngb translocation, it is also important to note that E2-dependent Ngb upregulation prevents the deleterious effects of oxidative stress.

E2-dependent Ngb upregulation within neuronal cells is pivotal to reducing the effects of oxidative stress (De Marinis et al., 2013; Fiocchetti et al., 2013). Hydrogen peroxide treatment of MCF-7 cells (Fiocchetti et al., 20145) and DLD-1 cells (Fiocchetti et al., 2015) triggered the apoptotic pathway, but the pretreatment with E2 prevented apoptosis. It was shown that E2 treatment with hydrogen peroxide upregulated Ngb levels; in Ngb-silenced MCF-7 cells (Fiocchetti et al., 2014) and DLD-1 cells (Fiocchetti et al., 2015), E2 treatment was unable to prevent the apoptosis triggered by hydrogen peroxide. This suggests that the E2-dependent Ngb upregulation is important to counteract the detrimental effects of hydrogen peroxide.

1.1.14 Neuroglobin Translocation into Mitochondria

Proteins that are normally imported (Figure 1.8) into the mitochondria are of two different classes: proteins that carry the N-terminus targeting sequence with cleavable extensions or proteins that carry internal signals without cleavable extensions (Pfanner and Geissler, 2001; Truscott et al., 2003; Chacinska et al., 2009). In case of the former, the N-terminus targeting sequence is recognized by TOM (translocase of outer membrane). Once the recognition is complete, the protein becomes imported into the mitochondria to serve its destined purpose (Schatz and Dobberstein, 1996). The lack of mitochondrial targeting sequence within the Ngb structure still does not justify the localization of Ngb. An explanation to the localization of Ngb without the N-terminus presequence is that the mitochondrial targeting sequence is not highly conserved (Truscott et al., 2003), which would mean that Ngb has a unique targeting sequence. Another justification is that mRNA and ribosomes are recognized (Marc et al., 2002; Riemer et al., 2011), which would mean that the import of Ngb could be possible through co-translational transport.

The translocation of Ngb into the mitochondria might also be related to the VDAC and MPT, as a study that used inhibitors of VDAC and MPT yielded a reduction in the increased Ngb translocation into the mitochondria that is expected during OGD (Yu et al., 2012). The translocation of Ngb into the mitochondria would indicate that the expression of Ngb takes place in the nuclear DNA (Burmester et al., 2000). Evidence of the translocation of Ngb from the cytoplasm into the mitochondria has been elucidated by the interaction of Ngb with multiple proteins within the mitochondria, such as Etfa (Electron-transfer flavoprotein) (Yu et al., 2012), Cyc1 (a subunit of the third respiratory complex) and VDAC (Zhu et al., 2011). However, the exact mechanism of mitochondrial importing of Ngb is not well known.

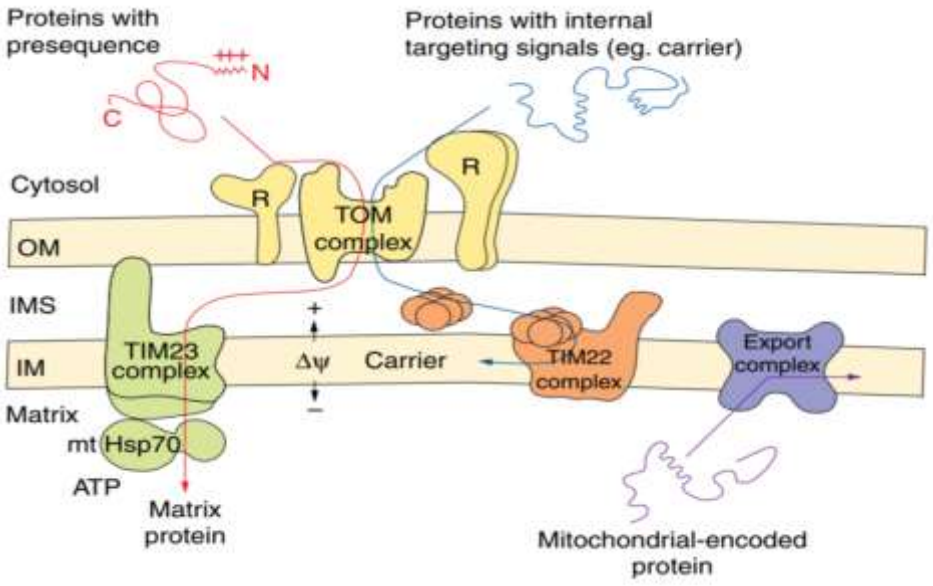

Figure 1.9 Protein Import into Mitochondrion
The complexes TOM, TIM23 and TIM22 are responsible for importing proteins destined to the internal compartments, while the Export complex is responsible for exporting proteins from the matrix and into the inner membrane. The specific receptor (R) is the site of binding for proteins with the N-terminal sequence or internal signals, which then directs the protein through the general import pore (GIP) of the translocase of the outer membrane (TOM). The proteins with the N-terminal presequence are imported across the inner membrane via the TIM23 complex and into the matrix. The proteins with the internal targeting sequences are destined for the inner membrane, and are directed by the Tim factors to the TIM22. Membrane insertion at the TIM22 complex is dependent on the membrane potential. The export complex export proteins that are encoded in the mitochondria and some imported proteins to the inner membrane. IM:

1.1.15 Insights into Ngb Function via Overexpression and Knockdown

Ngb overexpression has been associated with reduction in brain injury caused by intracerebral hemorrhage (Jin et al., 2011.), which would further confirm Ngb's role in neuroprotection. An *in vivo* study using exogenous Ngb demonstrated that it could be taken up by the neurons of the mice used, and even protects the brain from ischemic injury (Cai et al.,

2011.). Furthermore, overexpression of Ngb, through a transfection of the SH-SY5Y cells, protected the cells against H_2O_2 injury (Antao et al., 2010.). Moreover, Ngb overexpression in SH-SY5Y cells and cortical neurons of transgenic mice lead to a decrease in calcium levels, maintaining the integrity of the mitochondrial membrane and its potential in the process (Duong et al., 2009; Liu, et al., 2009). In addition, Ngb overexpression has been shown to defend against cell death that has been caused by OGD, H_2O_2, paraquat and amyloid beta peptide (Sun et al., 2001; Fordel et al., 2006; Li et al., 2008; Li et al., 2008; Raychaudhuri et al., 2010; Antao et al., 2010). To further determine the protective measures of Ngb, Ngb overexpression was implemented in transgenic mice in a study by Li et al., 2010; the results showed that the production of RNS and ROS, as well as the peroxidation of lipids, decreased in neurons, hinting at an association between Ngb and its antiapoptotic activities (Li et al., 2010.). Even though the *in vivo* protective role of Ngb is contradictory to the in vitro studies (Hundahl et al., 2006), there have been *in vivo* studies that show that Ngb overexpression in transgenic animals was associated with a reduction in cerebral infarct size (Khan et al., 2006; Wang et al., 2008).

As for knockdowns, *in vitro* studies regarding the knockdown of Ngb has been associated with a decrease in neuroblastoma cell viability under oxidative stress (Ye et al., 2009) and an increase in cortical neuronal death as a result of hypoxia (Szymanski et al., 2008). Sun et al., 2003 administred an adeno-associated viral vector that would express Ngb into the cerebrum of rats that underwent Ngb knockdown, and it was observed that the size of the infarct was reduced as well (Sun et al., 2003).

1.1.16 Neuroglobin Mechanism of Action

Other than its interaction with Cyt c, evidence indicates that Ngb interacts with the G-proteins (Wakasugi et al., 2003); the ferric form of Ngb was shown to bind to the Gα subunit in

the GDP-bound state, where it acts as a GDI (guanine-nucleotide dissociation inhibitor) (Wakasugi et al., 2003.). This action inhibits the conversion of GDP to GTP, which prevents the Gα subunit from binding to the G$\beta\gamma$ complex, causing the release of the Gβγ subunit (Wakasugi et al., 2003; Schwindinger and Robishaw, 2001). This in turn activates the neuroprotective effect of NGF (nerve growth factor), which works through the activation of the PI3K/Akt pathway (Dudek *et al*., 1997.). To confirm that Gβγ is required for the neuroprotective effect to occur, Wu and Wong, 2006 demonstrated that the Gβγ inhibitor, transducin, prevented the neuroprotective effect of NGF, which in turn confirms the role of PI3K/Akt pathway involvement (Wu and Wong, 2006). Hypoxia and ischemia induce HIF-1α, which in turn, induces insulin growth factor, which activates the PI3K/Akt pathway (Li et al., 2006.). Since HIF-1α affects Ngb expression (Haines et al., 2012.), it might be a valid connection between Ngb and its effect through the PI3K/Akt pathway, which favours cell survival (Jover-Mengual et al., 2010). Hemin, a porphyrin, has been shown to upregulate Ngb mRNA and pAkt levels, indicating that there could be a connection between Ngb and pAkt (Zhang et al., 2013). Another study that shows the association between Ngb and Akt observed that Ngb protected cells against H_2O_2 injury by phosphorylating Akt and activating the mito-KATP channel (Antao et al., 2010.); pAkt (phosphorylated Akt) inhibits apoptosis by preventing the release of Cyt c and AIF from the mitochondria (Tapodi et al., 2005).

There is an increase in the activity of nNOS after ischemia (Lipton, 1999), which will eventually lead to cell death, as the continuously produced NO will induce mitochondrial permeabilization, which will then lead to the release of Cyt c and the eventual activation of the caspase cascade (Zhu et al., 2004). Since the ferric and ferrous forms of Ngb show reactive potential with nitrogen in vitro, the neuroprotective mechanisms of Ngb could lie within NO

(even though it is not as significant as Hb or Mb (Smagghe et al., 2008)) and RNS scavenging; the latter has been observed within reactions between Ngb and the nitrite and peroxynitrite anions (Zhu et al., 2004), which does not require a ferryl intermediate (Herold et al., 2004). The ferrous form of Ngb is important due to its NO scavenging capabilities (Brunori et al., 2005), which would indicate that the continuous reduction and oxidation of Ngb is important. The protective function of Ngb could also be related to its scavenging abilities for peroxynitrite anion ($ONOO^-$) (Fago et al., 2004a), which constitutes RNS, as well scavenging for ROS, during hypoxia (Fordel et al., 2007). It could also be attributed to nitric oxide homeostasis (Brunori et al., 2005; Brunori and Vallone, 2006) and acting as a sensor for hypoxia (Wakasugi and Morishima, 2005) in neurons. The management of the reactive species may not be a result of a direct interaction between Ngb and the reactive species however, as it could also be due to an interaction between Ngb and the respiratory complexes, which was observed in the works of Yu et al., 2012 and Yu et al., 2012 (Yu et al., 2012; Yu et al., 2012.). The direct effect of Ngb on reactive species has been documented however, in a study by Li et al., 2011; recombinant human Ngb has been shown to directly scavenge reactive species effectively, including hydrogen peroxide, superoxide anion and hydroxyl radicals (Li et al., 2011). The scavenging capabilities of the recombinant human Ngb were lesser than vitamin C, but were greater than GSH (Li et al., 2011.).

The ferric Ngb has been shown to inhibit the GPCR (G-protein coupled receptor) (Wakasugi et al., 2003), which is required for the formation of IP3 from PIP2. IP3 is required for the release of calcium from the endoplasmic reticulum when bound to the IP3 receptor, which will lead to an increase in the release of calcium. Thus, the inhibition of IP3 production by Ngb will lead to a decrease in calcium levels within the cytoplasm, which agrees with the findings

that showed Ngb colocalizing with orexin, an excitatory neuropeptide that increases calcium levels within neurons, as well as amyloid beta, and lead to the eventual death of the cell, hinting further at the neuroprotective capabilities of Ngb.

Another protective mechanism for Ngb involves the inhibition of Pak1 kinase and the interaction with members of the RhoGTPase family; this mechanism induces reorganization in the cytoskeleton and prevents the aggregation of mitochondria at the lipid raft, preventing any hypoxia-induced death signaling (Khan et al., 2008). This mechanism has also been shown in death signaling induced by NMDA excitatoxicity and amyloid beta in neurons as well (Khan et al., 2007).

1.2 Objectives

1.2.1 To determine if Ngb inhibits apoptosis via the inhibition of cytochrome c peroxidase activity.

1.2.2 To determine if the phytoestrogen resveratrol (RES), like estradiol (E2) stimulates Ngb expression and affects Ngb subcellular localization.

1.2.3 To determine if Ngb stabilizes mitochondrial network stability under physiological stress.

Chapter 2.0: The effect of Ngb on cytochrome c peroxidase activity

2.1 Introduction

Cyt c is part of the cytochrome c family haemproteins, and seems to be normally localized within the intermembrane space of the mitochondrion (Neupert 1997), particularly at the inner membrane portion. It is part of the electron transport chain (ETC), where it transfers electrons from Complex III (Coenzyme Q – Cyt C reductase or cytochrome bc_1 complex) to Complex IV (Cyt C oxidase). The 12 kDA protein contains a haem group that binds to the two cysteine side chains via thioether bonds (Kang and Carey, 1999). The ability of the haem group to be reduced grants cytochrome c multiple functions, which affects the kinetics of electron transfer (Zhao et al., 2003); this haem group accepts the electron from Complex III and transfers it to Complex IV. In addition to its function in the ETC, cyt c plays a role in apoptosis, particularly the intrinsic apoptotic pathway, with the peroxidation of the lipid of the inner mitochondrial membrane – cardiolipin.

Cardiolipin is a type of diphosphatidylglycerol lipid that compromises the inner membrane of a mitochondrion. As it is the main component of the inner mitochondrial membrane, the functions of cardiolipin involve proteins integrated in that membrane. It has been shown that cardiolipin is associated with maintaining the quaternary structure of Complex III as well as the function of the enzyme (Gomez and Robinson, 1999). Also, it seems that ATP synthase has a high-binding affinity to cardiolipin (Eble et al., 1990) and that function of Complex IV is maintained via cardiolipin. In addition to the role that cardiolipin plays in the structure and function of the inner membrane, the lipid seems to play a role in apoptosis as well; the peroxidation of cardiolipin causes the release of the pro-apoptotic protein – cytochrome c.

When cyt c interacts with cardiolipin at the inner mitochondrial membrane, the haem group becomes exposed to hydrogen peroxide (H_2O_2), which is produced during the electron transport; the hydrogen peroxide binds to the haem group, which activates the intrinsic peroxidase activity of cyt c (Kagan et al., 2005; Gonzalvez and Gottlieb, 2007; Ott et al., 2007). Cardiolipin becomes oxidized from the peroxidase activity, and forms cardiolipin hydroperoxides that have a different structural conformity; the oxidized cardiolipin becomes distributed at the outer mitochondrial membrane, creating pores that aid in the release of cyt c (Orrenius and Zhivotovsky, 2005; Paradies et al., 2009). The release of cyt c from the intermembrane space to the cytoplasm triggers the intrinsic apoptotic pathway. A role of cyt c in apoptosis is that it binds to the IP3 receptor on the endoplasmic reticulum, which leads to the release of calcium. Calcium then enters the mitochondria and induces swelling and eventual fragmentation of the mitochondria, which creates an increase in cyt c release in a positive feedback mechanism (Boehning et al., 2003). The other role of cyt c is to create the apoptosome (a multimolecualr holoenzymatic complex) that cleaves and activates procaspase 9, which leads to the formation of caspase 9 and the eventual activation of the caspase cascade (Kroemer et al., 1998).

Ngb seems to have an anti-apoptotic effect, possibly due to the interaction with cyt c (Brittain et al., 2010; Yu et al., 2012). The active form of cyt c that leads to the activation of the intrinsic apoptotic pathway is the ferric cyt c form (Brittain et al., 2010; Ascenzi et al., 2011). It has been shown that Ngb reduces ferric cyt c to ferrous cyt c, which inhibits the apoptotic activity of cyt c (Suto et al., 2005; Borutaite and Brown, 2007; Brown and Borutaite, 2008; Raychaudhuri et al., 2010). The interaction between Ngb and cyt c was thought to occur exclusively within the cytoplasm (Brittain and Skommer, 2012). However, studies have shown

that Ngb translocates to mitochondria under some conditions. It has been shown that Ngb translocation to the mitochondria occurs via the mPTP, which is located on the inner mitochondrial membrane, and VDAC, which is located on the outer mitochondrial membrane (Yu et al., 2012). De Marinis et al., 2013 also showed that there is an association between cyt c and Ngb within the mitochondria. The interaction with cyt c within the mitochondria could be putatively associated with Ngb's ability to reduce cyt c; the role of Ngb in inhibiting apoptosis by interacting with cyt c within the mitochondria has not been fully elucidated.

The evidence shows that Ngb interacts with cyt c and is able to translocate into the mitochondria to prevent cyt c release. Since Ngb is able to prevent the release of cyt c from the mitochondria, it could be hypothesized that Ngb could have an effect on the intrinsic peroxidase activity of cyt c.

In order to assess the effect of Ngb on the intrinsic peroxidase of cyt c on cardiolipin, the cyt c peroxidase activity assay was undertaken. The assay involves the use of Amplex Red reagent (as described in Atkinson et al., 2011 and Birk et al., 2013) using the Varian Cary Eclipse fluorescence spectrophotometer equipped with the microplate reader (obtained from Agilent Technologies, Santa Clara, CA, USA). The assay involves the formation of resorufin from the oxidation of the Amplex Red alongside the activation of the cyt c peroxidase intrinsic activity (Zhou et al., 1997).

2.2 Materials and Methods

2.2.1 Materials

Cytochrome c from bovine heart (Catalogue# C3131), cardiolipin (from bovine heart) in ethanol (Catalogue# C1649) and 9.79 M hydrogen peroxide (Catalogue# 216763) were obtained

from Sigma-Aldrich (St. Louis, MO, USA) HEPES (4-(2-hydroxyethyl)-1-piperazineethanesulfonic acid) and DMSO (Dimethylsulfoxide) were obtained from BioShop (Burlington, ON, Canada).

Amplex Red (10-Acetyl-3,7-dihydroxyphenoxazine) was obtained from Cayman Chemical (Ann Arbor, MI, USA).

Purified Recombinant Human Neuroglobin (Catalogue# ab63278) was obtained from Abcam (Cambridge, UK).

2.2.2 Methods

2.2.2.1 Cytochrome c peroxidase activity assay

The intrinsic activity of cyt c was measured with purified cyt c, purified cardiolipin and the reagent Amplex Red as mentioned above. The spectrophotometer measures the fluorescence from resorufin, which is formed as a result of the oxidation of Amplex Red during the activity of cyt c peroxidase. The assay involves the usage of cyt c (1 μM; from bovine heart) was incubated with cardiolipin (15 μM; ≥80% polyunsaturated fatty acid content, primarily linoleic acid, from bovine heart) in HEPES buffer (20 mM, pH 7.4) with or without purified Ngb for 20 minutes. H_2O_2 and Amplex Red (both at the final concentration of 50 μM) were then added to initiate the activity, with the resorufin formation rate being measured over 10 minutes using excitation of 525 nm and emission wavelengths of 590 nm. Maximal reaction rates (measured in Arbitrary Fluorescence Units (AFU) per minute) were calculated from the initial linear range of the formation of resorufin using Cary Eclipse Kinetics softaware (obtained from Walnut Creek, USA). The entirety of the assay was performed at room temperature, protected from light.

2.3 Results

2.3.1 Neuroglobin does not inhibit cytochrome c peroxidase activity

The intrinsic cardiolipin peroxidase activity of cyt c was measured with cyt c alone as well as cyt c with cardiolipin using an Amplex Red/horseradish peroxidase-based fluorometric assay (Fig. 2.1), with the latter condition mimicing the normal peroxidation process; the linearity of the fluorescence change measured till 10 minutes. The change in fluorescence witth cyt c alone was 2.5 times less than the measurement for cyt c with cardiolipin and was significantly different (p-value ≤ 0.001). The fluorescence measurement of the reaction with the presence of cardiolipin and Ngb alongside cyt c and cardiolipin was around 7.6 Fluorescence Arbitrary Units, which is around 2.4 times greater than the measurement with the presence of cytochrome c alone. However, the measurement with presence of cardiolipin alongside cyt c was not statistically significant (p-value = 0.24).

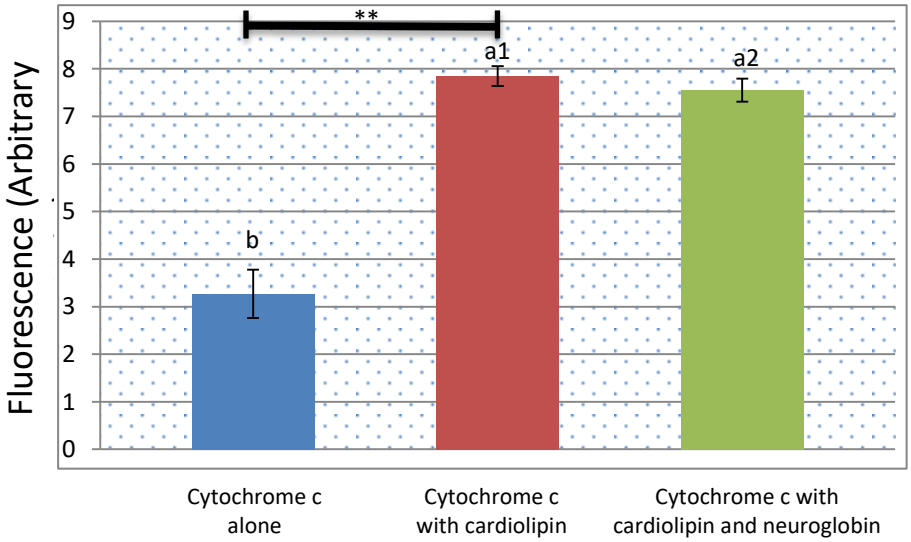

Figure 2.1: Neuroglobin does not inhibit Cytochrome c Peroxidase Activity

The bar chart shows the three different experimental conditions: cytochrome c alone (negative control), cytochrome c with cardiolipin (positive control) and cytochrome c with cardiolipin and neuroglobin. The bars represent means ± SEM from triplicates for each condition. The statistical analysis between the positive control (a1) and the experimental condition (a2) were analyzed with the independent T-test (p-value = 0.24). ** indicates a p-value less than 0.001.

2.4 Discussion

2.4.1 Neuroglobin lacks inhibitory effect on cytochrome c peroxidase activity

The lack of increase in the fluorescent measurement in the presence of cyt c alone relative to the measurement in the presence of cyt c and cardiolipin, was expected, as the peroxidase activity of cyt c is largely activated when cyt c interacts with cardiolipin; the exposure of the haem group within cyt c towards H_2O_2 would activate the peroxidase activity. The increase in fluorescence after the addition of cardiolipin agrees with multiple authors (Figure 2.2) (Petrosillo et al., 2001; Kagan et al., 2005), since cardiolipin exposes the haem group of cyt c during their

interaction, allowing H_2O_2 to react with the haem group; the activation of the peroxidase activity of cyt c correlates with the increase in the fluorescence of the assay.

However, the non-significant difference between the measurement of the fluorescence after the addition of Ngb and the measurement with cardiolipin and cyt c only could show that Ngb does not interact with cyt c through the inhibition of the intrinsic peroxidase activity. This lack of inhibition could be because the ratio of Ngb to cyt c used was 1:1, where there is evidence that the anti-apoptotic effects occur when the ratio of Ngb to cyt c is 3:1 (Raychaudhuri et al., 2010). Another explanation could be due to the differences in localization of cyt c and Ngb.

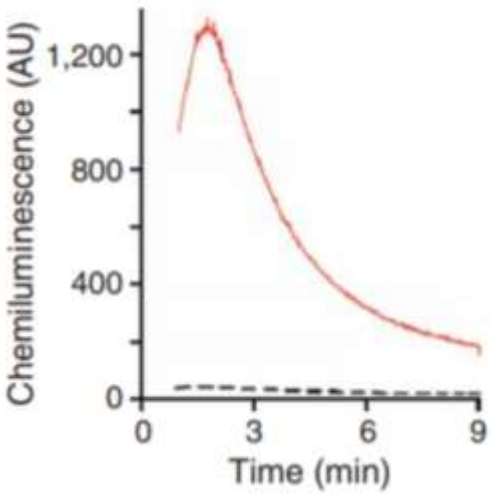

Figure 2.2 H_2O_2-Induced oxidation chemiluminescence response

The figure depicts the oxidation of luminol via H_2O_2 in a manner similar to the Amplex Red reagent. The red curve shows cyt c with cardiolipin, while the black dotted curve shows cyt c without cardiolipin. The figure was obtained from Kagan et al., 2005.

Cyt c is exclusively localized in the intermembrane space of the mitochondria, where it peroxidizes the cardiolipin at the inner membrane, leading to the release of cyt c. Even though Ngb localizes in the mitochondria, its exact location has not been elucidated. Lechauve et al., 2012 has shown that Ngb localizes within the mitochondrial matrix, which was confirmed when Ngb presence was detected in mitoplasts (mitochondrion devoid of the outer membrane and the intermembrane space). This location would explain the lack of any Ngb inhibitory activity towards the cyt c peroxidase activity; a putative ratiocination is that Ngb is unable to reach cyt c and interact with it in the intermembrane space, as the inner membrane acts as a barrier. However, the lack of interaction between the two proteins contradicts results from certain authors (De Marinis et al., 2013). Another putative explanation is that Ngb does not affect cyt c's peroxidase activity as it acts as a scavenger for ROS (Herold et al., 2004; Fordel et al., 2007) within the matrix, which means that it will not interfere with the reaction between H_2O_2 and the haem group of cyt c.

A third supposed deduction could be that Ngb binding with cyt c requires the ferric form of cyt c, which is required for the apoptosome to form (Pan et al., 1999; Suto et al., 2005). This would suggest that the interaction between Ngb and cyt c is possible upon the release of the cyt c into the cytoplasm. That interaction contrasts with the evidence that shows that Ngb and cyt c interact together within the mitochondria (De Marinis, 2013). It would be safe to assume that the Ngb role within the mitochondria would be the scavenging of ROS and RNS.

2.5 Conclusion

Given the data provided, Ngb does not inhibit the peroxidase activity of cyt c in a 1:1 ratio as there was no significant difference between the fluorescence measurement in the cyt c and cardiolipin group and the cyt c, cardiolipin and Ngb group.

Chapter 3.0: The Effect of E2 and RES on Ngb expression and subcellular localization

3.1 Introduction

Ngb has been shown to be cytoplasmic (Reuss et al., 2002; Zhang et al., 2002; Schmidt et al., 2003; Wystub et al., 2003) via evaluations of bioinformatical sequences (Schmidt et al., 2004), which involves predictive systems to predict localization such as SCLpred (Mooney et al., 2011), and has been shown to translocate and localize in the mitochondria (Bentmann et al., 2005), where it is thought to prevent the release of cyt c and the eventual activation of apoptosis. This mechanism is the hypothesized role of Ngb in promoting cell survival. Literature has been shown that the role of Ngb is dependent on its upregulation via E2 stimulation.

Transcriptioanl upregulation of Ngb (via ERβ) has been shown to reach approximately 300% in SK-N-BE neuroblastoma cells, mouse hippocampal neurons and mouse astrocytes (De Marinis et al., 2010; Marinis et al., 2013). The release of cyt c from the mitochondria was prevented as a result of E2-dependent Ngb upregulation, leading and to its translocation into the mitochondria and preventing the cyt c release (De Marinis et al., 2010; Fiocchetti et al., 2012; De Marinis et al., 2013; Fiocchetti et al., 2013). Recent studies have also shown that Ngb translocates into the mitochondria in MCF-7 (breast cancer cells) (Fiocchetti et al., 2014), HepG2 (liver cancer cells) (Fiocchetti et al., 2014) and DLD-1 (colorectal cells) (Fiocchetti et al., 2015). The upregulation of Ngb does not only occur in nervous cells (such as SK-N-BE and SH-SY5Y cells), but there is evidence that elucidates the E2-dependent Ngb upregulation in non-neuronal cells, including MCF-7 (Fiocchetti et al., 2014), HepG2 (Fiocchetti et al., 2014) and DLD-1 (Fiocchetti et al., 2015); the upregulation was both time-dependent and dose-dependent these cells (Fiocchetti et al., 2014; Fiocchettis et al., 2015). Since ERs have a transcriptional and

non-genomic activity (Ascenzi et al., 2006; Marino et al., 2006; Acconcia and Marino, 2011), the effect of E2 stimulation on Ngb mRNA transcript levels and protein levels were elucidated.

Fiocchetti et al., 2014 elucidated the effect of 10 nM E2 stimulation across different time points on HepG2 and MCF-7 cells; it was shown that E2 has upregulated the Ngb mRNA transcripts, with a significant increase peaking at 4 hours of E2 treatment, then decreasing and after that till 24 hours. In another study, 10 nM E2 stimulation across different time points in the DLD-1 cells showed that there was no significant effect on the Ngb mRNA transcript (Fiocchetti et al., 2015). In addition to measuring mRNA expression levels, studies show the effect of the transcription inhibitor actinomycin D (Act) on the E2-dependent Ngb upregulation. It was shown that E2-dependent Ngb upregulation was inhibited as a result of Act (Fiocchetti et al., 2014), which would confirm that Ngb upregulation is transcriptionally modulated. Intriguingly, Act did not inhibit the E2-dependent Ngb upregulation, but rather reduced the upregulation signicantly.

In order to assess the effect of RES on the upregulation of Ngb protein levels, western blots were undertaken for SH-SY5Y cells. The detection of Ngb protein levels after E2 stimulation via western blots, were used as a positive control. Ngb mRNA levels were detected via quantitative real-time PCR after E2 stimulation; Ngb mRNA levels in SH-SY5Y cells were first detected in hypoxic and OGD conditions as a positive control to validate the PCR technique. To assess subcellular localization of Ngb, a fusion protein of Ngb and GFP (Green Fluorescent Protein) was created using Gibson Assembly between a GFP-containing plasmid (mEmerald mito-7) and Ngb-containing plasmid (pCMV3-GFPSpark-Ngb).

3.2 Materials and Methods

3.2.1 Materials

PVDF (Polyvinylidene fluoride) 0.45 µm membrane (Catalogue# 1620112), Microseal 'B' Adhesive Seals (Catalogue# MSB1001), Multiplate Low Profile 96-Well Unskirted PCR Plates (Catalogue# MLL9601), iScript cDNA Synthesis Kit (Catalogue# 170-8891), SsoAdvanced Universal SYBR Green Supermix (Catalogue# 172-5270) and thick filter paper (Catalogue# 1703969) were obtained from Bio-rad (Mississauga, ON, Canada).

Charcoal-stripped fetal bovine Serum (Catalogue# 080-750) was obtained from Wisent, Inc. (Saint-Jean-Baptiste, QC, Canada).

Supplement-free Dulbecco's Modified Eagle Medium powdered media (Catalogue# 5030), Dulbecco's Modified Eagle Phenol Red-Free Medium (Catalogue# D1145), Dulbecco's Modified Eagle Medium (Catalogue# D6429), L-glutamine, sodium pyruvate (Catalogue# D7777, nonessential amino acids, fetal bovine serum (Catalogue# F6178), penicillin/streptomycin solution and 0.25% trypsin/EDTA solution were obtained from Sigma-Aldrich (St. Louis, MO, USA).

10 cm cell culture plates, 6 cm cell culture plates and cell scrapers were obtained from Sarstedt, Inc. (Newton, SC, USA).

mEmerald-Mito-7 was a gift from Michael Davidson (Addgene plasmid # 54160).

pCMV3-GFPSpark-NGB (Catalogue# HG15110-ANG) was obtained from Sino Biological Inc. (North Wales, PA, USA).

Anti-Ngb mouse monoclonal primary antibody (13C8) (Catalogue# ab37258) and Purified Recombinant Human Neuroglobin (Catalogue# ab63278) were obtained from Abcam (Cambridge, UK). was obtained from Abcam (Cambridge, UK).

Anti-Ngb mouse monoclonal primary antibody (Catalogue# AA 1-152) was obtained from Merck (Boston, MA, USA).

Turbo DNA-free Kit (Catalogue# AM1907) was obtained from Thermo Fisher (Burlington, ON, Canada).

Monarch Plasmid Miniprep Kit (Catalogue# T1010S), Gibson Assembly Master Mix (Catalogue# E2611S) and Monarch DNA Gel Extraction Kit (T1020S) was obtained from New England Biolabs Inc.(Whitby, ON, Canada)

Total RNA Purification Kit (Catalogue# 37500) was obtained from Norgen Biotek (Thorold, ON, Canada).

Unless otherwise indicated, all other chemicals, reagents and solutions were purchased from Sigma-Aldrich (St. Louis, MO, USA), BioShop (Burlington, ON, Canada) or Fisher Scientific (Mississauga, ON, Canada).

3.2.2 Methods

3.2.2.1 Cell Culture

MCF-7 breast cancer cells and DLD-1 colorectal cancer cells (obtained from ATCC, Manassas, VA, USA) were grown in Dulbecco's Modified Eagle Phenol Red-Free Medium (DMEM), supplemented with 2 mM L-glutamine, 10% charcoal-stripped FBS, 2X MEM nonessential amino acids, penicillin (50 I.U./mL)/streptomycin (50 µg/mL) and 4500 mg/L glucose.

SH-SY5Y neuroblastoma cells (obtained from ATCC, Manassas, VA, USA) were grown in Dulbecco's Modified Eagle Medium (DMEM), supplemented with 10% FBS, 2X MEM nonessential amino acids, penicillin (50 I.U./mL)/streptomycin (50 µg/mL), 4500 mg/L glucose,

4 mM L-glutamine and 1 mM sodium pyruvate for the hypoxia experiment, and were grown in DMEM without glucose or serum.

The cells were cultured in a 37℃ humidified 5% CO2 atmosphere in a Forma Series II water-jacketed CO2 incubator. Cells were grown until 80% confluency, before being split for subculturing. Growth medium was removed, followed by Dulbecco PBS rinsing and addition of 0.25% Trypsin/EDTA solution. Cells were trypsinized for approximately 3 minutes within the incubator. After trypsinization, media-containing FBS was added to neutralize trypsin activity. The mixture was then placed into conical tubes, and centrifuged for 5 minutes at 240 g; the supernatant was discarded and the pellet was resuspended in fresh growth medium and cells were replated.

For the hypoxia and OGD experiments, the cells were grown in a humidified hypoxia chamber, with all media used in these experiments pre-equilibrated in the hypoxia chamber before usage.

All solutions and media were pre-warmed to 37℃ in an Isotemp 110 water bath (obtained from Fisher Scientific, Mississauga, ON, Canada) and cell culture work was implemented within a Class II Type A2 biological safety cabinet (obtained from Esco Inc., Hatboro, PA, USA).

3.2.2.2 Lysate Preparation

Cells were harvested using ice-cold RIPA lysis buffer (150 mM NaCl, 1% Triton-X 100, 0.5% sodium deoxycholate, 0.1% SDS and 50 mM Tris pH 8) and kept on ice for 30 minutes. The resulting lysate was centrifuged for 10 minutes at 4℃ and 10,000 g. The supernatant was then collected where Bradford assay was used to quantify total protein concentration; all lysates were stored at -80℃.

3.2.2.3 Western Blot

20 µg of total protein from lysates were added to loading buffer (containing 10%/200 mM DTT) in a ratio of 1:1, then boiled at 100℃ for 5 minutes. The samples were then electrophoresed using SDS-PAGE (sodium dodecyl sulphate-polyacrylamide gel electrophoresis) in a Bio-rad Mini-PROTEAN Tetra Cell apparatus for around 2 hours at 100V; 15% resolving gel and 5% stacking gel were used. Proteins from the gel were transferred onto PVDF 0.45 µm membrane within a Bio-Rad Trans-Blot semi-dry transfer apparatus for 2 hours and 30 minutes at 25V. The membranes were blocked with 5% milk/PBS solution at room temperature for 1 hour.

For antibody incubation, membranes were incubated with anti-Ngb (1:1000) overnight on a rotisserie at 4℃ then washed with PBS-T 3 times (with each wash lasting 5 minutes), then incubated with secondary anti-mouse antibody (1:2500) for 1 hour at room temperature. For loading and transfer controls, membranes were incubated with anti-Actin (1:1000) overnight on a rotisserie at 4℃ then washed with PBS-T 3 times (with each wash lasting 5 minutes), then incubated with secondary unconjugated anti-rabbit antibody (1:2500) for 1 hour at room temperature. Membranes after secondary incubation were visualized via Odyssey infrared imaging system (LI-COR Biosciences).

3.2.2.4 RNA Extraction and Quantitative RT-PCR

Cells were washed with ice-cold PBS and RNA was extracted using the Total RNA Purification Kit according the manufacturer's instructions. 1 µg RNA underwent reverse transcription to form cDNA via iScript cDNA Synthesis Kit in a thermocycler (25℃ for 5 minutes, then 42℃ for 30 minutes, then 85℃ for 5 minutes and lastly 4℃ on hold). Real-Time

PCR was performed using CFX96 Touch Real-Time PCR Detection System (obtained from Bio-Rad), with the Ngb forward primer sequence being: AAGGGCGGTTCTCTGGGAGCTT and the Ngb reverse primer sequence being: AGAGGATGTGCAGGGCCAGCTT. Each PCR was performed in triplicates, including the non-template control (NTC). The VEGF gene was used as a positive control gene for the hypoxia experiments. The housekeeping genes used were GAPD and PPIA for hypoxia, and GAPD only for OGD as PPIA levels changed in the OGD experiments. The relative level for NGB gene (shown in arbitrary units), was calculated using the 2-ΔΔCt method.

3.2.2.5 Ngb-EGFP Fusion Protein Construction

Ngb sequence from the pCMV3-GFPSpark-Ngb plasmid was amplified via PCR, using the Ngb forward primer sequence: ATGGAGCGCCCGGAGC and the Ngb reverse primer sequence: TTACTCGCCATCCCAGCCTC (see image in Appendix). The mEmerald mito-7 plasmid underwent two different restriction cut reactions to form two different plasmid constructs. The NheI and BamHI restriction enzymes were used to remove the mitochondrial targeting sequence from the plasmid, while NheI and NotI restriction enzymes were used to remove both the mitochondrial targeting sequence and the EGFP (see images in Appendix). The plasmid backbone from the cutting reactions of the mEmerald mito-7 plasmid and the Ngb sequence from the pCMV3-GFPSpark-Ngb plasmid, were extracted from their gels using the Monarch DNA Gel Extraction Kit. The Ngb sequence and the mEmerald plasmid backbone were ligated using the Gibson Assembly to form a plasmid containing either Ngb alone, EGFP alone or both Ngb and GFP sequences; the Ngb forward primer sequence was: GTTTAGTGAACCGTCAGATCCGCTAGCATGGAGCGCCCGGAGC, the Ngb reverse primer sequence was:

CACCATGGTGGCGACCGGTGGATCCCTCGCCATCCCAGCCTCGA, the Ngb alone reverse primer sequence was: GGCTGATATGATCTAGAGTCGCGGCCGCTTACTCGCCATCCCAGCCTC, the EGFP forward sequence was: GTTTAGTGAACCGTCAGATCCGCTAGCATGGTGAGCAAGGGCGAG and the EGFP reverse primer sequence was: GGCTGATATGATCTAGAGTCGCGGCCGCTTACTTGTACAGCTCGTCCATGC. The seams at which the ligation of the inserts occurred were sequenced at the SickKids Lab (Toronto, ON, Canada) to validate the success of the assembly (see sequencing results in the Appendix).

3.2.2.6 Transient Transfection of SH-SY5Y with the newly constructed Plasmid Variants

SH-SY5Y cells were transiently transfected with the variants Ngb alone, EGFP alone or the Ngb-EGFP fusion plasmid constructs using Lipofectamine 2000 reagent, where the reagent and plasmid DNA were diluted in serum-free and antibiotic-free DMEM. The two solutions are then added to one another to form the lipid complexes and then added to the culture dishes after 5 minutes of incubation; the ratios (µg:µL) of plasmid DNA to Lipofectamine 2000 were 1:3. After 24 hours, the media is replaced with normal growth media, and then the cells were used for live imaging and western blots.

3.2.2.7 Confocal Microscopy

Live imaging of SH-SY5Y cells was undertaken using the Carl Zeiss Axio Observer.Z1 inverted light/epifluorescence microscope equipped with ApoTome.2 optical sectioning and a Hamamatsu ORCA-Flash4.0 V2 digital camera. Cells were grown in phenol-red free medium and were viewed via a Plan-Apochromat 63x/1.40 Oil DIC M27 microscope objective. The

microscope stage and objective lens were warmed to 37℃ via TempModule S-controlled stage heater and objective heater (obtained from PeCon, Erbach, Germany); CO2 environment was maintained at 5% using a culture incubator. For green fluorescence detection, the fluorescence channel possesses excitation and emission wavelength filter sets 450-490 nm and 500-550 nm respectively, and set excitation and emission wavelengths of 488 nm and 509 nm respectively (Zeiss Item# 411003-0004-000). Z-stack series were made up of 30-40 slices, and were captured as single 2D images using the extended depth of focus tool using Zeiss Zen 2 (blue edition) software (see images in the Appendix).

3.3 Results

3.3.1 Ngb is not detectable in SHSY5Y cells under basal conditions or after E2 or RES stimulation

SH-SY5Y cells were treated with 10 nM E2 for 24 hours and then Ngb was probed using the Abcam antibody; no Ngb bands were seen (Figure 3.1). However, purified recombinant Ngb was detectable under the same conditions (Figure 3.2), indicating that the Abcam antibody can detect Ngb. The western blot procedure was repeated using the same Abcam antibody while adjusting conditions. This time semi-dry transfer was performed (see images in Appendix) with or without an alternative transfer buffer (Bjerrum Schaefer-Nielson Buffer: 48 mM Tris, 39 mM

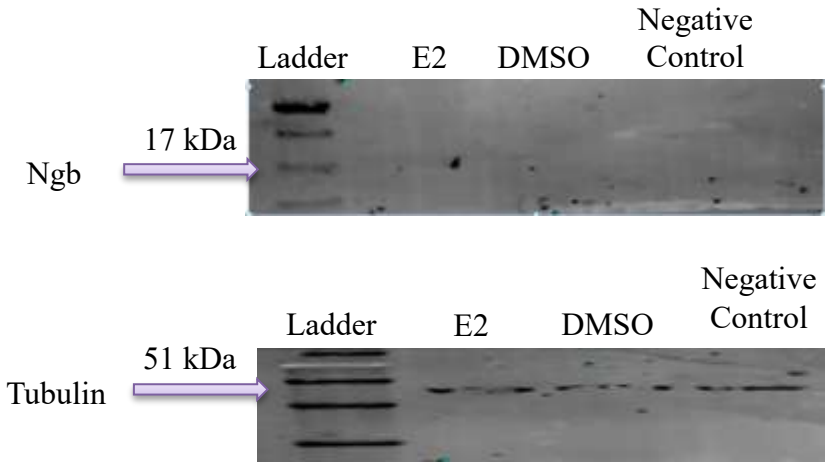

Figure 3.1 Western Blot Visualization of Ngb

The images of the membranes show the attempted detection of Ngb after treatment with 10 nM E2, vehicle and negative controls for 24 hours. The top image shows Ngb detection and the bottom image shows tubulin loading control.

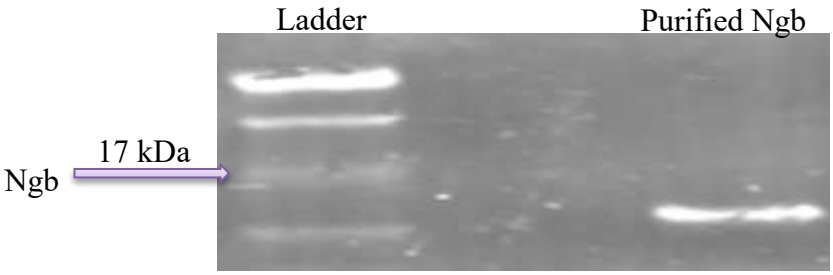

Figure 3.2 Western Blot Visualization of Purified Ngb

The images of the membrane show the detection of 2 µg of purified Ngb.

glycine, 20% methanol (pH 9.2); see images in Appendix). Nonetheless, no Ngb was detected in SH-SY5Y cells.

The SH-SY5Y cells were also treated with different concentrations of E2 for 24 hours and then Ngb was visualized, and still, the Ngb bands remained absent on the nitrocellulose membrane (Figure 3.3). The cells were then treated with 10 µM of E2 (Figure 3.4a) or RES (Figure 3.4b) for 24 hours and then Ngb was visualized; there were no Ngb bands.

3.3.2 Ngb mRNA expression levels were variable and similar

The SH-SY5Y cells were treated in the hypoxia chamber for 32 hours, with normal growth medium in the hypoxia experiment and with a glucose- and serum-free medium in the OGD experiment for 32 hours. The cells were then harvested via ice-cold PBS and centrifuged for 10 minutes at 10000 g; the supernatant was discarded and the pellet was collected. The cells were then lysed using the lysis buffer provided by the kit before the RNA isolation procedure started. The results show that there was a significant 5 times increase in the mRNA transcript for the OGD experiment with respect to the control group (Figure 3.5); the Ngb mRNA transcript did not have a significant increase in the hypoxia experiment (Figure 3.5). The levels for VEGF mRNA transcripts were upregulated in the hypoxia experiment as expected (see figure in Appendix).

MCF-7 cells and DLD-1 cells were treated with 10 nM E2 for 24 hours, and then the cells were harvested and underwent quantitative RT-PCR. The results show that Ngb mRNA levels of MCF-7 (Figure 3.6a) and DLD-1 (3.6b) were quite variable, and inferences based on those results could not be made. The Cq values of the Non-reverse transcriptase (NRT) samples were similar to the actual samples, indicating genomic contamination; to eliminate genomic

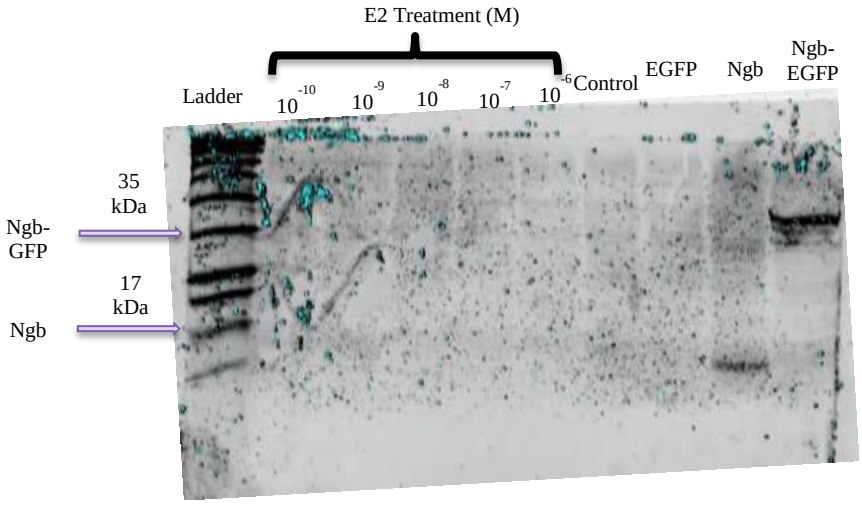

Figure 3.3 Western Blot Visualization of Ngb with Different E2 Concentrations and Plasmid Variant Transfections

The image of the membrane shows the detection of Ngb after treatment of different E2 concentrations and negative control for 24 hours. The last three lanes show the attempted detection of Ngb bands after SH-SY5Y transient transfection; the Ngb bands appear in the last two lanes.

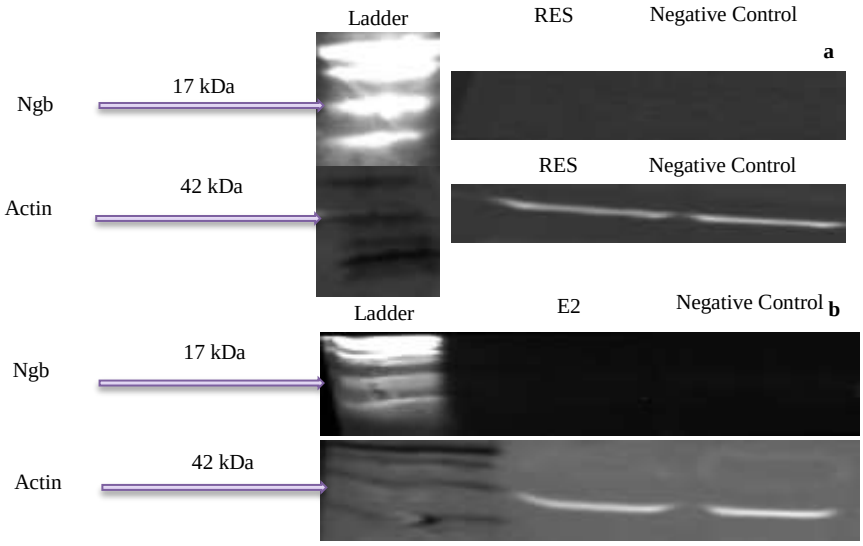

Figure 3.4 Western Blot Visualization of Ngb after Treatment with 10 µM E2 or RES for 24 hours

The top half images of the membranes show the detection of Ngb after treatment of a) E2 and b) RES. The bottom half images of a) and b) show the actin loading control.

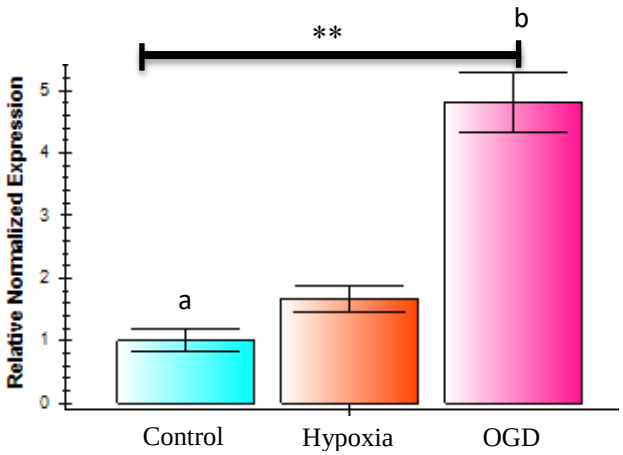

Figure 3.5 Ngb mRNA Transcript Levels in SH-SY5Y with OGD and Hypoxia

The hypoxia and OGD (b) PCR was used as a positive control for the success of the technique. The mRNA level is greatly upregulated in OGD with respect to the control (a), but is not significant in hypoxia. The housekeeping gene used here is GAPD.

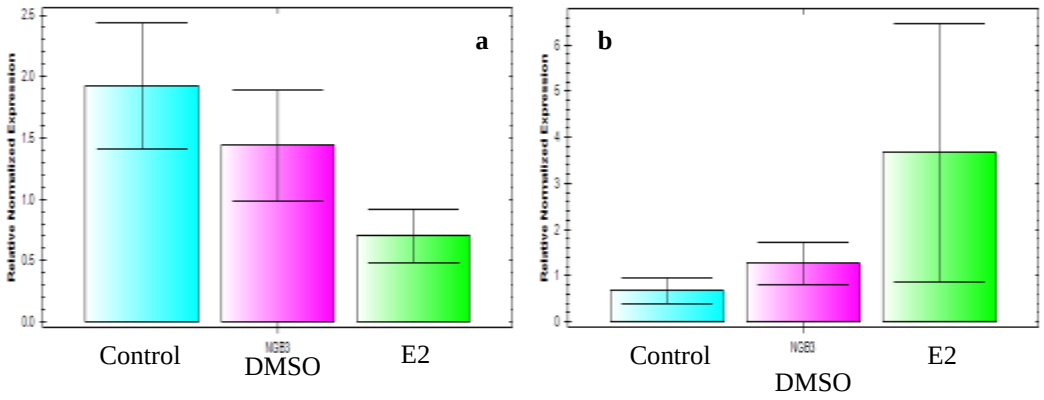

Figure 3.6 Ngb mRNA Transcript Levels in MCF-7 and DLD-1 cells after 10 nM E2 stimulation for 24 hours

The figure depicts the levels of Ngb mRNA transcripts after 24 hour stimulation with 10 nM E2. a) Shows the mRNA transcript expression level in MCF-7 and b) shows the mRNA transcript expression level in DLD-1. The housekeeping genes used here are GAPD and PPIA.

contamination, the Turbo DNA-free Kit was used. MCF-7 cells were treated with 10 nM E2 for 24 hours, then the RNA was extracted and subjected to DNAse treatment via the aforementioned kit; the RNA then underwent reverse transcription and PCR. The mRNA levels were still contaminated, indicated by the similarities between the NRTs and the actual samples (see figure

in Appendix). The MCF-7 cells were treated 10 nM E2 for 4 hours, as literature showed that mRNA transcript levels peak at 4 hours (Fiocchetti et al., 2014), and then the RNA was extracted. The total RNA was divided into groups, where one group was subjected to DNAse treatment, and the second group remained without DNAse treatment. The results showed that genomic contamination persisted in the samples (see figure in Appendix).

3.3.3 Ngb-EGFP fusion protein subcellular localization could not be determined

The SH-SY5Y cells were transfected with the three constructs (EGFP alone, Ngb alone and Ngb-EGFP fusion), were visualized with the confocal microscope using live imaging. As expected, the cells transfected with the Ngb alone plasmid construct did not show any green fluorescence. The cells transfected with the EGFP alone plasmid construct showed green fluorescence (Figure 2.3.7a) but the cells transfected with the Ngb-EGFP fusion plasmid construct did not show any green fluorescence (Figure 2.3.7b).

3.3.4 Transfection confirmation was successful via western blot

The transiently-transfected SH-SY5Y cells were harvested after live imaging and underwent western blots to confirm the success of the transfection. The results showed that the bands of Ngb in the transfected cells were present, but the Ngb bands in the non-transfected cells were absent (see images in Appendix).

3.4 Discussion

Protein levels of Ngb have been shown to be greatly upregulated by E2 in MCF-7 (Fiocchetti et al., 2014), HepG2 (Fiocchetti et al., 2014) and DLD-1 (Fiocchetti et al., 2015) across different concentrations and different time points. mRNA transcript levels have been shown to be greatly

by upregulated by E2 in the MCF-7 and HepG2 cells (Fiocchetti et al., 2014), but did not have a significant effect on DLD-1 cells (Fiocchetti et al., 2015). Literature also shows that E2 stimulates the translocation of Ngb into the mitochondrial compartment in the MCF-7 (Fiocchetti et al., 2014), HepG2 (Fiocchetti et al., 2014) and DLD-1 cells (Fiocchetti et al., 2015).

3.4.1 Ngb was not detectable in western blots after E2 or RES stimulation in SH-SY5Y

The results show that Ngb was not detectable in the western blots, whether in the negative control groups or in the experimental groups treated with E2 or RES; the Ngb bands detected were from the transfection experiments. The absence of Ngb bands could be due to low levels of Ngb in the SH-SY5Y cells, which is not possible as literature shows that SH-SY5Y cells express Ngb (Fordel et al., 2007; Fordel et al., 2007) and that E2 increase the levels of Ngb in neuroblastomas (De Marinis et al., 2013; Fiocchetti et al., 2013). An approach towards detection enhancement that could provide further insight is the horseradish peroxidase (HRP). The enzyme of plant origins catalyzes the conversion of certain chromogenic substrates to produce colour or light (depending on the substrate) which could be detected via spectrophotometry (Akkara et al., 1991; Veitch, 2004); this catalytic activity is stimulated via an oxidizing agent, such as H2O2. Antibodies conjugated to HRP have been shown to have the capability of locating proteins of interest and producing strong and detectable signals (Chau and Lu, 1995), which is due to the high turnover rate of HRP (Beyzavi et al., 1987). The implementation of western blots using antibody-HRP conjugation could provide insight as to the basal levels of Ngb in cells. Another approach is to use purified Ngb in a western blot by using different dilutions in a wide dilution range; the detection of Ngb across different dilutions could provide further insight into Ngb's levels and detectability.

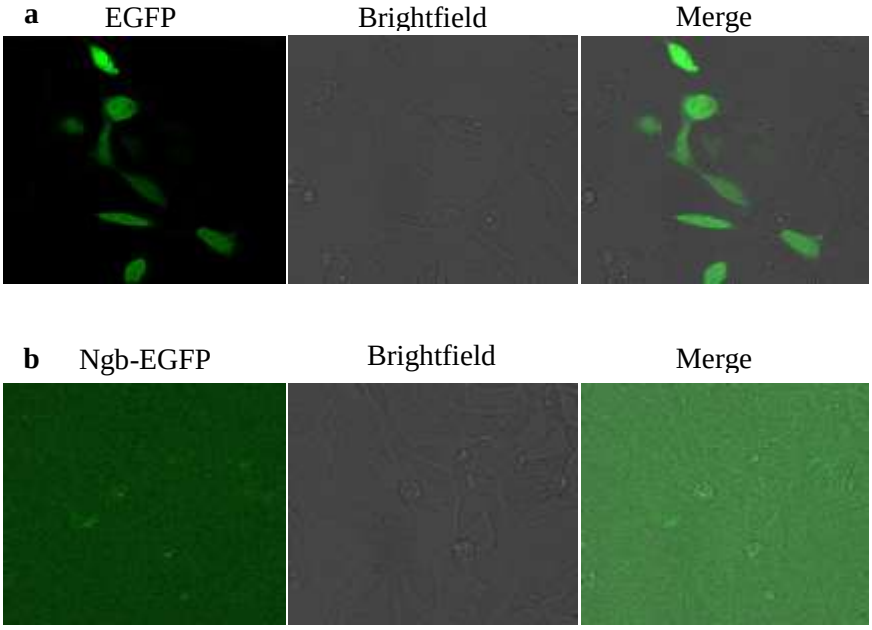

Figure 3.7 Confocal Microscope Live Images of EGFP Alone Protein and the Ngb-EGFP Fusion Protein

The images depict the images of SHY-SY5Y cells after the transfection of EGFP alone plasmid construct and the Ngb-EGFP fusion plasmid construct. a) Shows the fluorescence of the EGFP, with the brightfield channel being used to create contrast to view both transfected and non-transfected cells. These images were captured at 350 ms exposure time. b) Shows the fluorescence of the Ngb-EGFP fusion protein, with the brightfield channel being used to create contrast to view both transfected and non-transfected cells. These images were captured at 1500 ms exposure time.

3.4.2 Ngb mRNA transcript levels were variable in MCF-7 and DLD-1

10 nM E2 stimulation for 24 hours was shown to upregulate the Ngb mRNA expression levels in MCF-7 cells (Fiocchetti et al., 2014), but it did not have any effect on DLD-1 cells (Fiocchetti et al., 2015). The results show great variability in mRNA transcript levels, which is due to the presence of genomic contamination as indicated by the Cq levels in the NRT samples. The presence of significant genomic contamination could be an indication that the homogenization of the samples during RNA extraction was not efficient due to the viscosity of the lysate as a result

of DNA. Another explanation is that the Ngb mRNA transcript level is absent in the cells, which proves controversial as there are results that show Ngb expression in breast cancer cells (Fiocchetti et al., 2014; Fiocchetti et al., 2016) and there are results that state that mRNA transcripts are absent in breast cancer cells (Gorr et al., 2011). The variability in the mRNA transcript levels could be explained through the inhibition of PCR as a result of reverse transcription (RT); it has been shown that RT has a binding site on the Taq polymerase, which leads to the inhibition of the PCR and could lead to different expression levels amongst the different samples (Chumakov, 1994; Suslov and Steindler, 2005); heating RT before the start of PCR inacitivates RT (Chumakov 1994).

In addition to RT, but since the SYBR present in the PCR supermix solution is a dye that binds to double-stranded DNA in a sequence-independent manner, it could be more specific and sensitive if a fluorescently-labeled hybridization probe, which binds to DNA sequences in a specific manner, could be used (Deprez et al., 2002). Another factor that could have prevented results from being obtained could be the presence of DTT during the synthesis of cDNA (Deprez et al., 2002). Moreover, nucleic acid could adsorb to surfaces of tubes during extraction (Gassilloud et al., 2007; Gonzalez et al., 2007; Butot et al., 2007; Fox et al., 2007), which would hinder efficient RNA isolation; a detailed review of various PCR inhibitors (Schrader et al., 2012) provide an insight to the variability of PCR results, with Sur et al., 2010 showing an effective method of improving PCR efficiency.

3.4.3 Ngb-EGFP fusion protein does not fluoresce

Literature has shown that Ngb does re-allocate into the mitochondrial compartment via E2 stimulation (Fiocchetti et al., 2014; Fiocchetti et al., 2015). To assess the subcellular re-

allocation, EGFP was fused with Ngb to detect Ngb's translocation into the mitochondria under stress via confocal microscopy. However, even though the western blots confirm the success of the transfection, the confocal microscopy failed to detect fluorescence. The absence of fluorescence might be attributed to the misfolding of the Ngb-EGFP fusion protein. Another explanation to the absence of a detectable signal is the presence of a degron sequence on Ngb.

A degron is a part of the protein, which includes structural motif (Fortmann et al., 2015), amino acid sequence (Cho and Dreyfuss, 2010) and exposed arginine (Varshavsky, 1996) and lysine (Dohmen et al., 1994) residues, that regulates its degradation (Jariel-Encontre et al., 2008; Ravid and Hochstrasser, 2008; Erales and Coffino, 2014). Since Ngb undergoes proteasomal degradation, it could be speculated that the degron on Ngb is ubiquitin-dependent (Ravid and Hochstrasser, 2008), where it activates the polyubiquitination reaction for proteasomal degradation targeting (Coux et al., 1996; Lecker et al., 2006). In order to identify degrons, a three-step procedure must be undertaken (Ju and Xie, 2006; Schrader et al., 2009; Fortmann et al., 2015).

Firstly, the suspected degron sequence is fused to a stable protein (such as GFP) and then the concentrations of the altered protein and the unaltered protein over time is observed (Li et al., 1998). If the suspected degron is actually a degron, the altered protein will degrade faster than the unaltered protein (Ravid and Hochstrasser, 2008; Jariel-Encontre et al., 2008; Erales et al., 2014). To confirm the identity of the degron, a mutation of the protein containing the degron is formed, where the degron is removed; the mutated protein concentration should degrade slower than the unmutated protein (Ravid and Hochstrasser, 2008; Jariel-Encontre et al., 2008; Erales et al., 2014). The third step involves identifying whether the degron is ubiquitin-dependent (Ravid and Hochstrasser, 2008) or ubiquitin-independent (Jariel-Encontre et al., 2008; Erales et al.,

2014). The attachment will be measured to the protein with the degron present and the protein with the degron absent (Loetscher et al., 1991; Shrader et al., 2009; Fortmann et al., 2015); if the degron is ubiquitin-dependent, then polyubiquitination will be witnessed on the protein with the degron present (Ravid and Hochstrasser, 2008; Fortmann et al., 2015). Since the fusion protein created in this study had Ngb on the terminus, it could prove insightful if the EGFP is placed on the N-terminus to create EGFP-Ngb, as the degron on Ngb might be on the N-degron.

3.5 Conclusion

The constructed plasmids expressing Ngb and EGFP-Ngb proteins were detected via western blots, confirming the success of transfection. However, the latter protein did not fluoresce compared to the control EGFP plasmid. Multiple western blot attempts failed to detect endogenous Ngb in SH-SY5Y cells, and the qRT-PCR results were variable in MCF-7 and DLD-1 cells due to genomic contamination; the qRT-PCR experimentation for the hypoxia and OGD experiments on SH-SY5Y cells was successful, functioning as a positive control.

Chapter 4.0: The Effect of E2 and RES on Mitochondrial Networks under Physiological Stress with respect to Ngb Upregulation

4.1 Introduction

Mitochondrial biogenesis is the process of increasing the number of mitochondria as a result of different environmental and stressful stimuli, such as an increase in ATP usage (Valero 2014; Sanchis-Gomar et al., 2014). Mitochondrial biogenesis affects the number of mitochondria within cells, but other processes are required to modulate their morphology, distribution and function - mitochondrial fission and fusion (Bertholet et al., 2016; Mishra and Chan, 2016). The balance between mitochondrial fusion and fission is referred to as mitochondrial dynamics.

Mitochondrial fission involves the fragmentation of single mitochondrial structures, while mitochondrial fusion involves the merger of multiple mitochondrial structures into elongated or networked mitochondria (Chan 2006; Mishra and Chan, 2016). Different stimuli have been shown to affect the mitochondrial network, by affecting the balance between fusion and fission (Youle and Van Der Bliek, 2012; Bertholet et al., 2016), such as the need for transporting more mitochondria to energy-demanding areas (Bo et al., 2010; Youle and Van Der Bliek, 2012).

Mitochondrial fission is controlled by a cytosolic dynamin (Mishra and Chan, 2016; Bertholet et al., 2016) – Dynamin-related Protein (DRP), which surrounds the mitochondria then constricts, fragmenting both the inner and outer mitochondrial membranes (Figure 4.1b; Bo et al., 2010). Mitochondrial fusion on the other hand is controlled by membrane-anchored dynamin proteins: Mitofusin (Mfn) and Optic Atrophy (Opa) (Figure 4.1a). The former is responsible for

the fusion of the outer membrane, while the latter is responsible for the fusion of the inner membrane

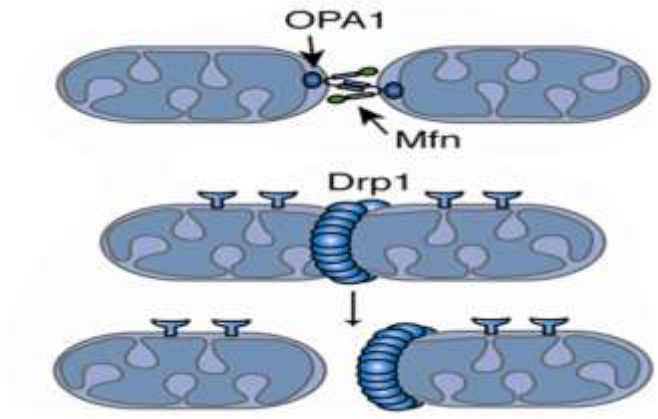

Figure 4.1 Mitochondrial fusion and fission

The figure depicts the GTPases that control fusion and fission and the process that they undertake. a) portrays OPA1 and Mfn and the process of mitochondrial fusion. b) portrays Drp1 and the process of mitochondrial fission.

(Ventura-Clapier et al., 2008; Youle and Van Der Bliek, 2012; Mishra and Chan, 2016). Cellular stress affects the balance between fusion and fission, and that balance is responsible for maintaining mitochondrial functionality.

Cellular stress threatens the cells by triggering apoptosis, and a defensive mechanism to prevent or delay apoptosis involves damaged mitochondria fusing together to undertake genetic complementation; complementation of the mitochondrial genome allows defective mitochondria to compensate for their lack of functionality. This procedure helps in the generation of functional mitochondria (Hales 2010). To provide the cell with resistance to stress, mitochondria tend to hyperfuse and form a highly connected network, in a process called stress-induced mitochondrial hyperfusion (SIMH). This form of fusion has been shown to promote ATP

production (Tondera et al., 2009). The increase in mitochondrial mass, ATP production, activation of Bax as well as a delay in cyt c release (Tondera et al., 2009) elucidate SIMH's anti-apoptotic role. Tondera et al., 2009 elucidated the role of SIMH in causing cyclin E buildup and regulating the progression of G1-S transition. Other studies have shown that SIMH compensates the reduction of ATP production in the G1-S transition (Stanton et al., 1991), protects the cells against apoptosis during that transition and aids in genetic complementation (Detmer and Chan, 2007). In addition to mitochondrial fusion, the translocation of Ngb into the mitochondria seems to have a putative anti-apoptotic role as well.

Yu et al., 2012 showed that Ngb translocates into the mitochondria during stress to exert a supposed anti-apoptotic role, the mechanism(s) of which has not been fully elucidated. However, the role of Ngb in promoting cell survival combined with its translocation into the mitochondria could have a connection. Khan et al., 2008 showed that Ngb helped maintain mitochondrial membrane potential and improved ATP production after hypoxia. Moreover, other studies have shown that the absence of Ngb in cells reduced the activities of Complex I and III of the mitochondria (Lechauve et al., 2012). Interestingly, even though Ngb translocates into the mitochondria, its precise localization Ngb within the mitochondrial compartment has only been speculated. Moreover, hyperfusion is an approach for stress resistance and fragmentation is a marker of apoptosis, and since Ngb translocates into the mitochondria to exert its anti-apoptotic, it could prove insightful to study the effects of Ngb on mitochondrial dynamics.

Ngb over-expression can inhibit mitochondrial aggregation that occurs during hypoxia (Khan et al., 2008); mitochondrial aggregation is a process that precedes the release of cyt c (Haga et al., 2003), which would eventually lead to apoptosis. Mitochondrial aggregation occurs due to mitochondrial transport (Haga et al., 2003), and short-term mitochondrial movement relies

on the actin cytoskeleton; Antao et al., 2010 has shown that actin condensation as a result of hydrogen peroxide has been abrogated by Ngb. Since Ngb overexpression inhibits mitochondrial aggregation, which precedes the release of cyt c, and since Ngb prevents the release of cyt c, it could be postulated that Ngb plays a role in mitochondrial dynamics regulation.

In order to test the effect of Ngb on mitochondrial dynamics, as well as the effect of E2 and RES on Ngb-mediated mitochondrial dynamic regulation, a plasmid containing Ngb sequence was co-transfected into SH-SY5Y cells stably expressing mEmerald mito-7. The Ngb EGFP fusion plasmid (mentioned in Chapter 3.0) was planned to be used in the assessment of mitochondrial dynamics, but since there the fluorescence was absent (see Figure 3.7 in Chapter 3.0), the experiments could not be undertaken. The cells were treated with E2 and/or RES and the mitochondrial networks were visualized using Carl Zeiss microscope. Mitochondrial fusion and fission were assessed using an ImageJ macro called Mitochondrial Network Analysis (MiNA) (Valente et al., 2017). MiNA skeletonizes (Figure 4.2) mitochondrial networks, and quantifies the different shapes of mitochondria that indicate fusion or fission (Figure 4.3).

4.2 Materials and Methods

4.2.1 Materials

3.5 cm cell culture plates and cell scrapers were obtained from Sarstedt, Inc. (Newton, SC, USA).

Supplement-free Dulbecco's Modified Eagle Medium powdered media (Catalogue# 5030), L-glutamine, sodium pyruvate (Catalogue# D7777), nonessential amino acids, penicillin/streptomycin solution and 0.25% trypsin/EDTA solution were obtained from Sigma-Aldrich (St. Louis, MO, USA).

Charcoal-stripped fetal bovine Serum (Catalogue# 080-750) was obtained from Wisent, Inc. (Saint-Jean-Baptiste, QC, Canada).

Nitrocellulose, 0.2 µm membrane (Catalogue# 1620112) and thick filter paper (Catalogue# 1703969) were obtained from Bio-rad (Mississauga, ON, Canada).

Anti-Ngb mouse monoclonal primary antibody (Catalogue# AA 1-152) was obtained from Merck (Boston, MA, USA).

Alexa Fluor 647 donkey anti-mouse (Catalogue# A31571) was obtained from Life Technologies (Grand Island, NY, USA).

mEmerald-Mito-7 was a gift from Michael Davidson (Addgene plasmid # 54160).

pCMV3-GFPSpark-NGB (Catalogue# HG15110-ANG) was obtained from Sino Biological Inc. (North Wales, PA, USA).

Monarch Plasmid Miniprep Kit (Catalogue# T1010S) and Monarch DNA Gel Extraction Kit (T1020S) were obtained from New England Biolabs Inc.(Whitby, ON, Canada).

Unless otherwise indicated, all other chemicals, reagents and solutions were purchased from Sigma-Aldrich (St. Louis, MO, USA), BioShop (Burlington, ON, Canada) or Fisher Scientific (Mississauga, ON, Canada).

4.2.2 Methods

4.2.2.1 Cell Culture

SH-SY5Y neuroblastoma cells (obtained from ATCC, Manassas, VA, USA) were grown in Dulbecco's Modified Eagle Medium (DMEM), supplemented with 10% charcoal-stripped

FBS, 2X MEM nonessential amino acids, penicillin (50 I.U./mL)/streptomycin (50 µg/mL), 4500 mg/L glucose, 4 mM L-glutamine and 1 mM sodium pyruvate. The cells were cultured in a 37℃ humidified 5% CO2 atmosphere in a Forma Series II water-jacketed CO2 incubator. Cells were grown until 80% confluency, before being split for subculturing. Growth medium was removed, followed by Dulbecco PBS rinsing and addition of 0.25% Trypsin/EDTA solution. Cells were trypsinized for approximately 3 minutes within the incubator. After trypsinization, media-containing FBS was added to neutralize trypsin activity. The mixture was then placed into conical tubes, and centrifuged for 5 minutes at 240 g; the supernatant was discarded and the pellet was resuspended in fresh growth medium and cells were replated.

All solutions and media were pre-warmed to 37℃ in an Isotemp 110 water bath (obtained from Fisher Scientific, Mississauga, ON, Canada) and cell culture work was implemented within a Class II Type A2 biological safety cabinet (obtained from Esco Inc., Hatboro, PA, USA).

4.2.2.2 Stable Transfection of SH-SY5Y with mEmerald mito-7 Plasmid

The mEmerald mito-7 plasmid encoding for emerald green fluorescent protein (EGFP) contains an N-terminal mitochondrial targeting sequence, obtained from subunit VIII of human Complex IV (Planchon et al., 2011). It was a gift from Michael Davidson (Planchon et al., 2011). Bacteria containing the plasmid were inoculated onto agar plates containing 100 mg/mL kanamycin and were incubated overnight at 37℃. Single colonies from these plates were inoculated into LB medium containing kanamycin and incubated overnight at 37℃ in a C25KC shaker incubator (New Brunswick Scientific, Edison, NJ, USA). Plasmids were isolated from

bacterial cultures using the DNA Miniprep Kit (obtained from Norgen Biotek, Thorold, ON, Canada).

SH-SY5Y cells were stable-transfected with mEmerald mito-7 plasmid using Lipofectamine 2000 reagent, where the reagent and plasmid DNA were diluted in serum-free and antibiotic-free DMEM. The two solutions are then added to one another to form the lipid complexes and then added to the culture dishes after 5 minutes of incubation; the ratios (µg:µL) of plasmid DNA to Lipofectamine 2000 were 0.5:0.5, 1:1, 1:1.5, 1.5:1.5 and 1:3. After 24 hours, the media is replaced with the selection DMEM with 10% FBS, 2X nonessential amino acids and G418 (400 µg/mL); the selection medium was changed every other day. After 10 days, the G418 concentration was lowered to 100 µg/mL and used as a maintenance dose. The ratio used for co-transfection experiments and live imaging involved the 1:3 ratio.

4.2.2.3 Confocal Microscopy

Live imaging of SH-SY5Y cells was undertaken using the Carl Zeiss Axio Observer.Z1 inverted light/epifluorescence microscope equipped with ApoTome.2 optical sectioning and a Hamamatsu ORCA-Flash4.0 V2 digital camera. Cells were grown in phenol-red free medium and were viewed via a Plan-Apochromat 63x/1.40 Oil DIC M27 microscope objective. The microscope stage and objective lens were warmed to 37℃ via TempModule S-controlled stage heater and objective heater (obtained from PeCon, Erbach, Germany); CO2 environment was maintained at 5% using a culture incubator. For green fluorescence detection, the fluorescence channel possesses excitation and emission wavelength filter sets 450-490 nm and 500-550 nm respectively, and set excitation and emission wavelengths of 488 nm and 509 nm respectively (Zeiss Item# 411003-0004-000). Z-stack series were made up of 30-40 slices, and were captured

as single 2D images using the extended depth of focus tool using Zeiss Zen 2 (blue edition) software.

4.2.2.4 Lysate Preparation

Cells were harvested using ice-cold "YY" lysis buffer (2X: 100 mM HEPES pH 7.5, 20% Glycerol, 300 mM NaCl, 2% Triton-X 100, 2 mM EDTA pH 8 and 2 mM EGTA pH 8 with 10% SDS added to create 1X lysis buffer and a final concentration of 0.75% SDS; protease inhibitor cocktail was also added to the 1X dilution) and kept on ice for 10 minutes. The resulting lysate was boiled at 100℃ for 5 minutes, then Bradford assay was used to quantify total protein concentration; all lysates were stored at -80℃.

4.2.2.5 Western Blots

35 µg of total protein from lysates were added to 4X loading buffer (containing 5% β-mercaptoethanol final concentration) in a ratio of 1:3, then boiled at 100℃ for 5 minutes. The samples were then electrophoresed using SDS-PAGE (sodium dodecyl sulphate-polyacrylamide gel electrophoresis) in a Bio-rad Mini-PROTEAN Tetra Cell apparatus for around 1 hour and 35 minutes at 125V; 13.5% resolving gel and 3% stacking gel were used. Proteins from the gel were transferred onto nitrocellulose 0.2 µm membrane within Owl VEP-2 Mini Tank Electroblotting System (obtained from Thermo Fisher, Burlington, ON, Canada) for 1 hour at 100V, with the apparatus being kept on ice. The membranes were blocked with 5% Bovine Serum Albumin (BSA)/TBS-T solution at room temperature for 1 hour.

For antibody incubation, membranes were incubated with anti-Ngb (1:1000) overnight on a rotisserie at 4℃ then washed with TBS-T 3 times (with each wash lasting 5 minutes), then incubated with secondary anti-mouse antibody (1:5000) for 1 hour at room temperature. For

loading and transfer controls, membranes were incubated with anti-Actin (1:1000) overnight on a rotisserie at 4℃ then washed with TBS-T 3 times (with each wash lasting 5 minutes), then incubated with secondary anti-rabbit antibody (1:5000) for 1 hour at room temperature. Membranes after secondary incubation were visualized via ChemiDoc Imaging System (obtained from Bio-Rad).

4.2.2.6 Statistical Analysis

The statistical analyses were carried out using Statistical Package for Social Sciences (SPSS) using one-way ANOVAs that contained more than two groups. Normal distribution of the data was determined via homoscedastic checks, kurtosis, skewness and mean similarities. If the ANOVA tests showed a statistical significance, the post hoc tests Games-Howell (for heteroscedastic data) and Bonferroni (for homoscedastic data) were carried out. Statistical significance was determined at p-value of < 0.05.

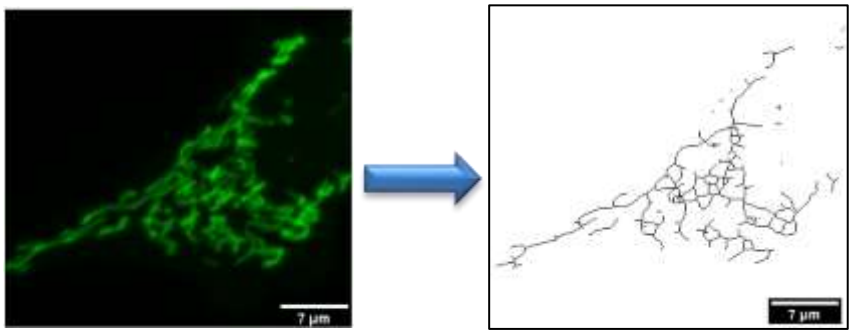

Figure 4.2 Skeletonizing Mitochondrial Network of Stable-Transfected SH-SY5Y

The image on the left shows an image from Carl Zeiss microscope, with the mitochondrial network coloured green. The image on the right depicts MiNA skeletonization for quantification.

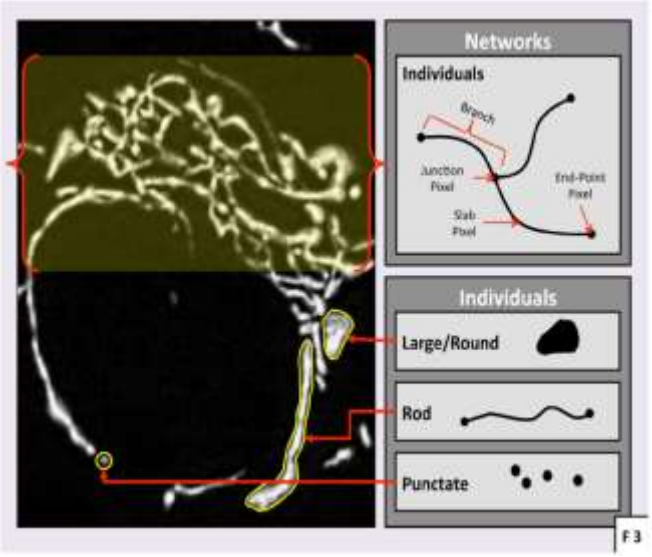

Figure 4.3 Quantification of Mitochondria based on Different Shapes

The image on the left depicts mitochondrial networks, with different mitochondrial shapes being highlighted in yellow. The diagrams on the right portray the different shapes that assess fusion or fission, with networks indicating fusion and individuals indicating fission. The image was obtained from Valente et al.. 2017.

4.3 Results

4.3.1 Mitochondrial morphology with RES and E2 pretreatment in the presence of hydrogen peroxide stress for non-transfected and Ngb-transfected SH-SY5Y cells

4.3.1.1 E2 pretreatment in Ngb-transfected SH-SY5Y cells decreased mitochondrial individual number but did not affect network number or mean network size

Both Ngb-transfected and non-transfected SH-SY5Y cells were treated with 10 µM E2 for 24 hours, then were treated with 300 µM H2O2 for 2 hours. The cells were then imaged and analyzed as mentioned above. For the individuals parameter, there was a significant increase in mitochondrial individuals of the H_2O_2 treatment in Ngb-transfected SH-SY5Y cells in

comparison with the non-transfected cells of the control group (p-value < 0.05) (Figure 4.4a) and the non-transfected cells treated with H_2O_2 (p-value < 0.01) (Figure 4.4b). In addition, the Ngb-transfected cells that have been pretreated with E2 then treated with H_2O_2 had a significant decrease in mitochondrial individual number with respect to the Ngb-transfected cells treated with H_2O_2 (p-value < 0.05) (Figure 4.4c).

For the network parameter, there were no significant differences in mitochondrial network numbers between the H_2O_2 treatment in Ngb-transfected SH-SY5Y cells, the non-transfected cells of the control group (Figure 4.5a) and the non-transfected cells treated with H_2O_2 (Figure 4.5b). Moreover, the Ngb-transfected cells that have been pretreated with E2 then treated with H_2O_2 did not show any significant differences in network number with the Ngb-transfected cells treated with H_2O_2 (Figure 4.5c).

As for the mean network size (Figure 4.6), there was no significant effect on the number of branches per network across all treatment groups with respect to both the Ngb-transfected and non-transfected cells.

4.3.1.2 RES pretreatment in Ngb-transfected SH-SY5Y cells decreased mitochondrial individual number but did not affect network number or mean network size

The Ngb-transfected and non-transfected SH-SY5Y cells were treated with 10 µM RES for 24 hours, then were treated with 300 µM H2O2 for 2 hours in the similar manner as the E2 pretreatment groups, before undergoing imaging and analysis. With regards to the individuals parameter, there was no significant difference between the H_2O_2 treatment in Ngb-transfected SH-SY5Y cells and the non-transfected cells of the control group (Figure 4.7a), but showed a significant increase with respect to and the non-transfected cells treated with H_2O_2 (p-value <

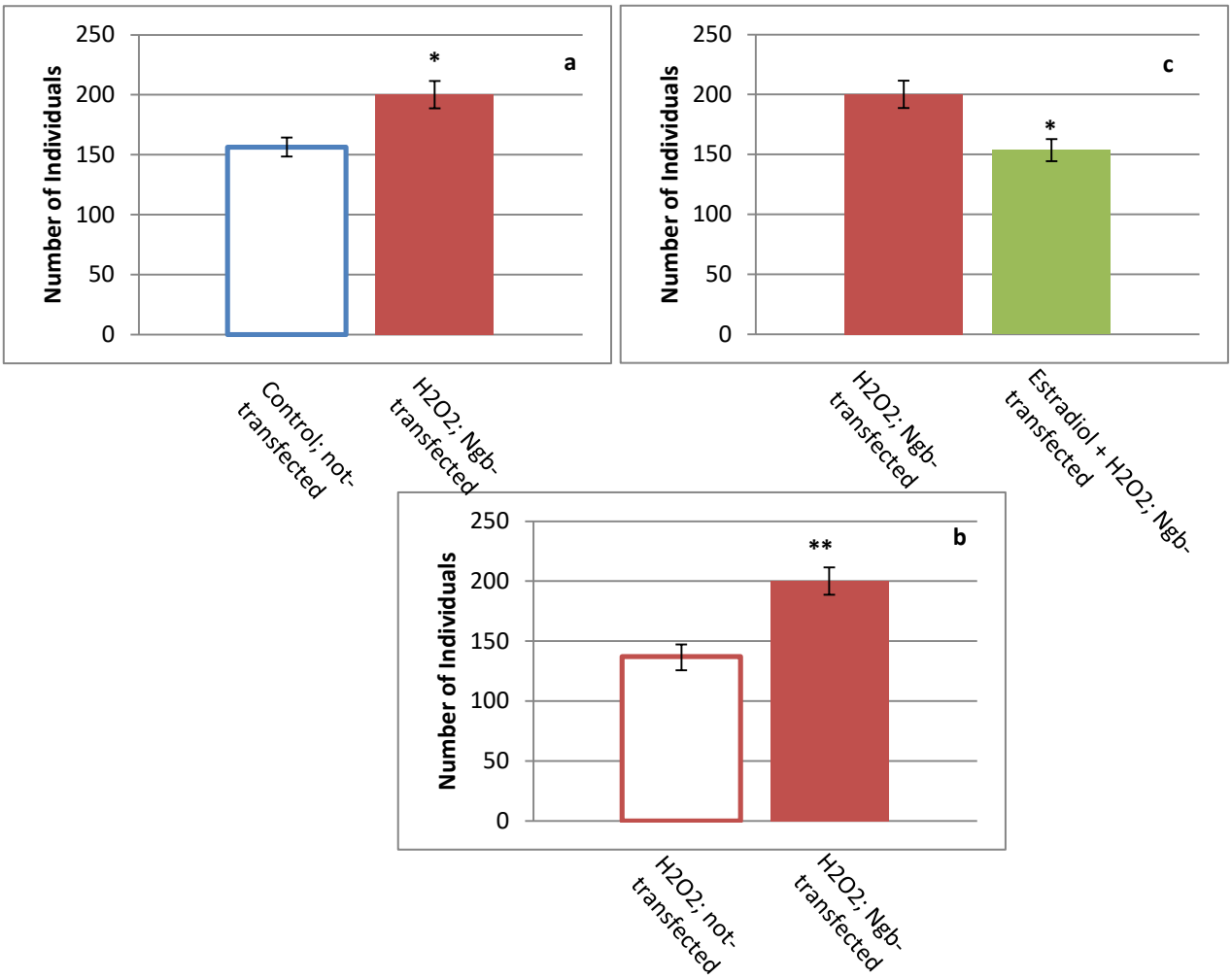

Figure 4.4 Quantification of Mitochondrial Individuals after Estradiol Pretreatment under Hydrogen Peroxide Stress

The figures portray the differences in the number of mitochondrial individuals. (a) shows the comparison between the non-transfected SH-SY5Y cells of the control group with the Ngb-transfected SH-SY5Y cells under H2O2 stress. (b) shows the comparison between the non-transfected SH-SY5Y cells under H2O2 stress with the Ngb-transfected SH-SY5Y cells under H2O2 stress. (c) shows the comparison between the Ngb-transfected SH-SY5Y cells under H2O2 stress and Ngb-transfected SH-SY5Y cells under H2O2 stress after estradiol pretreatment. Data is represented as mean ± SEM.

*: indicates p-value <0.05

**: indicates p-value <0.01

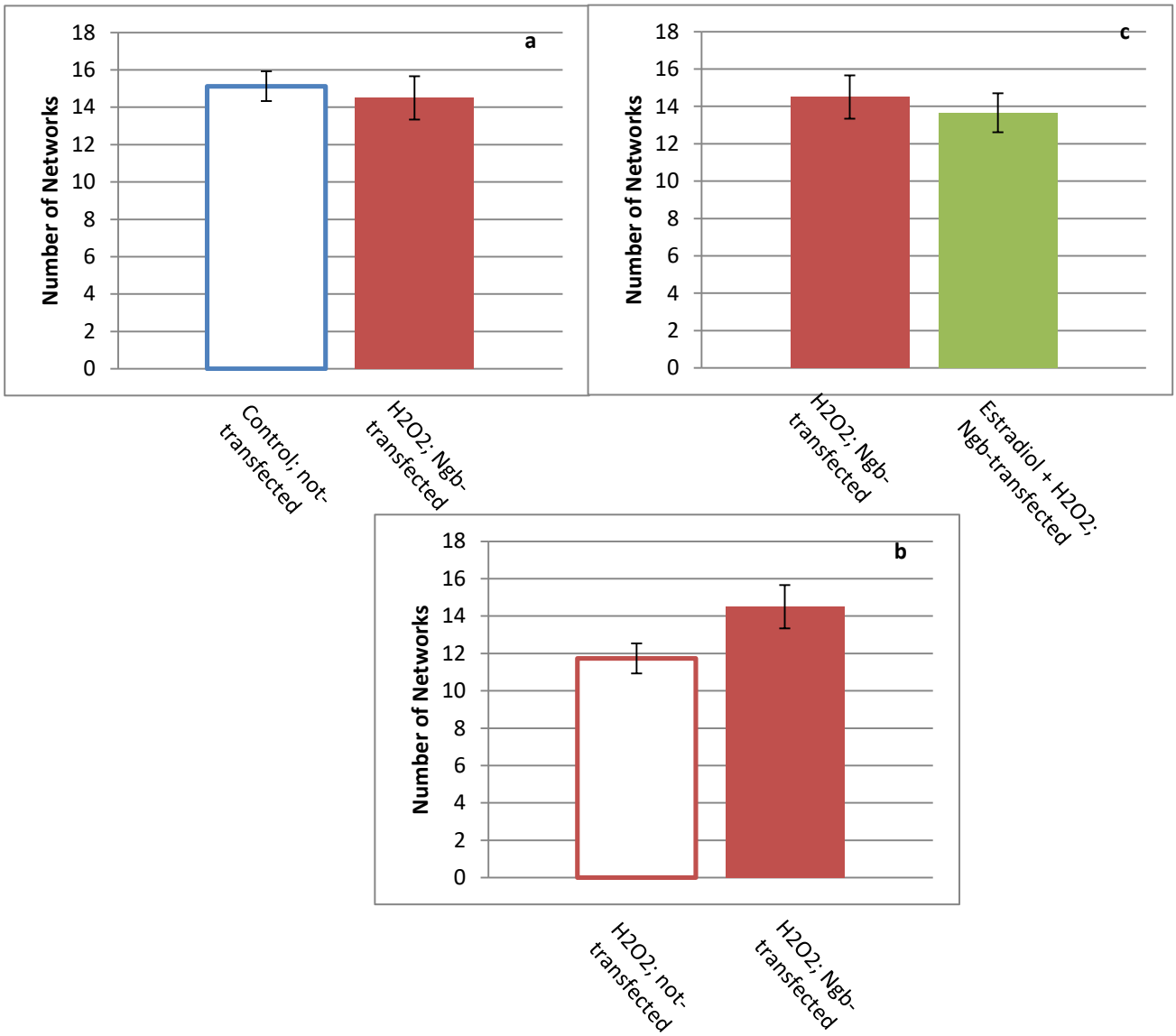

Figure 4.5 Quantification of Mitochondrial Networks after Estradiol Pretreatment under Hydrogen Peroxide Stress

The figures portray the differences in the number of mitochondrial networks. (a) shows the comparison between the non-transfected SH-SY5Y cells of the control group with the Ngb-transfected SH-SY5Y cells under H2O2 stress. (b) shows the comparison between the non-transfected SH-SY5Y cells under H2O2 stress with the Ngb-transfected SH-SY5Y cells under H2O2 stress. (c) shows the comparison between the Ngb-transfected SH-SY5Y cells under H2O2 stress and Ngb-transfected SH-SY5Y cells under H2O2 stress after estradiol pretreatment. Data is represented as mean ± SEM.

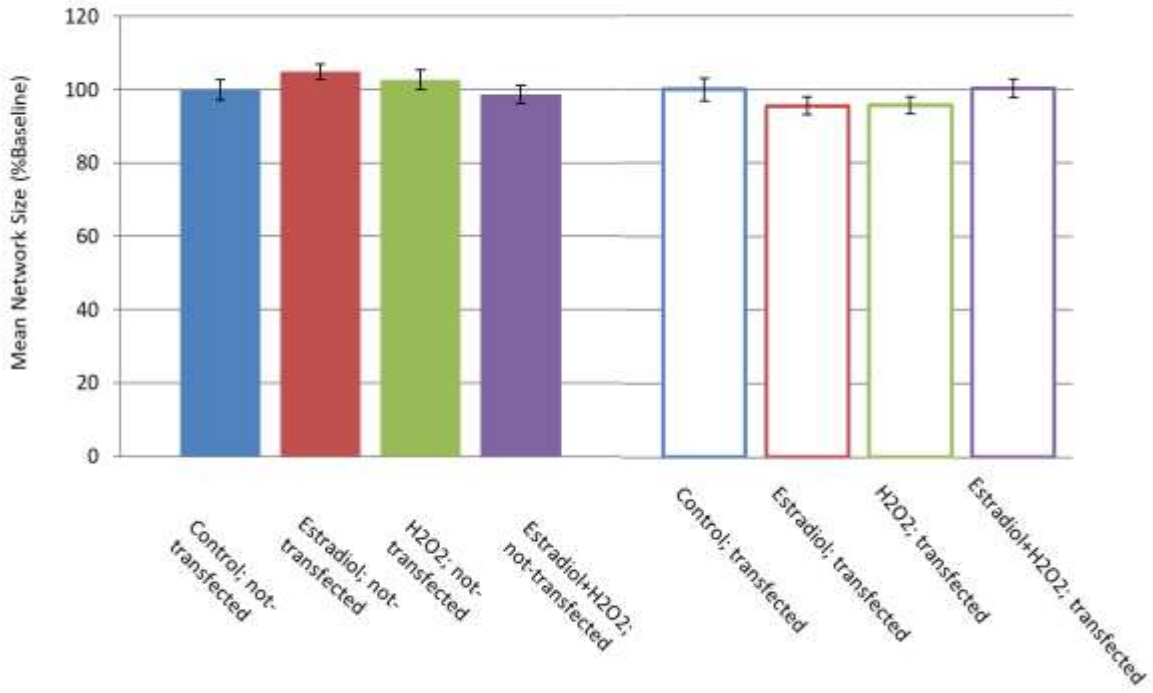

Figure 4.6 Quantification of Mitochondrial Mean Network Sizes after Estradiol Pretreatment under Hydrogen Peroxide Stress

The figure portrays the differences in the number of mitochondrial branches per network. The left side of the figure depicts the non-transfected SH-SY5Y cells under various conditions of treatments, while the right side of the figure depicts the Ngb-transfected SH-SY5Y cells under the same conditions of treatment. Data has been normalized to the controls of each form of transfection and is represented as mean ± SEM.

0.01) (Figure 4.7b). Furthermore, the Ngb-transfected cells that have been pretreated with RES then treated with H_2O_2 had a significant decrease in individuals in comparison to the non-transfected cells treated with H_2O_2 (p-value < 0.05) (Figure 4.7c).

With regards to the number of networks, there were no significant differences between the H_2O_2 treatment in Ngb-transfected SH-SY5Y cells, the non-transfected cells of the control group (Figure 4.8a) and the non-transfected cells treated with H_2O_2 (Figure 4.8b). In addition, the Ngb-transfected cells that have been pretreated with RES then treated with H_2O_2 did not show any

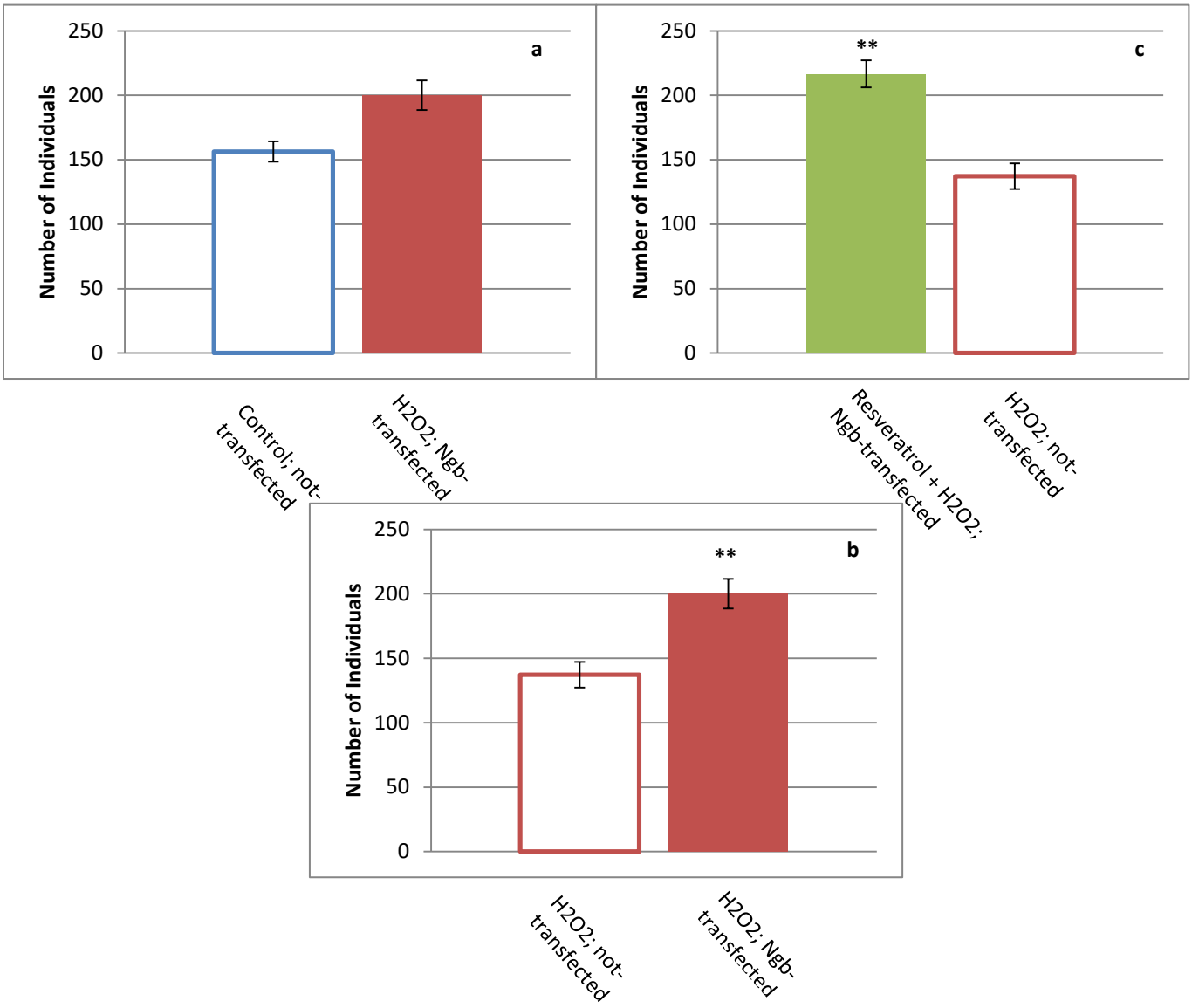

Figure 4.7 Quantification of Mitochondrial Individuals after Resveratrol Pretreatment under Hydrogen Peroxide Stress

The figures portray the differences in the number of mitochondrial individuals. (a) shows the comparison between the non-transfected SH-SY5Y cells of the control group with the Ngb-transfected SH-SY5Y cells under H2O2 stress. (b) shows the comparison between the non-transfected SH-SY5Y cells under H2O2 stress with the Ngb-transfected SH-SY5Y cells under H2O2 stress. (c) shows the comparison between the non-transfected SH-SY5Y cells under H2O2 stress and Ngb-transfected SH-SY5Y cells under H2O2 stress after resveratrol pretreatment. Data is represented as mean ± SEM.

**: indicates p-value <0.01

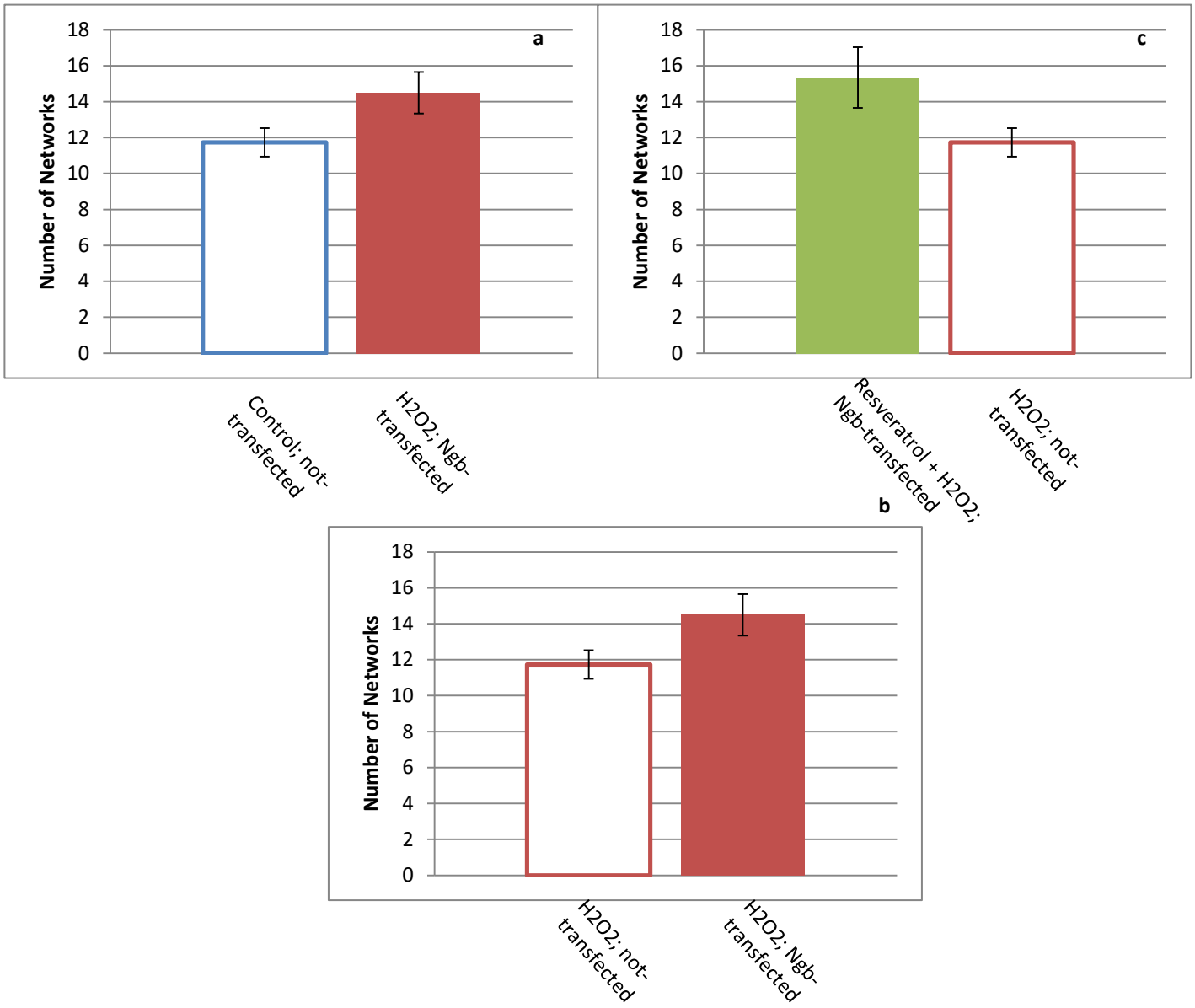

Figure 4.8 Quantification of Mitochondrial Networks after Resveratrol Pretreatment under Hydrogen Peroxide Stress

The figures portray the differences in the number of mitochondrial networks. (a) shows the comparison between the non-transfected SH-SY5Y cells of the control group with the Ngb-transfected SH-SY5Y cells under H2O2 stress. (b) shows the comparison between the non-transfected SH-SY5Y cells under H2O2 stress with the Ngb-transfected SH-SY5Y cells under H2O2 stress. (c) shows the comparison between the non-transfected SH-SY5Y cells under H2O2 stress and Ngb-transfected SH-SY5Y cells under H2O2 stress after resveratrol pretreatment. Data is represented as mean ± SEM.

significant differences in mitochondrial network number in comparison with the non-transfected cells treated with H_2O_2 (Figure 4.8c).

For the mean network size (Figure 4.9), there were no significant differences in branch number per network across all treatment groups with regards to both the Ngb-transfected and non-transfected cells.

4.3.2 Mitochondrial morphology with RES and E2 pretreatment in hypoxic conditions for non-transfected and Ngb-transfected SH-SY5Y cells

4.3.2.1 E2 pretreatment in Ngb-transfected SH-SY5Y cells increased mitochondrial individual number and mitochondrial network number but did not affect mean network size

The Ngb-transfected cells and the non-transfected cells were pretreated with 10 μM E2 for 24 hours then incubated in hypoxic conditions for 24 hours, before undergoing reoxygenation for 3 hours. After that, the cells were visualized using the Carl Zeiss microscope then the mitochondrial networks were quantified using the MiNA macro. With regards to the mitochondrial individual number, there was no significant difference in the individuals of hypoxia/reoxygenation-treated Ngb-transfected cells in comparison with the non-transfected cells of the control group (Figure 4.10a), but there was a significant increase in the individual number of the former with respect to the hypoxia/reoxygenation-treated non-transfected cells (p-value < 0.01) (Figure 4.10b). The E2-pretreated hypoxia/reoxygenation-treated Ngb-transfected cells showed a significant increase in individuals in comparison with hypoxia/reoxygenation-treated Ngb-transfected cells (Figure 4.10c).

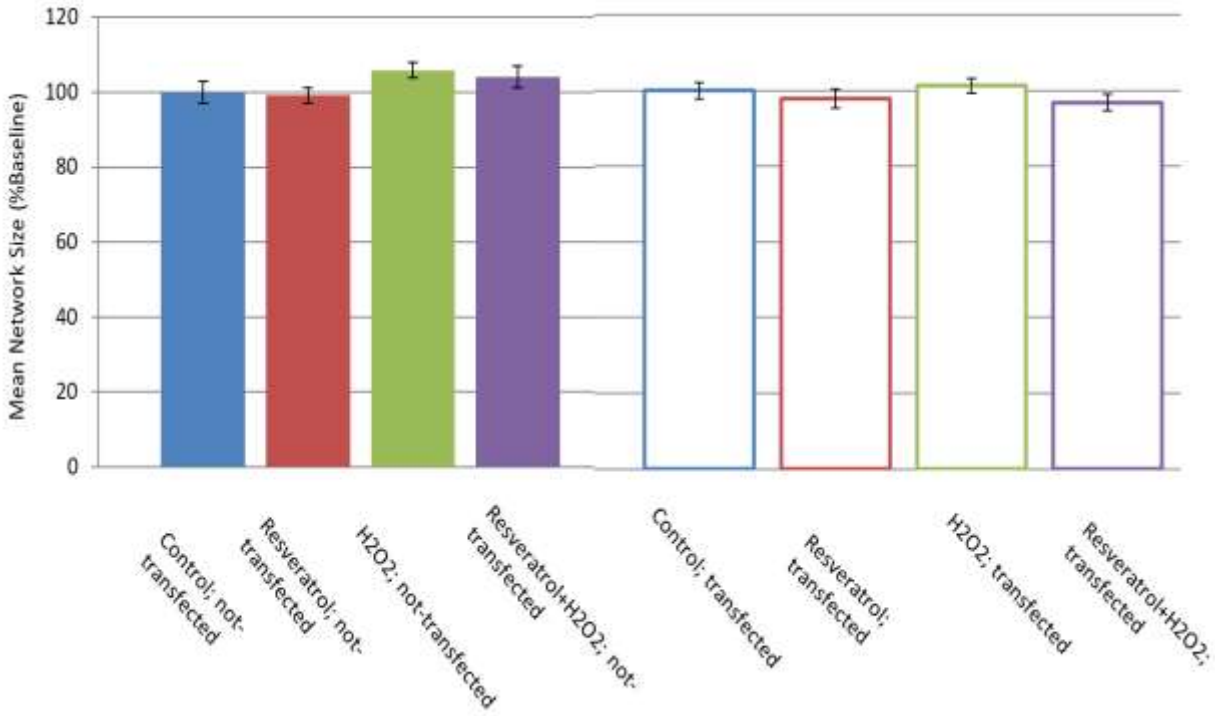

Figure 4.9 Quantification of Mitochondrial Mean Network Sizes after Resveratrol Pretreatment under Hydrogen Peroxide Stress

The figure portrays the differences in the number of mitochondrial branches per network. The left side of the figure depicts the non-transfected SH-SY5Y cells under various conditions of treatments, while the right side of the figure depicts the Ngb-transfected SH-SY5Y cells under the same conditions of treatment. Data has been normalized to the controls of each form of transfection and is represented as mean ± SEM.

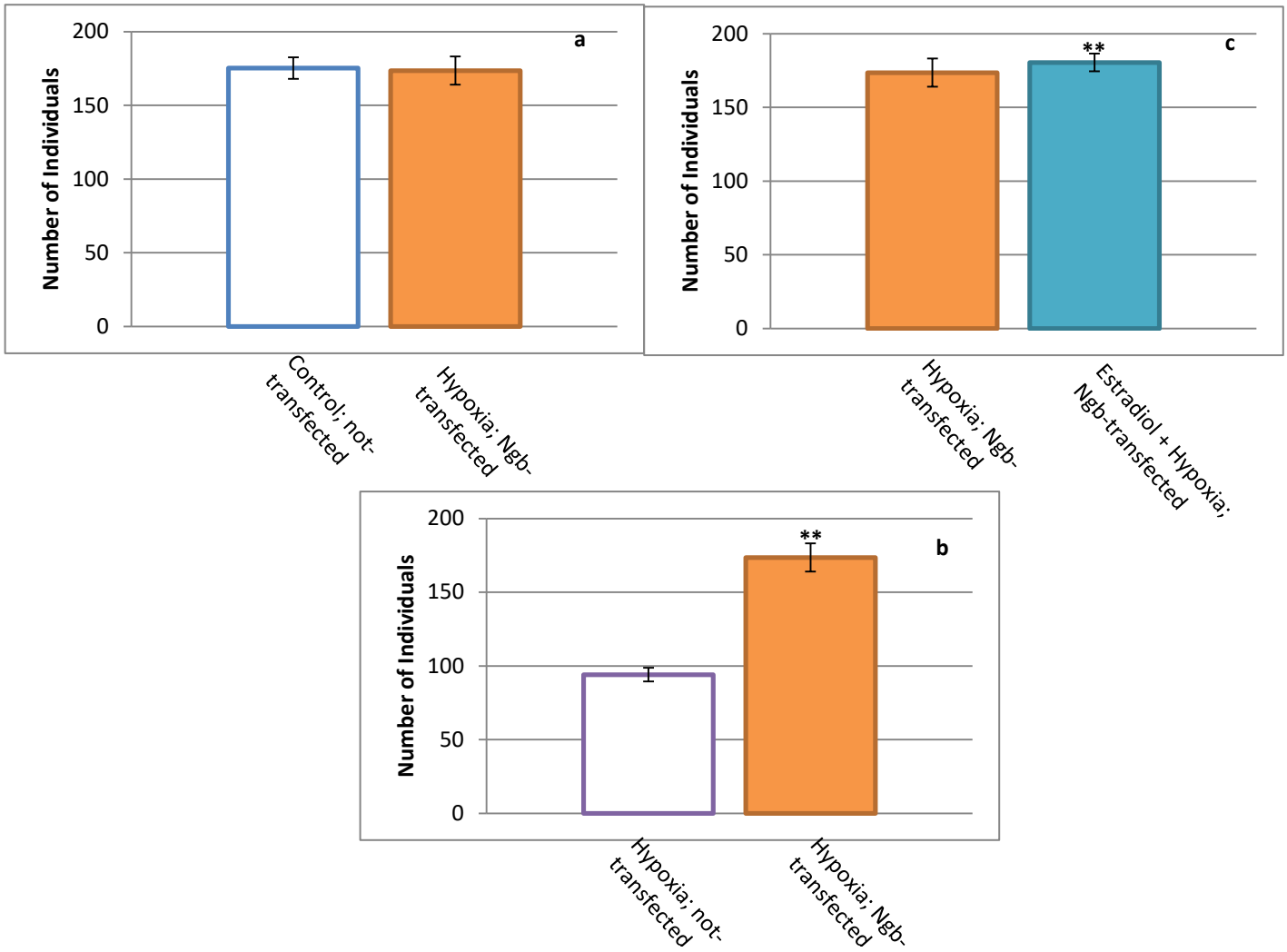

Figure 4.10 Quantification of Mitochondrial Individuals after Estradiol Pretreatment under Hypoxic Stress

The figures portray the differences in the number of mitochondrial individuals. (a) shows the comparison between the non-transfected SH-SY5Y cells of the control group with the Ngb-transfected SH-SY5Y cells under hypoxic stress. (b) shows the comparison between the non-transfected SH-SY5Y cells under hypoxic stress with the Ngb-transfected SH-SY5Y cells under hypoxic stress. (c) shows the comparison between the Ngb-transfected SH-SY5Y cells under hypoxic stress and Ngb-transfected SH-SY5Y cells under hypoxic stress after estradiol pretreatment. Data is represented as mean ± SEM.

**: indicates p-value <0.01

For the number of mitochondrial networks, there was no significant difference in networks between hypoxia/reoxygenation-treated Ngb-transfected cells and the non-transfected cells of the control group (Figure 4.11a), but a significant increase in networks was shown in the former with respect to hypoxia/reoxygenation-treated non-transfected cells (p-value < 0.01) (Figure 4.11b). Lastly, the E2-pretreated hypoxia/reoxygenation-treated Ngb-transfected cells showed a significant increase in network number in comparison with the hypoxia/reoxygenation-treated non-transfected cells (p-value < 0.01) (Figure 4.11c).

As for the mean network size (Figure 4.12), there was no significant effect on the number of branches per network under hypoxic conditions with respect Ngb-transfection and non-transfection.

4.3.2.2 RES pretreatment in Ngb-transfected SH-SY5Y cells decreased mitochondrial individual number, increased mitochondrial network number but did not affect mean network size

Both the Ngb-transfected cells and the non-transfected cells were pretreated with 10 μM RES for 24 hours before undergoing a 24-hour incubation period in hypoxic conditions for 24 hours; the cells were then reoxygenated for 3 hours before imaging and analysis. For the mitochondrial individual parameter, there was a significant increase in the individuals of hypoxia/reoxygenation-treated Ngb-transfected cells in comparison with the non-transfected cells of the control group (p-value < 0.01) (Figure 4.13a), but there was a significant decrease in the individual number of the former with respect to the hypoxia/reoxygenation-treated non-transfected cells (p-value < 0.01) (Figure 4.13b). The RES-pretreated hypoxia/reoxygenation-

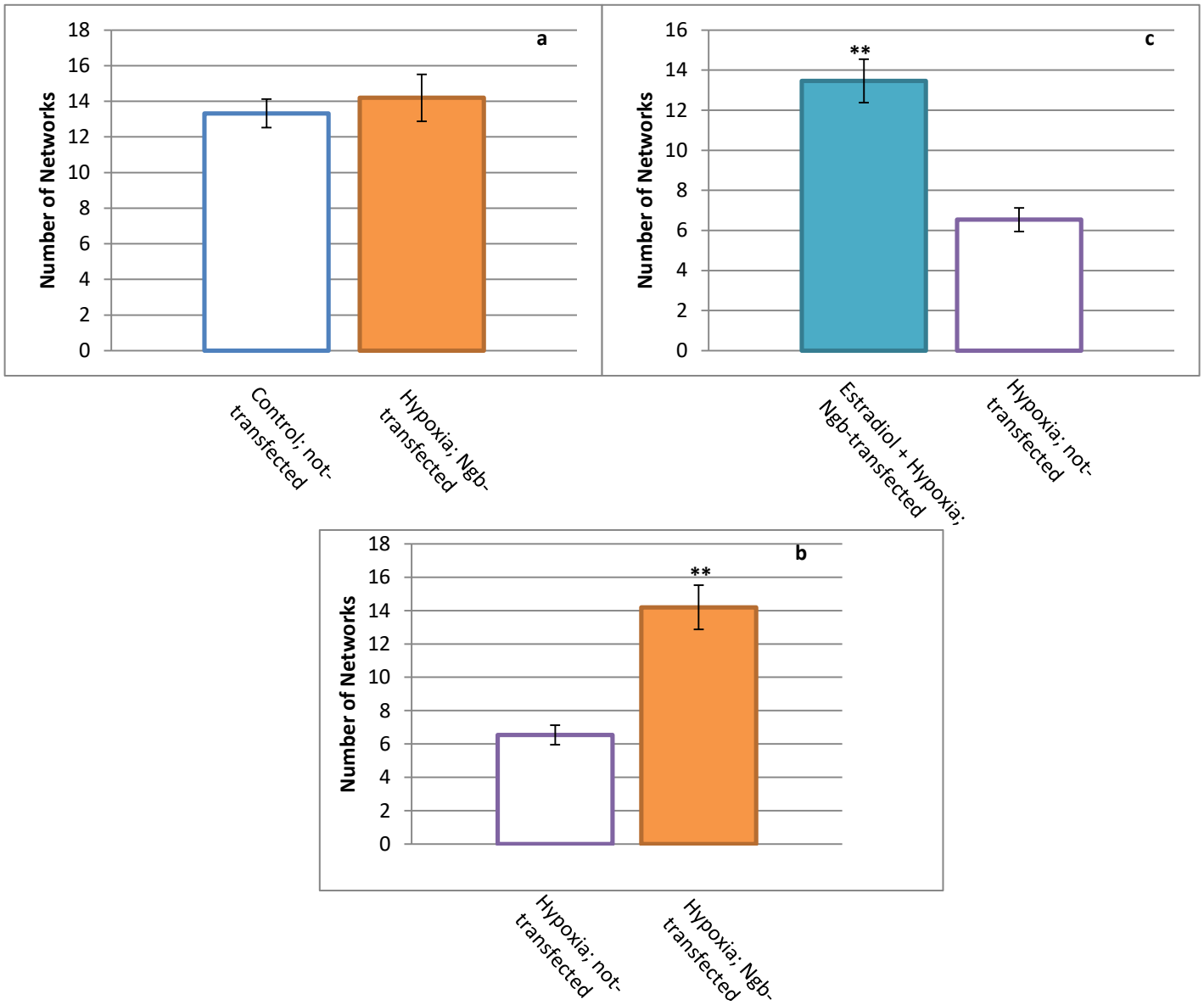

Figure 4.11 Quantification of Mitochondrial Networks after Estradiol Pretreatment under Hypoxic Stress

The figures portray the differences in the number of mitochondrial networks. (a) shows the comparison between the non-transfected SH-SY5Y cells of the control group with the Ngb-transfected SH-SY5Y cells under hypoxic stress. (b) shows the comparison between the non-transfected SH-SY5Y cells under hypoxic stress with the Ngb-transfected SH-SY5Y cells under hypoxic stress. (c) shows the comparison between the non-transfected SH-SY5Y cells under hypoxic stress and Ngb-transfected SH-SY5Y cells under hypoxic stress after estradiol pretreatment. Data is represented as mean ± SEM.

**: indicates p-value < 0.01

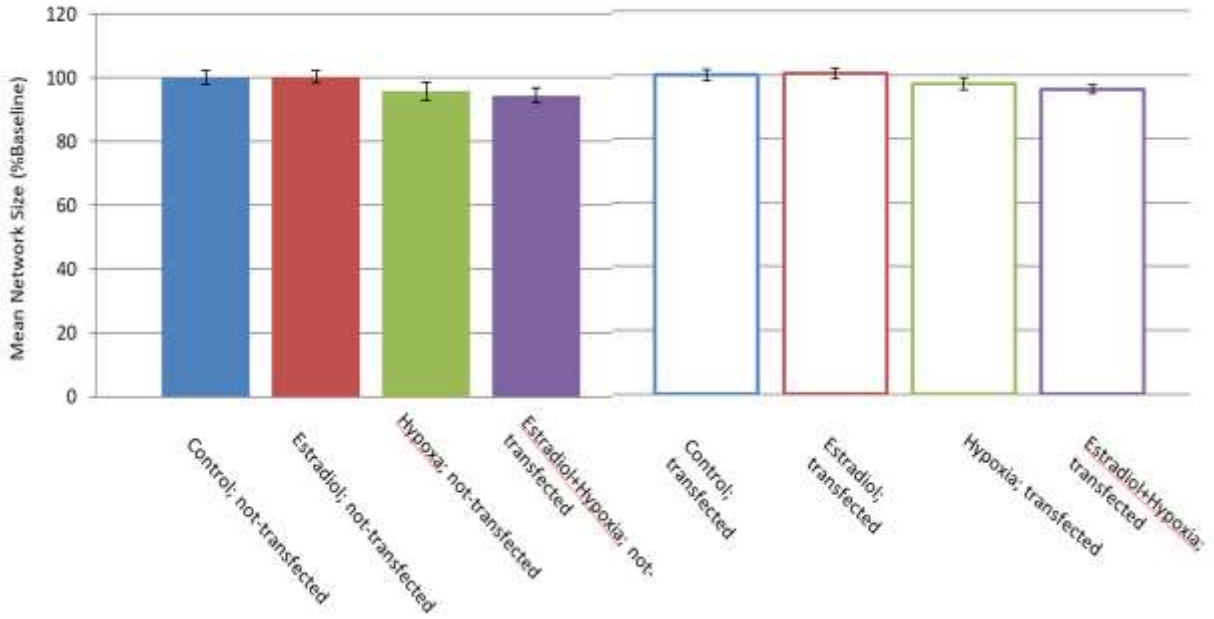

Figure 4.12 Quantification of Mitochondrial Mean Network Sizes after Estradiol Pretreatment under Hypoxic Stress

The figure portrays the differences in the number of mitochondrial branches per network. The left side of the figure depicts the non-transfected SH-SY5Y cells under various conditions of treatments, while the right side of the figure depicts the Ngb-transfected SH-SY5Y cells under the same conditions of treatment. Data has been normalized to the controls of each form of transfection and is represented as mean ± SEM.

treated Ngb-transfected cells showed a significant decrease in individuals in comparison with hypoxia/reoxygenation-treated Ngb-transfected cells (Figure 4.13c).

As for the mitochondrial network parameter, there was no significant difference shown between hypoxia/reoxygenation-treated Ngb-transfected cells and the non-transfected cells of the control group (Figure 4.14a), but a significant increase in networks was shown in the former with respect to hypoxia/reoxygenation-treated non-transfected cells (p-value < 0.01) (Figure 4.14b). For the RES-pretreated hypoxia/reoxygenation-treated Ngb-transfected cells, a significant increase was shown in comparison with the hypoxia/reoxygenation-treated non-transfected cells (p-value < 0.01) (Figure 4.14c).

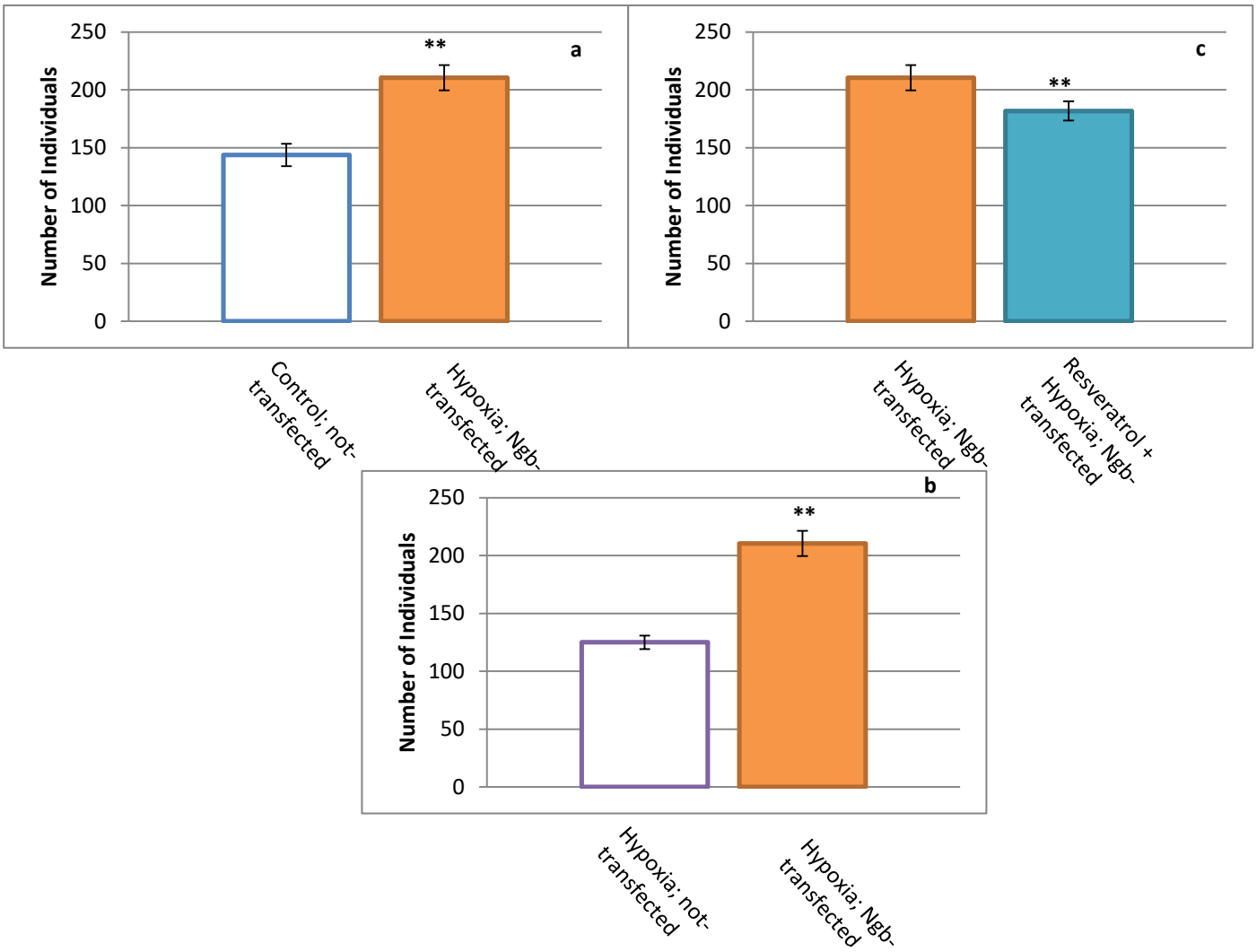

Figure 4.13 Quantification of Mitochondrial Individuals after Resveratrol Pretreatment under Hypoxic Stress

The figures portray the differences in the number of mitochondrial individuals. (a) shows the comparison between the non-transfected SH-SY5Y cells of the control group with the Ngb-transfected SH-SY5Y cells under hypoxic stress. (b) shows the comparison between the non-transfected SH-SY5Y cells under hypoxic stress with the Ngb-transfected SH-SY5Y cells under hypoxic stress. (c) shows the comparison between the Ngb-transfected SH-SY5Y cells under hypoxic stress and Ngb-transfected SH-SY5Y cells under hypoxic stress after estradiol pretreatment. Data is represented as mean ± SEM.

**: indicates p-value <0.01

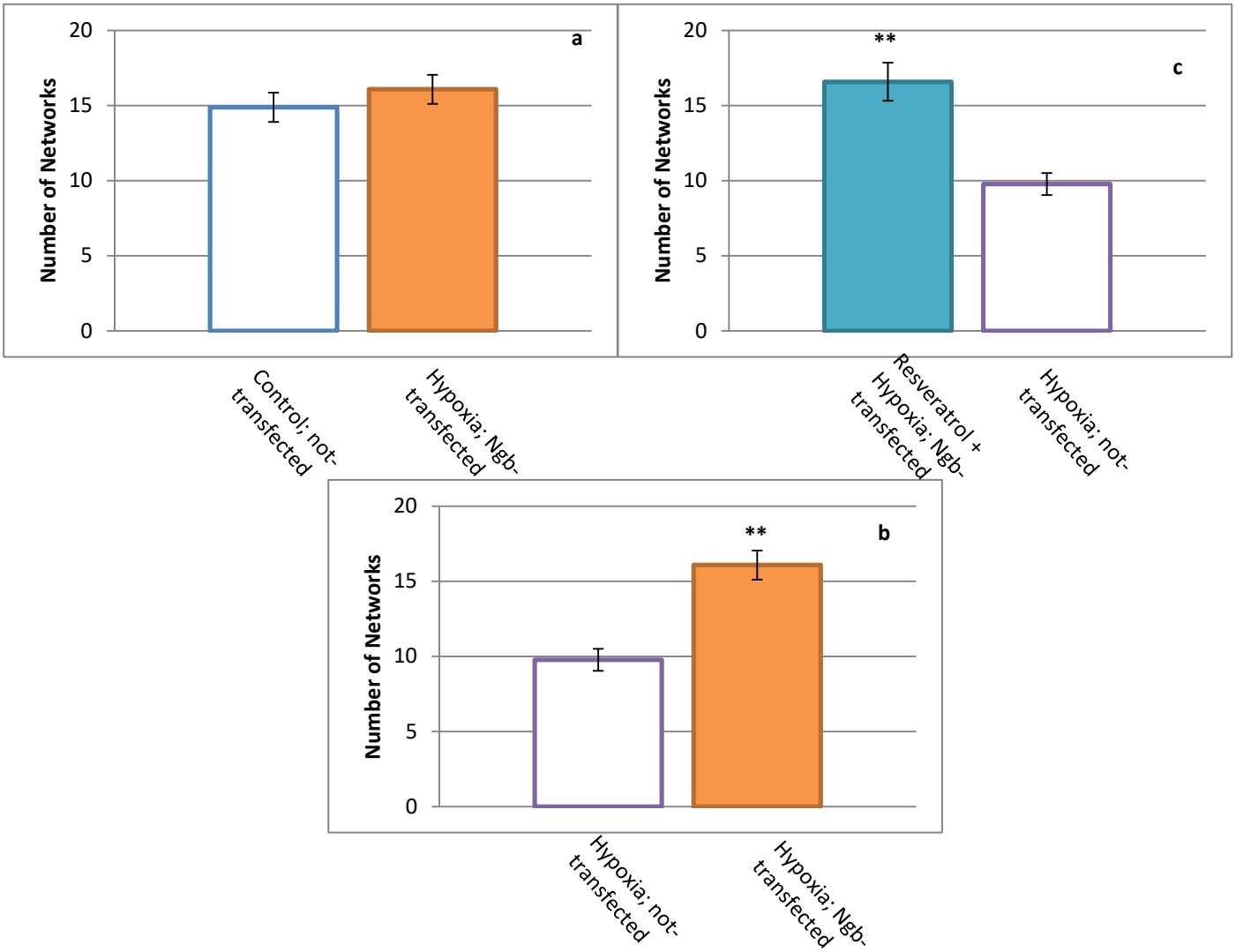

Figure 4.14 Quantification of Mitochondrial Networks after Resveratrol Pretreatment under Hypoxic Stress

The figures portray the differences in the number of mitochondrial networks. (a) shows the comparison between the non-transfected SH-SY5Y cells of the control group with the Ngb-transfected SH-SY5Y cells under hypoxic stress. (b) shows the comparison between the non-transfected SH-SY5Y cells under hypoxic stress with the Ngb-transfected SH-SY5Y cells under hypoxic stress. (c) shows the comparison between the non-transfected SH-SY5Y cells under hypoxic stress and Ngb-transfected SH-SY5Y cells under hypoxic stress after estradiol pretreatment. Data is represented as mean ± SEM.

**: indicates p-value < 0.01

Lastly, there was no significant difference on the mean network size (Figure 4.16) under hypoxic conditions regardless of the transfection and treatment Ngb-transfection and non-transfection.

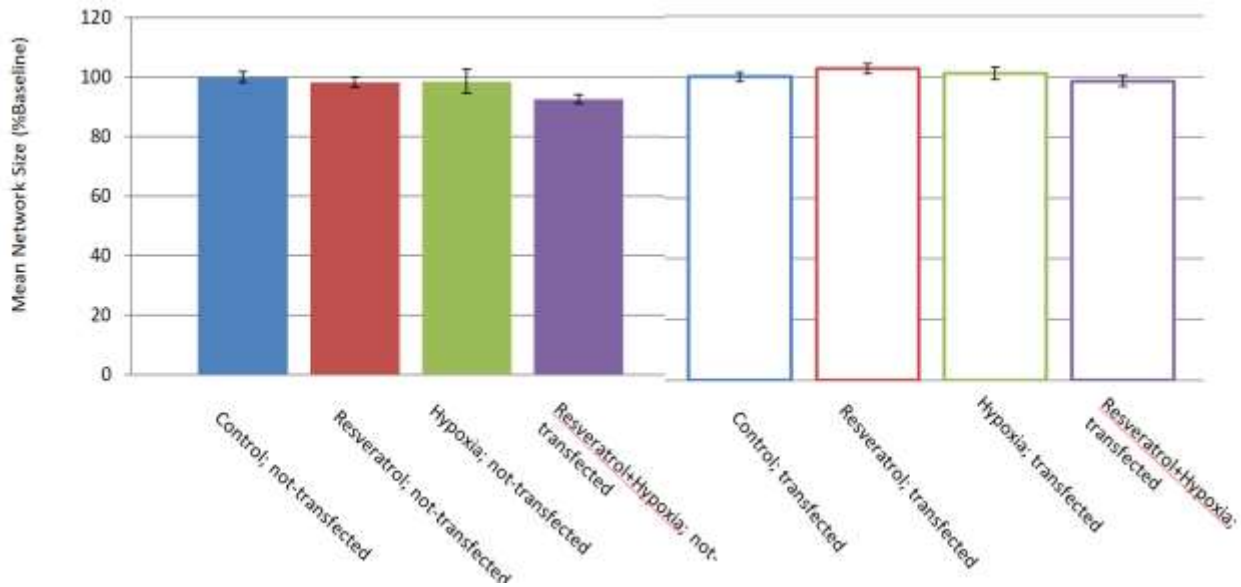

Figure 4.15 Quantification of Mitochondrial Mean Network Sizes after Resveratrol Pretreatment under Hypoxic Stress

The figure portrays the differences in the number of mitochondrial branches per network. The left side of the figure depicts the non-transfected SH-SY5Y cells under various conditions of treatments, while the right side of the figure depicts the Ngb-transfected SH-SY5Y cells under the same conditions of treatment. Data has been normalized to the controls of each form of transfection and is represented as mean ± SEM.

4.4 Discussion

Ngb is a haem protein that has been shown to protect cells against oxidative stress. Ngb silencing promotes apoptosis caused by various forms of oxidative stress (Li et al., 2007; Watanabe et al., 2012;). In contrast, Ngb overexpression confers neuronal cells with protective capabilities against oxidative stress or hypoxia/ischemia stress (Sun et al., 2001; Li et al., 2008; Li et al., 2008; Watanabe and Wakasugi, 2008). Ngb upregulation has been shown to occur

immediately following exposure to an oxidative stress (Watanabe and Wakasugi, 2008; Emara et al., 2010; Oleksiewicz et al., 2011), which could explain how cancer cells survive oxidative stress or hypoxic insults that occur in neoplastic tissue (Emara et al., 2010; Oleksiewicz et al., 2011). Since fission is a marker of cellular stress and fusion is a marker of stress resistance, Ngb translocates into mitochondria during cellular stress, combined with Ngb's translocation into mitochondria under stress, it could be hypothesized that Ngb affects mitochondrial dynamics.

4.4.1 Ngb alone does not prevent mitochondrial fragmentation

For the hydrogen peroxide stress experiment, an increase in individual number was shown in the Ngb-transfected SH-SY5Y cells. The individual number parameter indicates mitochondrial fragmentation and it could be assumed that the results indicate that the aforementioned group showed a phenotype with an increase in mitochondrial fragmentation. Combined with the non-significant differences in network number and mean network size, it could be postulated that the overexpression of Ngb without any form of pretreatment did not prevent the formation of punctae and rod-shaped mitochondria, a sign of fragmentation. However, E2 or RES pretreatment in the Ngb-transfected cells showed a significant decrease in individual formation, hinting at the prevention of fragmentation, which agrees with the evidence that shows RES's ability to ameliorate mitochondrial fission under stress (Wang et al., 2014; Li et al., 2016); the protective effects of RES on mitochondria have been reviewed by Ungvari et al., 2011.

The overexpression of Ngb alone did not seem to abrogate mitochondrial fragmentation as a result of H2O2 insult, which could argue Ngb's role in mitochondrial dynamics as one of its anti-apoptotic effects; Ngb's role could be limited to other elucidated mechanisms, such as ROS

scavenging (Herold et al., 2004; Fordel et al., 2006; Fordel et al., 2007; Li et al., 2008) and GDI activity (Watanabe et al., 2012). It could also be due to the misfolding of the Ngb protein from the plasmid transfection, as mentioned in Chapter 2.

Hypoxia has been shown to increase production of ROS (Fridovich, 1978; Yoshikawa et al., 1982; Block et al., 1989; Chang et al., 1989; Kehrer et al., 1990), although other evidence exists that shows a reduction in ROS production as a result of hypoxic insult (de Groot and Littauer, 1989). There is also evidence that reoxygenation induces an increase in ROS production (Arroyo et al., 1990). As mentioned earlier, an increase in ROS production would lead to mitochondrial fragmentation, and eventually apoptosis.

For the hypoxic stress experiments, the overexpression of Ngb without any form of pretreatment showed an increase in the number of punctae and rod-shaped mitochondria. In addition to the increase of individual number, the increase in network number and the non-significant difference in mean network size indicate that the larger networks are being fragmented into smaller networks as well as punctae and rod-shaped mitochondria; this evidence shows that Ngb overexpression, by itself, could not ameliorate mitochondrial fragmentation. However, RES pretreatment in Ngb-transfected cells showed a decrease in individual number and an increase in network number, which would indicate that fragmentation, was limited to the formation in smaller networks from larger networks, instead of punctae and rod-shaped mitochondria; this could be due to RES's promotion of the expression of mitochondrial fission protein (Peng et al., 2015).

Moreover, E2 pretreatment in Ngb-transfected cells showed a significant increase in individual and network number. Combined with the lack of significant difference in mean

network size, the larger networks seem to undergo fragmentation into smaller networks as well as punctae and rod-shaped mitochondria. The failure to ameliorate fragmentation by the ERβ agonists could have been associated with the low concentrations used (10 μM) for a short pretreatment period (24 hours); an increase in the concentration of RES combined with a longer pretreatment period could help with the reduction of fragmentation, as a similar approach was undertook by Wang et al., 2014.

4.4.2 Ngb does not induce mitochondrial fusion

The number of network parameters is used to quantitavely asses the degree of mitochondrial fusion, as fission fragments mitochondrial networks during apoptosis to aid in the release of pro-apoptotic proteins (Parone and Martinou, 2006; Suen et al., 2008); there is evidence that elucidates the inhibition of fusion during apoptosis (Karbowski et al, 2004), indicating that fusion has an antiapoptotic activity.

An increase in the number of branches per network (mean network size) indicates that networks are elongating and creating more branches, a sign of fusion. Increased fusion with mitochondria leads to a highly connected network (hyperfusion), and provides resistance towards apoptosis. Tondera et al., 2009 has shown the different effects of hyperfusion within the cell, such as delaying the release of cyt c and increasing ATP production; it could be postulated that Ngb exacts its anti-apoptotic also by preventing cyt c release through the induction of hyperfusion. Across all forms of groups, regardless of presence or absence of overexpressed Ngb, there were no significant differences in the number of branches per network. The overexpression of Ngb alone did not show any significant increases in the elongation of networks through the formation of more branches within the mitochondrion, indicating that Ngb may not

have a role in mitochondrial fusion. The pretreatment with E2 and RES in the Ngb-transfected cells also did not increase the formation of branches in a network. These results could be explained by the lack of any role Ngb has on mitochondrial dynamics as a protective mechanism for SH-SY5Y cells. With regards to the pretreatment, it could be that the low concentrations for a short pretreatment period, as mentioned above, was not enough to abrogate the deleterious effects of hypoxia and reoxygenation.

4.5 Conclusion

The constructed plasmid expressing the Ngb protein was present within cells, indicated by the Ngb bands from western blots that validate the success of transfection. However, Ngb alone did not prevent mitochondrial fragmentation nor did it induce mitochondrial fusion and network elongation, while the combined effects of E2 and RES pretreatments with Ngb seemed to abrogate mitochondrial fragmentation in oxidative stress.

5.0 Discussion

5.1 No evidence that neuroglobin inhibits cytochrome c peroxidase activity

As previously mentioned, Ngb interacts with cyt c by reducing it and preventing apoptosome formation. This interaction, which was shown to be very rapid (Fago et al., 2008), is thought to be electrostatic, as the pI of Ngb is 4.6 (acidic) and that of cyt c is 10.2 (basic) (Brittain et al., 2010). Another form of interaction is a direct docking interaction (Figure 5.1), which showed that the cyt c residues (Lys25 and Lys72) binding with Ngb are also pivotal for cyt c – Apaf-1 binding (Kluck et al., 2000; Yu et al., 2001; Abdullaev et al., 2002; Chertkova et al., 2008) and apoptosome formation. Due to these interactions between cyt c and Ngb, combined with Ngb's translocation into the mitochondria to interact with cyt c and inhibit apoptosis as mentioned earlier, it could be hypothesized that Ngb could prevent cyt c release by inhibiting its peroxidase activity; cyt c peroxidase activity leads to cyt c's detachment from cardiolipin and its eventual release.

The significant increase in the fluorescence measurement of the peroxidase activity with cyt c and cardiolipin compared to cyt c alone was expected, since the cyt c peroxidase activity is prominently activated as a result of cyt c and cardiolipin interaction, which agrees with literature (see Figure 2.2 in Chapter 2; Petrosillo et al., 2001; Kagan et al., 2005); this increase in fluorescence is a result of the exposure of cyt c's haem group towards H_2O_2 due to the interaction with cardiolipin, which inexorably activates cyt c's peroxidase activity. However, the fluorescence measurement with the addition of Ngb (cyt c, cardiolipin and Ngb) was not significantly different from the measurements of cyt c and cardiolipin, which shows that Ngb did not inhibit cyt c's peroxidase activity.

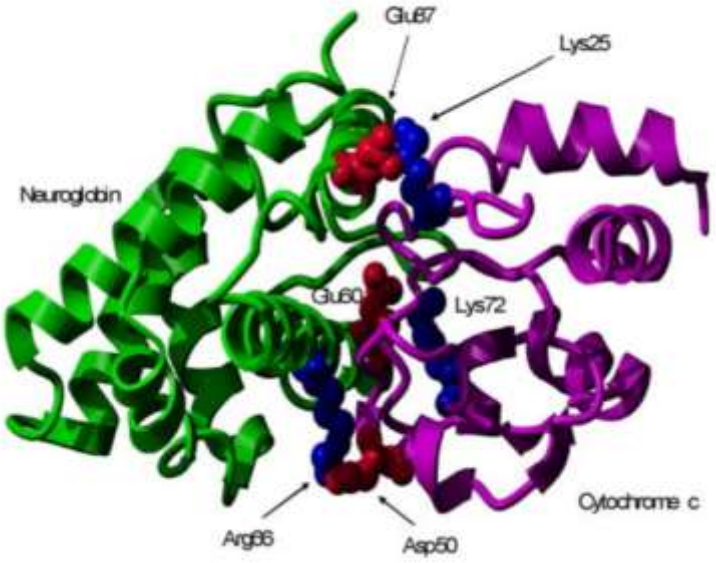

Figure 5.1 Docking Structure of Ngb-Cytochrome c Complex

The figure depicts a physical interaction between cyt c and Ngb, where the Lys25 and Lys72 on cyt c bind with Gluc67 and Glu60 on Ngb. This structure was calculated using BIGGER (Palma et al., 2000) and rendered using YASARA. This image was obtained from Raychaudhuri et al., 2010.

The non-significant difference between the measurement of the fluorescence after the addition of Ngb and the measurement with cardiolipin and cyt c only indicates that Ngb does not inhibit the activation of cyt c's peroxidase activity in a 1:1 ratio. The concentrations of cyt c differ amongst organs and species (Potter and DuBois, 1942). Forman and Azzi, 1997 showed that cyt c's concentration in cardiomyocytes within the intermembrane space ranges from 0.5 to 5 mM, with its cytosolic concentration being approximately 0.46 mM (van Beek-Harmsen and van der Laarse, 2005; another study showed that 0.04 ng/mL cyt c is released from intact isolated rat heart mitochondria (Appaix et al., 2000). In the HL-60 promyeolocytic leukemia cells, it was shown that intracellular cyt c concentration was around 7 µM (Ripple et al., 2010). Ott et al., 2002, showed that around 0.1 µM of cyt c is free in the intermembrane space and can be released

easily once a mild apoptotic signal is triggered, with more cyt c being released if a strong apoptotic signal is triggered. Ngb concentrations in retinal rods and endocrine tissues reach levels as high as 100 µM (Hankeln et al., 2005). Although the concentrations of Ngb within the mitochondria, as well as ratios of Ngb to cyt c concentrations, have not been elucidated, Raychaudhuri et al., 2010 showed decreased apoptosome formation and inhibition of caspase 9 at different Ngb concentrations (0, 0.01 µM and 0.1 µM) and constant cyt c levels (0.1 µM); it was shown that the apoptosome formation inhibition was Ngb dose-dependent. Increasing the levels of cyt c from 0.1 µM to 0.2 µM showed a 15-fold increase in caspase 3 activation (non-linear manner), requiring higher levels of Ngb to inhibit apoptosis; Ngb levels at 0.5 µM with respect to cyt c levels at 0.2 µM inhibited apoptosis (Raychaudhuri et al., 2010). This shows that effective ratio between Ngb and cyt c with regards to inhibition to apoptosis is 3:1. Although there is no evidence with regards to Ngb inhibiting the peroxidase activity of cyt c, it could prove insightful if a 3:1 Ngb to cyt c ratio is investigated for that assay. However, the results from such an experiment might not be extrapolated as the probability of the 3:1 ratio occurring physiologically within the mitochondria is too low.

The lack of inhibition could be attributed to nature of interaction between Ngb and cyt c, where Ngb inactivates the apoptotic effect of cyt c by reducing it to the ferrous form (Suto et al., 2005; Borutaite and Brown, 2007; Brown and Borutaite, 2008). The lack of inhibition could also be due to the fact the anti-apoptotic effects occur when the ratio of Ngb to cyt c is 3:1 (Raychaudhuri et al., 2010). Other than the nature of interaction, the differences in localization between cyt c and Ngb could justify these results.

Ngb translocates into the mitochondria, however its exact location has not been clearly indicated. Ngb has been shown to localize in the mitochondrial matrix, as a result of Ngb

presence detected in mitoplasts; mitoplasts are mitochondria that lack outer membranes and intermembrane spaces (Lechauve et al., 2012). However, interaction between Ngb and cyt c has been elucidated in the literature (De Marinis et al., 2013); although the nature of the interaction between Ngb and cyt c has not been elucidated, immunopreciptation blots of the mitochondrial fraction for Ngb and cyt c indicates that Ngb interacts with cyt c in the mitochondrial fraction. Another explanation for the lack of inhibition of the cyt c peroxidase activity with Ngb is that Ngb does not interfere with the peroxidase activity, but mainly functions as a ROS scavenger (Herold et al., 2004; Fordel et al., 2007), and thus, Ngb does not prevent the activity of cyt c peroxidase. Furthermore, Ngb binding with cyt c could require the released active ferric form of cyt c (Pan et al., 1999; Suto et al., 2005), hinting that the interaction between Ngb and cyt c occurs only in the cytoplasm, which still contradicts the literature that a Ngb-cyt c interaction in the mitochondria occurs (De Marinis, 2013).

5.2 Endogenous Ngb is undetectable in SH-SY5Y cell lysates

The western blots performed to visualize endogenous Ngb and the effects of E2 and RES on its expression failed to detect Ngb under any condition tested. On the other hand, Ngb bands were readily detectable in lanes with pure recombinant Ngb or with cells in which Ngb had been overexpressed, indicating that the technique undertaken was efficient. The absence of endogenous Ngb bands could not be interpreted as lack of Ngb expression in this cell line, as SH-SY5Y cells have been shown previously to express Ngb protein (Fordel et al., 2007a; Fordel et al., 2007b), and that E2 greatly increases the levels of Ngb in the SK-N-BE neuroblastoma cell lines (De Marinis et al., 2013; Fiocchetti et al., 2013). It could be speculated that the reasons behind the lack of Ngb bands are that Ngb protein levels are quite low combined with a low sensitivity detection method, evident by the lack of bands on a 0.2 µm nitrocellulose membrane.

To provide insight into the levels of Ngb, a western blot with a wide dilution range of purified Ngb protein should be undertaken, to determine the lowest dilution at which the band could be visualized. Another method to aid in Ngb detection could be the use of chemiluminescence, which uses substrates for HRP, as the infra-red detection method for the unconjugated antibodies and the fluorescence detection for the Alexa-Fluor conjugated antibody were ineffective. The HRP detection has been shown to provide strong and detectable signals (Chau and Lu, 1995). In multiple attempts to replicate various studies (Fiocchetti et al 2014; Fiocchetti et al., 2015; Fiocchetti et al., 2016), the visualization detection method of Ngb bands on the membranes was different from those studies; the aforementioned studies used the super power ECL (enhanced chemiluminescence) HRP substrate, which was successful in visualizing Ngb bands. Since the western blots failed to show any Ngb bands, it could be safe to assume that the detection via chemiluminescence is essential to Ngb visualization.

5.3 Ngb mRNA transcript levels could not be accurately quantified in MCF-7 or DLD-1 cells but showed overexpression in SH-SY5Y cells that underwent OGD

Quantitative RT-PCR was performed on SH-SY5Y cells that were treated in hypoxic and OGD conditions to be used as a positive control for the success of the technique (chapter 3.0). Briefly, SH-SY5Y cells were placed in a humidified hypoxic chamber for both the hypoxia and OGD experiments, with the media for OGD lacking in FBS and glucose. The cells were incubated for 32 hours, and then were harvested via ice-cold PBS and the pellet collected. After the RNA isolation and cDNA synthesis, the cDNA underwent PCR to quantify Ngb mRNA transcript levels. The levels of Ngb mRNA were significantly higher in comparison with the hypoxia and control groups, which is concordant with the results from Fordel et al., 2007a. The 10 nM E2 stimulation for 24 hours however showed great variability in the results, preventing

any solid conclusions. Fiocchetti et al., 2014 showed that 10 nM E2 stimulation for 24 hours increased the levels of Ngb mRNA transcripts in MCF-7 cells in contrast with the DLD-1 cells, where there was no significant effect on the Ngb mRNA transcript levels (Fiocchetti et al., 2015). The presence of genomic contamination caused great variability in the mRNA expression levels, which was confirmed by the similarities of NRT Cq levels. Even though a study shows the absence of Ngb mRNA transcripts within MCF-7 cells (Gorr et al., 2011), other studies confirm the presence of the Ngb mRNA transcript level in the cells (Fiocchetti et al., 2014; Fiocchetti et al., 2016).In this study, both the MCF-7 and DLD-1 cells were used for the quantification of Ngb mRNA transcript levels, and the levels were quite variable compared to the results used in Fiocchetti et al., 2014, Fiocchetti et al., 2015 and Fiocchetti et al., 2016. The RNA isolation used in the aforementioned studies involved the use of the TRIzol reagent, while the RNA isolation used in this study was the Total RNA Isolation Kit from Norgen, using the "on-column" method. The on-column method was used to extract pure RNA with minimal genomic contamination. However, due to the nature and morphology of the MCF-7 and DLD-1 cells, which tend to adhere together during lysis, a TRIzol reagent would prove useful for such a great amount of contamination presence. This is because the TRIzol reagent separates the homogenate into different layers, with the RNA being separated into a layer of its own, allowing for a more effective RNA isolation; the RNA is then precipitated via isopropanol.

5.4 Ngb-EGFP fusion protein could not be visualized despite being detectable by western blot

Studies have shown that Ngb translocates into mitochondria when cells are stressed, and that translocation is E2-dependent (De Marinis et al., 2013; Fiocchetti et al., 2014; Fiocchetti et al., 2015; Fiocchetti et al., 2016). To visualize this translocation, I constructed EGFP, Ngb and

Ngb-EGFP fusion constructs for the fusion protein expression. SH-SY5Y cells were transfected with either of Ngb or Ngb-EGFP fusion plasmids expressing either Ngb alone or an Ngb-EGFP fusion protein respectively. Unfortunately, I was unable to detect the fusion protein using confocal microscopy, though positive controls including EGFP alone could be detected. The western blots performed to confirm the success of transfection showed Ngb bands, indicating expression from plasmids; however, western blots do not indicate functionality. The absence of fluorescence could be due to misfolding of the fusion protein, or the presence of a degron in its sequence.

Degrons are sequences of proteins that regulate protein degradation (Jariel-Encontre et al., 2008; Ravid and Hochstrasser, 2008; Erales and Coffino, 2014). As mentioned before, Ngb has been shown to undergoe proteasomal degradation, indicating that Ngb's degron is ubiquitin-dependent (Ravid and Hochstrasser, 2008). An N-degron sequence on Ngb has been identified, and could explain the lack of fluorescence from the Ngb-EGFP fusion protein, and would lead to the degradation of Ngb, which would lead to a higher turnover rate, preventing the correct formation and maturation of Ngb-EGFP. A solution to such a predicament is fusing the EGFP sequence at the N-terminus, overcoming the high turnover rate of Ngb. The EGFP-Ngb fusion plasmid construct could then be transfected into the SH-SY5Y cells and visualized using the confocal microscope to determine correct folding and the presence of fluorescence; once the fluorescence presence is confirmed, Ngb translocation under different conditions could be assessed and mitochondrial network characteristics could be quantified more directly.

5.5 Ngb overexpression did not affect mitochondrial network characteristics

Ngb's role in inducing mitochondrial fusion and hyperfusion has not been elucidated. Due to the translocation of Ngb into mitochondria, where it exerts its protective action, it could be speculated that Ngb might induce mitochondrial fusion (Wang, 2013) to prevent apoptosis. MiNA was used to quantify mitochondrial networking characteristics, which involves the skeletonizing mitochondria after taking images of mitochondria-containing EGFP in SH-SY5Y. The skeletonized mitochondria are then categorized into their respective parameters and quantified; interestingly, Ngb lacked a significant effect on mitochondrial network formation.

The parameters used to characterize mitochondrial networking included, but not limited to, individual number, network number and mean network size. The individual number parameter is a marker of mitochondrial fragmentation and it could be speculated that an increase in individual number is interpreted as an increase in mitochondrial fragmentation as fission fragments mitochondrial networks during apoptosis to aid in the release of pro-apoptotic proteins (Parone and Martinou, 2006; Suen et al., 2008). The network number parameter however, is a marker of mitochondrial fusion, and in contrast to the pro-apoptotic effect of fission, fusion promotes anti-apoptotic effects as there is evidence that shows inhibition of fusion during apoptosis (Karbowski et al, 2004). The mean network size (number of branches per network) parameter is a marker of fusion, which involves the formation of a highly connected network that confers different effects (Tondera et al., 2009) that resist cellular stress.

Cells under hydrogen peroxide stress showed an increase in number of individuals in the Ngb-transfected SH-SY5Y cells, while the Ngb-transfected cells pretreated with E2 and RES showed a decrease in individual number. These results show that Ngb overexpression alone could not inhibit mitochondrial fragmentation, but rather the synergistic effects of the ERβ agonists with Ngb overexpression abrogated the detrimental effects of fragmentation. For the

network number, Ngb overexpression alone or with ERβ agonists pretreatment did not have any significant effect on the number of networks under hydrogen peroxide stress, indicating that the mitochondrial networks were being fragmented into more punctae and rod-shaped mitochondrion.

As previously stated, increases in ROS production lead to mitochondrial fragmentation and apoptosis. ROS production has been shown to increase during hypoxia (Fridovich, 1978; Yoshikawa et al., 1982; Block et al., 1989; Chang et al., 1989; Kehrer et al., 1990), and reoxygenation (Arroyo et al., 1990), even though another study shows that hypoxic insults reduce ROS production (de Groot and Littauer, 1989). For the hypoxia/reoxygenation experiments, the Ngb-transfected SH-SY5Y cells with E2 and RES pretreatments as well as the E2-pretreated non-transfected cells showed a significant increase in individual number. These results show that Ngb overexpression combined with E2 and RES did not inhibit fission.

The number of mitochondrial individuals in the hypoxic experimentation showed a significant increase in Ngb-transfected SH-SY5Y cells and those that have been transfected with Ngb and pretreated with E2. This indicates that Ngb overexpression alone as well with E2 pretreatment did not inhibit the formation of more punctae and rod-shaped mitochondrion. However, Ngb overexpression and RES pretreatment showed a significant decrease in the number of individuals, which agrees with RES's role at ameliorating mitochondrial fission (Wang et al., 2014; Li et al., 2016). As for the number of networks, there was a significant increase in cells overexpressing Ngb, as well pretreated with E2 and RES, indicating that larger networks are being fragmented into smaller networks. The absence of fission amelioration could be as a result of low E2 and RES concentrations (10 μM) or that the pretreatment period (24 hours) was relatively short for the hypoxia/reoxygenation stress cells. Wang et al., 2014 showed

that a higher RES concentration and a longer pretreatment period do attenuate mitochondrial fission.

In addition to individual and network numbers, the number of branches per network (mean network size) was assessed as an indication of fusion or hyperfusion, as the networks elongated and become highly interconnected; Ngb overexpression did not show any significant effects on the number of branches, indicating that Ngb does not promote mitochondrial fusion.

These results suggest that the mechanism of action for Ngb does not involve induction of mitochondrial fusion, nor the inhibition of mitochondrial fission. Its anti-apoptotic effects, although not fully elucidated, could lie simply ROS scavenging (Herold et al., 2004; Fordel et al., 2006; Fordel et al., 2007; Li et al., 2008; Fago et al., 2008; Burmester and Hankeln, 2009), nitric oxide modulator (Herold et al., 2004; Brunori et al., 2005) and GDI inhibition (Watanabe et al., 2012). Moreover, the binding of Ngb to a plasma membrane lipid raft associated protein Flotillin-1 (Watanabe et al., 2012), could enforce the absence of a Ngb role in mitochondrial fusion promotion. Furthermore, Raychaudhuri et al., 2010 transfected SH-SY5Y cells with a Ngb-expressing plasmids that increased Ngb levels to 5 µM; this concentration was shown to protect cells against the stressor HA14-1 (BH3 mimetic) at low concentrations (12.5 µM and 25 µM) (Raychaudhuri et al., 2010), which shows that overexpression of Ngb was able to protect the cells from low-level stress, indicating that the stressors imposed onto the cells in this study could have been a high-level stress for Ngb to protect the cells. To provide further insight into Ngb's mechanism of action, cell viability after transfection, intracellular ROS measurement and direct ROS scavenging assays could be undertaken. Also, the overexpression of EGFP-Ngb fusion protein after transfection could provide more direct quantifications of mitochondrial network characteristics.

6.0 Bibliography

Abdullaev, Z. K., Bodrova, M. E., Chernyak, B. V., Dolgikh, D. A., Kluck, R. M., Pereverzev, M. O., ... & Newmeyer, D. D. (2002). A cytochrome c mutant with high electron transfer and antioxidant activities but devoid of apoptogenic effect.*Biochemical Journal*, *362*(3), 749-754.

Abdullaev, Z. K., Bodrova, M. E., Chernyak, B. V., Dolgikh, D. A., Kluck, R. M., Pereverzev, M. O., ... & Newmeyer, D. D. (2002). A cytochrome c mutant with high electron transfer and antioxidant activities but devoid of apoptogenic effect. *Biochemical Journal*, *362*(3), 749-754.

Acconcia, F., & Marino, M. (2011). The effects of 17b-estradiol in cancer are mediated by estrogen receptor signaling at the plasma membrane.*Frontiers in PHYSIOLOGY*, *2*, 30.

Acconcia, F., Totta, P., Ogawa, S., Cardillo, I., Inoue, S., Leone, S., ... & Marino, M. (2005). Survival versus apoptotic 17β-estradiol effect: Role of ERα and ERβ activated non-genomic signaling. *Journal of cellular physiology*, *203*(1), 193-201.

Akkara, J. A., Senecal, K. J., & Kaplan, D. L. (1991). Synthesis and characterization of polymers produced by horseradish peroxidase in dioxane. *Journal of Polymer Science Part A: Polymer Chemistry*, *29*(11), 1561-1574.

Antao, S. T., Duong, T. H., Aran, R., & Witting, P. K. (2010). Neuroglobin overexpression in cultured human neuronal cells protects against hydrogen peroxide insult via activating phosphoinositide-3 kinase and opening the mitochondrial KATP channel. *Antioxidants & redox signaling*, *13*(6), 769-781.

Appaix, F., Minatchy, M. N., Riva-Lavieille, C., Olivares, J., Antonsson, B., & Saks, V. A. (2000). Rapid spectrophotometric method for quantitation of cytochrome c release from isolated

mitochondria or permeabilized cells revisited. *Biochimica et Biophysica Acta (BBA)-Bioenergetics*, *1457*(3), 175-181.

Arroyo, C. M., Carmichael, A. J., Bouscarel, B., Liang, J. H., & Weglicki, W. B. (1990). Endothelial Cells as A Source of Oxygen-Free Radicals An Esr Study. *Free radical research communications*, *9*(3-6), 287-296.

Ascenzi, P., Bocedi, A., & Marino, M. (2006). Structure–function relationship of estrogen receptor α and β: impact on human health. *Molecular aspects of medicine*, *27*(4), 299-402.

Ascenzi, P., Polticelli, F., Marino, M., Santucci, R., & Coletta, M. (2011). Cardiolipin drives cytochrome c proapoptotic and antiapoptotic actions. *IUBMB life*,*63*(3), 160-165.

Atkinson, J., Kapralov, A. A., Yanamala, N., Tyurina, Y. Y., Amoscato, A. A., Pearce, L., ... & Maeda, A. (2011). A mitochondria-targeted inhibitor of cytochrome c peroxidase mitigates radiation induced death. *Nature communications*, *2*, 497.

Awenius, C., Hankeln, T., & Burmester, T. (2001). Neuroglobins from the zebrafish Danio rerio and the pufferfish Tetraodon nigroviridis. *Biochemical and biophysical research communications*, *287*(2), 418-421.

Baines, C. P., Kaiser, R. A., Purcell, N. H., Blair, N. S., Osinska, H., Hambleton, M. A., ... & Robbins, J. (2005). Loss of cyclophilin D reveals a critical role for mitochondrial permeability transition in cell death. *Nature*, *434*(7033), 658-662.

Barsoum, M. J., Yuan, H., Gerencser, A. A., Liot, G., Kushnareva, Y., Gräber, S., ... & Bossy-Wetzel, E. (2006). Nitric oxide-induced mitochondrial fission is regulated by dynamin-related GTPases in neurons.*The EMBO journal*, *25*(16), 3900-3911.

Bartella, V., Rizza, P., Barone, I., Zito, D., Giordano, F., Giordano, C., ... & Fuqua, S. A. W. (2012). Estrogen receptor beta binds Sp1 and recruits a corepressor complex to the estrogen receptor alpha gene promoter. *Breast cancer research and treatment, 134*(2), 569-581.

Bentmann, A., Schmidt, M., Reuss, S., Wolfrum, U., Hankeln, T., & Burmester, T. (2005). Divergent distribution in vascular and avascular mammalian retinae links neuroglobin to cellular respiration. *Journal of Biological Chemistry*, *280*(21), 20660-20665.

Bernad, S., Oellerich, S., Soulimane, T., Noinville, S., Baron, M. H., Paternostre, M., & Lecomte, S. (2004). Interaction of horse heart and thermus thermophilus type c cytochromes with phospholipid vesicles and hydrophobic surfaces. *Biophysical journal*, *86*(6), 3863-3872.

Bertholet, A. M., Delerue, T., Millet, A. M., Moulis, M. F., David, C., Daloyau, M., ... & Rojo, M. (2016). Mitochondrial fusion/fission dynamics in neurodegeneration and neuronal plasticity. *Neurobiology of disease*, *90*, 3-19.

Beyzavi, K., Hampton, S., Kwasowski, P., Fickling, S., Marks, V., & Clift, R. (1987). Comparison of horseradish peroxidase and alkaline phosphatase-labelled antibodies in enzyme immunoassays. *Annals of clinical biochemistry*, *24*(2), 145-152.

Birk, A. V., Liu, S., Soong, Y., Mills, W., Singh, P., Warren, J. D., ... & Szeto, H. H. (2013). The mitochondrial-targeted compound SS-31 re-energizes ischemic mitochondria by interacting with cardiolipin. *Journal of the American Society of Nephrology*, *24*(8), 1250-1261.

Block, E. R., Patel, J. M., & Edwards, D. E. B. O. R. A. H. (1989). Mechanism of hypoxic injury to pulmonary artery endothelial cell plasma membranes. *American Journal of Physiology-Cell Physiology*, *257*(2), C223-C231.

Bo, H., Zhang, Y., & Ji, L. L. (2010). Redefining the role of mitochondria in exercise: a dynamic remodeling. *Annals of the New York Academy of Sciences*, *1201*(1), 121-128.

Boehning, D., Patterson, R. L., Sedaghat, L., Glebova, N. O., Kurosaki, T., & Snyder, S. H. (2003). Cytochrome c binds to inositol (1, 4, 5) trisphosphate receptors, amplifying calcium-dependent apoptosis. *Nature cell biology*, *5*(12), 1051-1061.

Bønding, S. H., Henty, K., Dingley, A. J., & Brittain, T. (2008). The binding of cytochrome c to neuroglobin: a docking and surface plasmon resonance study. *International journal of biological macromolecules*, *43*(3), 295-299.

Borutaite, V., & Brown, G. C. (2007). Mitochondrial regulation of caspase activation by cytochrome oxidase and tetramethylphenylenediamine via cytosolic cytochrome c redox state. *Journal of Biological Chemistry*, *282*(43), 31124-31130.

Brand, M. D., Goncalves, R. L., Orr, A. L., Vargas, L., Gerencser, A. A., Jensen, M. B., ... & Dardov, V. J. (2016). Suppressors of Superoxide-H 2 O 2 Production at Site I Q of Mitochondrial Complex I Protect against Stem Cell Hyperplasia and Ischemia-Reperfusion Injury. *Cell Metabolism*, *24*(4), 582-592.

Brinton, R. D. (2001). Cellular and molecular mechanisms of estrogen regulation of memory function and neuroprotection against Alzheimer's disease: recent insights and remaining challenges.*Learning & Memory*, *8*(3), 121-133.

Brinton, R. D. (2008). The healthy cell bias of estrogen action: mitochondrial bioenergetics and neurological implications. *Trends in neurosciences*,*31*(10), 529-537.

Brittain, T., & Skommer, J. (2012). Does a redox cycle provide a mechanism for setting the capacity of neuroglobin to protect cells from apoptosis?.*IUBMB life*, *64*(5), 419-422.

Brittain, T., Skommer, J., Henty, K., Birch, N., & Raychaudhuri, S. (2010). A role for human neuroglobin in apoptosis. *IUBMB life*, *62*(12), 878-885.

Brittain, T., Skommer, J., Raychaudhuri, S., & Birch, N. (2010). An antiapoptotic neuroprotective role for neuroglobin. *International journal of molecular sciences*, *11*(6), 2306-2321.

Brittain, T., & Skommer, J. (2012). Does a redox cycle provide a mechanism for setting the capacity of neuroglobin to protect cells from apoptosis?.*IUBMB life*, *64*(5), 419-422.

Brown, G. C., & Borutaite, V. (2008). Regulation of apoptosis by the redox state of cytochrome c.*Biochimica et Biophysica Acta (BBA)-Bioenergetics*, *1777*(7), 877-881.

Brunori, M., & Vallone, B. (2006). A globin for the brain. *The FASEB Journal*, *20*(13), 2192-2197.

Brunori, M., Giuffrè, A., Nienhaus, K., Nienhaus, G. U., Scandurra, F. M., & Vallone, B. (2005). Neuroglobin, nitric oxide, and oxygen: functional pathways and conformational changes.*Proceedings of the National Academy of Sciences of the United States of America*, *102*(24), 8483-8488.

Burmester, T., & Hankeln, T. (2009). What is the function of neuroglobin?. *Journal of Experimental Biology*, *212*(10), 1423-1428.

Burmester, T., Ebner, B., Weich, B., & Hankeln, T. (2002). Cytoglobin: a novel globin type ubiquitously expressed invertebrate tissues.*Molecular biology and evolution*, *19*(4), 416-421.

Burmester, T., Weich, B., Reinhardt, S., & Hankeln, T. (2000). A vertebrate globin expressed in the brain. *Nature*, *407*(6803), 520-523.

Butot, S., Putallaz, T., Croquet, C., Lamothe, G., Meyer, R., Joosten, H., & Sánchez, G. (2007). Attachment of enteric viruses to bottles. *Applied and environmental microbiology*, *73*(16), 5104-5110.

Buytaert, E., Callewaert, G., Vandenheede, J. R., & Agostinis, P. (2006). Deficiency in apoptotic effectors Bax and Bak reveals an autophagic cell death pathway initiated by photodamage to the endoplasmic reticulum. *Autophagy*, *2*(3), 238-240.

Cadenas, E., & Davies, K. J. (2000). Mitochondrial free radical generation, oxidative stress, and aging. *Free Radical Biology and Medicine*, *29*(3), 222-230.

Cai, B., Lin, Y., Xue, X. H., Fang, L., Wang, N., & Wu, Z. Y. (2011). TAT-mediated delivery of neuroglobin protects against focal cerebral ischemia in mice. *Experimental neurology*, *227*(1), 224-231.

Caiazza, F., Galluzzo, P., Lorenzetti, S., & Marino, M. (2007). 17β-estradiol induces ERβ up-regulation via p38/MAPK activation in colon cancer cells. *Biochemical and biophysical research communications*, *359*(1), 102-107.

Carroll, J. S., Meyer, C. A., Song, J., Li, W., Geistlinger, T. R., Eeckhoute, J., ... & Wang, Q. (2006). Genome-wide analysis of estrogen receptor binding sites. *Nature genetics*, *38*(11), 1289-1297.

Celsi, F., Pizzo, P., Brini, M., Leo, S., Fotino, C., Pinton, P., & Rizzuto, R. (2009). Mitochondria, calcium and cell death: a deadly triad in neurodegeneration. *Biochimica et Biophysica Acta (BBA)-Bioenergetics*, *1787*(5), 335-344.

Chacinska, A., Koehler, C. M., Milenkovic, D., Lithgow, T., & Pfanner, N. (2009). Importing mitochondrial proteins: machineries and mechanisms. *Cell*, *138*(4), 628-644.

Chan, D. C. (2006). Mitochondrial fusion and fission in mammals. *Annu. Rev. Cell Dev. Biol.*, *22*, 79-99.

Chan, D. C. (2012). Fusion and fission: interlinked processes critical for mitochondrial health. *Annual review of genetics*, *46*, 265-287.

Chang, E. C., Frasor, J., Komm, B., & Katzenellenbogen, B. S. (2006). Impact of estrogen receptor β on gene networks regulated by estrogen receptor α in breast cancer cells. *Endocrinology*, *147*(10), 4831-4842.

Chang, S. W., Stelzner, T. J., Weil, J. V., & Voelkel, N. F. (1989). Hypoxia increases plasma glutathione disulfide in rats. *Lung*, *167*(1), 269-276.

Charn, T. H., Liu, E. T. B., Chang, E. C., Lee, Y. K., Katzenellenbogen, J. A., & Katzenellenbogen, B. S. (2010). Genome-wide dynamics of chromatin binding of estrogen receptors α and β: mutual restriction and competitive site selection. *Molecular endocrinology*, *24*(1), 47-59.

Chau, Y. P., & Lu, K. S. (1995). Investigation of the blood-ganglion barrier properties in rat sympathetic ganglia by using lanthanum ion and horseradish peroxidase as tracers. *Cells Tissues Organs*, *153*(2), 135-144.

Chaudhry, K., Rogers, R., Guo, M., Lai, Q., Goel, G., Liebelt, B., ... & Ding, Y. (2010). Matrix metalloproteinase-9 (MMP-9) expression and extracellular signal-regulated kinase 1 and 2 (ERK1/2) activation in exercise-reduced neuronal apoptosis after stroke. *Neuroscience letters*,*474*(2), 109-114.

Chen, J. Q., Delannoy, M., Cooke, C., & Yager, J. D. (2004). Mitochondrial localization of ERα and ERβ in human MCF7 cells. *American Journal of Physiology-Endocrinology and Metabolism*, *286*(6), E1011-E1022.

Chertkova, R. V., Sharonov, G. V., Feofanov, A. V., Ol'ga, V. B., Latypov, R. F., Chernyak, B. V., ... & Kirpichnikov, M. P. (2008). Proapoptotic activity of cytochrome c in living cells: effect of K72 substitutions and species differences. *Molecular and cellular biochemistry*, *314*(1-2), 85-93.

Chertkova, R. V., Sharonov, G. V., Feofanov, A. V., Ol'ga, V. B., Latypov, R. F., Chernyak, B. V., ... & Kirpichnikov, M. P. (2008). Proapoptotic activity of cytochrome c in living cells: effect of K72 substitutions and species differences. *Molecular and cellular biochemistry*, *314*(1-2), 85.

Chiang, C. W., Harris, G., Ellig, C., Masters, S. C., Subramanian, R., Shenolikar, S., ... & Yang, E. (2001). Protein phosphatase 2A activates the proapoptotic function of BAD in interleukin-3–dependent lymphoid cells by a mechanism requiring 14-3-3 dissociation. *Blood*, *97*(5), 1289-1297.

Cho, S., & Dreyfuss, G. (2010). A degron created by SMN2 exon 7 skipping is a principal contributor to spinal muscular atrophy severity. *Genes & development*, *24*(5), 438-442.

Chu, C. T., Ji, J., Dagda, R. K., Jiang, J. F., Tyurina, Y. Y., Kapralov, A. A., ... & Wang, K. Z. Q. (2013). Cardiolipin externalization to the outer mitochondrial membrane acts as an elimination signal for mitophagy in neuronal cells. *Nature cell biology*, *15*(10), 1197.

Chuang, P. Y., Conley, Y. P., Poloyac, S. M., Okonkwo, D. O., Ren, D., Sherwood, P. R., ... & Alexander, S. A. (2010). Neuroglobin genetic polymorphisms and their relationship to functional outcomes after traumatic brain injury. *Journal of neurotrauma*, *27*(6), 999-1006.

Chumakov, K. M. (1994). Reverse transcriptase can inhibit PCR and stimulate primer-dimer formation. *Genome Research*, *4*(1), 62-64.

Cossarizza, A., Pinti, M., Moretti, L., Bricalli, D., Bianchi, R., Troiano, L., ... & Vigano, A. (2002). Mitochondrial Functionality and Mitochondrial DNA Content in Lymphocytes of Vertically Infected Human Immunodeficiency Virus—Positive Children with Highly Active Antiretroviral Therapy—Related Lipodystrophy. *Journal of Infectious Diseases*,*185*(3), 299-305.

Coux, O., Tanaka, K., & Goldberg, A. L. (1996). Structure and functions of the 20S and 26S proteasomes. *Annual review of biochemistry*, *65*(1), 801-847.

De Arriba, G., Calvino, M., Benito, S., & Parra, T. (2013). Cyclosporine A-induced apoptosis in renal tubular cells is related to oxidative damage and mitochondrial fission. *Toxicology letters*, *218*(1), 30-38.

de Groot, H., & Littauer, A. (1989). Hypoxia, reactive oxygen, and cell injury. *Free Radical Biology and Medicine*, *6*(5), 541-551.

De Marinis, E., Ascenzi, P., Pellegrini, M., Galluzzo, P., Bulzomi, P., Arevalo, M. A., ... & Marino, M. (2011). 17β-Estradiol–a new modulator of neuroglobin levels in neurons: role in neuroprotection against H2O2-induced toxicity.*Neurosignals*, *18*(4), 223-235.

De Marinis, E., Fiocchetti, M., Acconcia, F., Ascenzi, P., & Marino, M. (2013). Neuroglobin upregulation induced by 17β-estradiol sequesters cytocrome c in the mitochondria preventing H2O2-induced apoptosis of neuroblastoma cells. *Cell death & disease*, *4*(2), e508.

De Marinis, E., Ascenzi, P., Pellegrini, M., Galluzzo, P., Bulzomi, P., Arevalo, M. A., ... & Marino, M. (2010). 17β-Estradiol–a new modulator of neuroglobin levels in neurons: role in neuroprotection against H2O2-induced toxicity.*Neurosignals*, *18*(4), 223-235.

Dejean, L. M., Martinez-Caballero, S., & Kinnally, K. W. (2006). Is MAC the knife that cuts cytochrome c from mitochondria during apoptosis?. *Cell Death & Differentiation*, *13*(8), 1387-1395.

Dent, P., Jelinek, T., Morrison, D. K., Weber, M. J., & Sturgill, T. W. (1995). Reversal of Raf-1 activation by purified and membrane-associated protein phosphatases. *SCIENCE-NEW YORK THEN WASHINGTON-*, 1902-1902.

Deprez, R. H. L., Fijnvandraat, A. C., Ruijter, J. M., & Moorman, A. F. (2002). Sensitivity and accuracy of quantitative real-time polymerase chain reaction using SYBR green I depends on cDNA synthesis conditions. *Analytical biochemistry*, *307*(1), 63-69.

Deroo, B. J., & Buensuceso, A. V. (2010). Minireview: estrogen receptor-β: mechanistic insights from recent studies. *Molecular endocrinology*, *24*(9), 1703-1714.

Detmer, S. A., & Chan, D. C. (2007). Functions and dysfunctions of mitochondrial dynamics. *Nature reviews. Molecular cell biology*, *8*(11), 870.

Dewilde, S., Kiger, L., Burmester, T., Hankeln, T., Baudin-Creuza, V., Aerts, T., ... & Moens, L. (2001). Biochemical characterization and ligand binding properties of neuroglobin, a novel member of the globin family. *Journal of Biological Chemistry*,*276*(42), 38949-38955.

Dohmen, R. J., Wu, P., & Varshavsky, A. (1994). Heat-inducible degron: a method for constructing temperature-sensitive mutants. *SCIENCE-NEW YORK THEN WASHINGTON-*, 1273-1273.

Dong, Y., Zhao, R., Chen, X. Q., & Yu, A. C. H. (2010). 14-3-3γ and neuroglobin are new intrinsic protective factors for cerebral ischemia. *Molecular neurobiology*, *41*(2-3), 218-231.

Drummond, A. E., & Fuller, P. J. (2010). The importance of ERβ signalling in the ovary. *Journal of Endocrinology*, *205*(1), 15-23.

Dudek, H., Datta, S. R., Franke, T. F., Birnbaum, M. J., Yao, R., Cooper, G. M., ... & Greenberg, M. E. (1997). Regulation of neuronal survival by the serine-threonine protein kinase Akt. *Science*,*275*(5300), 661-665.

Duong, T. T. H., Witting, P. K., Antao, S. T., Parry, S. N., Kennerson, M., Lai, B., ... & Harris, H. H. (2009). Multiple protective activities of neuroglobin in cultured neuronal cells exposed to hypoxia re-oxygenation injury. *Journal of neurochemistry*,*108*(5), 1143-1154.

Eble, K. S., Coleman, W. B., Hantgan, R. R., & Cunningham, C. C. (1990). Tightly associated cardiolipin in the bovine heart mitochondrial ATP synthase as analyzed by 31P nuclear magnetic resonance spectroscopy. *Journal of Biological Chemistry*, *265*(32), 19434-19440.

Emara, M., Turner, A. R., & Allalunis-Turner, J. (2010). Hypoxic regulation of cytoglobin and neuroglobin expression in human normal and tumor tissues. *Cancer cell international*, *10*(1), 33.

Erales, J., & Coffino, P. (2014). Ubiquitin-independent proteasomal degradation. *Biochimica et Biophysica Acta (BBA)-Molecular Cell Research*, *1843*(1), 216-221.

Fago, A., Hundahl, C., Dewilde, S., Gilany, K., Moens, L., & Weber, R. E. (2004). Allosteric Regulation and Temperature Dependence of Oxygen Binding in Human Neuroglobin and Cytoglobin MOLECULAR MECHANISMS AND PHYSIOLOGICAL SIGNIFICANCE. *Journal of Biological Chemistry*, *279*(43), 44417-44426.

Fago, A., Mathews, A. J., & Brittain, T. (2008). A role for neuroglobin: resetting the trigger level for apoptosis in neuronal and retinal cells. *IUBMB life*,*60*(6), 398-401.

Fago, A., Mathews, A. J., Moens, L., Dewilde, S., & Brittain, T. (2006). The reaction of neuroglobin with potential redox protein partners cytochrome b 5 and cytochrome c. *FEBS letters*, *580*(20), 4884-4888.

Fernandez, M. G., Troiano, L., Moretti, L., Nasi, M., Pinti, M., Salvioli, S., ... & Cossarizza, A. (2002). Early changes in intramitochondrial cardiolipin distribution during apoptosis. *Cell growth and differentiation*, *13*(9), 449-455.

Fesik, S. W., & Shi, Y. (2001). Controlling the caspases. *Science*, *294*(5546), 1477-1478.

Fiocchetti, M., Ascenzi, P., & Marino, M. (2012). Neuroprotective effects of 17β-estradiol rely on estrogen receptor membrane initiated signals. *Frontiers in physiology*, *3*.

Fiocchetti, M., Camilli, G., Acconcia, F., Leone, S., Ascenzi, P., & Marino, M. (2015). ERβ-dependent neuroglobin up-regulation impairs 17β-estradiol-induced apoptosis in DLD-1 colon cancer cells upon oxidative stress injury. *The Journal of steroid biochemistry and molecular biology*, *149*, 128-137

Fiocchetti, M., Cipolletti, M., Leone, S., Naldini, A., Carraro, F., Giordano, D., ... & Marino, M. (2016). Neuroglobin in breast cancer cells: effect of hypoxia and oxidative stress on protein level, localization, and anti-apoptotic function. *PloS one*, *11*(5), e0154959.

Fiocchetti, M., De Marinis, E., Ascenzi, P., & Marino, M. (2013). Neuroglobin and neuronal cell survival. *Biochimica et Biophysica Acta (BBA)-Proteins and Proteomics*, *1834*(9), 1744-1749.

Fiocchetti, M., Nuzzo, M. T., Totta, P., Acconcia, F., Ascenzi, P., & Marino, M. (2014). Neuroglobin, a pro-survival player in estrogen receptor α-positive cancer cells. *Cell death & disease*, *5*(10), e1449.

Fordel, E., Geuens, E., Dewilde, S., De Coen, W., & Moens, L. (2004). Hypoxia/ischemia and the regulation of neuroglobin and cytoglobin expression. *IUBMB life*, *56*(11-12), 681-687.

Fordel, E., Geuens, E., Dewilde, S., Rottiers, P., Carmeliet, P., Grooten, J., & Moens, L. (2004). Cytoglobin expression is upregulated in all tissues upon hypoxia: an in vitro and in vivo study by quantitative real-time PCR. *Biochemical and biophysical research communications*, *319*(2), 342-348.

Fordel, E., Thijs, L., Martinet, W., Lenjou, M., Laufs, T., Van Bockstaele, D., ... & Dewilde, S. (2006). Neuroglobin and cytoglobin overexpression protects human SH-SY5Y neuroblastoma cells against oxidative stress-induced cell death. *Neuroscience letters*, *410*(2), 146-151.

Fordel, E., Thijs, L., Martinet, W., Schrijvers, D., Moens, L., & Dewilde, S. (2007). Anoxia or oxygen and glucose deprivation in SH-SY5Y cells: a step closer to the unraveling of neuroglobin and cytoglobin functions. *Gene*, *398*(1), 114-122.

Fordel, E., Thijs, L., Moens, L., & Dewilde, S. (2007). Neuroglobin and cytoglobin expression in mice. *The FEBS journal*, *274*(5), 1312-1317.

Forman, H. J., & Azzi, A. (1997). On the virtual existence of superoxide anions in mitochondria: thoughts regarding its role in pathophysiology. *The FASEB Journal*, *11*(5), 374-375.

Fortmann, K. T., Lewis, R. D., Ngo, K. A., Fagerlund, R., & Hoffmann, A. (2015). A regulated, ubiquitin-independent degron in IκBα. *Journal of molecular biology*, *427*(17), 2748-2756.

Fox, D. H., Huang, C. K., Du, J., Chang, T. Y., & Pan, Q. (2007). Profound inhibition of the PCR step of CF V3 multiplex PCR/OLA assay by the use of UV-irradiated plastic reaction tubes. *Diagnostic Molecular Pathology*, *16*(2), 121-123.

Fox, E. M., Andrade, J., & Shupnik, M. A. (2009). Novel actions of estrogen to promote proliferation: integration of cytoplasmic and nuclear pathways.*Steroids*, *74*(7), 622-627.

Frasor, J., Danes, J. M., Komm, B., Chang, K. C., Lyttle, C. R., & Katzenellenbogen, B. S. (2003). Profiling of estrogen up-and down-regulated gene expression in human breast cancer cells: insights into gene networks and pathways underlying estrogenic control of proliferation and cell phenotype. *Endocrinology*, *144*(10), 4562-4574.

Fridovich, I. (1978). Hypoxia and oxygen toxicity. *Advances in neurology*, *26*, 255-259.

Galkin, A., & Moncada, S. (2007). S-nitrosation of mitochondrial complex I depends on its structural conformation. *Journal of Biological Chemistry*,*282*(52), 37448-37453.

Galluzzi, L., Blomgren, K., & Kroemer, G. (2009). Mitochondrial membrane permeabilization in neuronal injury. *Nature Reviews Neuroscience*,*10*(7), 481-494.

Galluzzo, P., Caiazza, F., Moreno, S., & Marino, M. (2007). Role of ERβ palmitoylation in the inhibition of human colon cancer cell proliferation. *Endocrine-related cancer*, *14*(1), 153-167.

Gao, L., Laude, K., & Cai, H. (2008). Mitochondrial pathophysiology, reactive oxygen species, and cardiovascular diseases. *Veterinary Clinics of North America: Small Animal Practice*, *38*(1), 137-155.

Gassilloud, B., Huguet, L., Maul, A., & Gantzer, C. (2007). Development of a viral concentration method for bottled water stored in hydrophobic support. *Journal of virological methods*, *142*(1), 98-104.

Geuens, E., Brouns, I., Flamez, D., Dewilde, S., Timmermans, J. P., & Moens, L. (2003). A globin in the nucleus!. *Journal of Biological Chemistry*,*278*(33), 30417-30420.

Gnaiger, E. (2003). Oxygen conformance of cellular respiration. A perspective of mitochondrial physiology. *Adv Exp Med Biol*, *543*, 39-55.

Gomez, B., & Robinson, N. C. (1999). Phospholipase digestion of bound cardiolipin reversibly inactivates bovine cytochrome bc 1. *Biochemistry*, *38*(28), 9031-9038.

Gonzalez, A., Grimes, R., Walsh, E. J., Dalton, T., & Davies, M. (2007). Interaction of quantitative PCR components with polymeric surfaces. *Biomedical microdevices*, *9*(2), 261-266.

Gonzalvez, F., & Gottlieb, E. (2007). Cardiolipin: setting the beat of apoptosis. *Apoptosis*, *12*(5), 877-885.

Gorr, T. A., Wichmann, D., Pilarsky, C., Theurillat, J. P., Fabrizius, A., Laufs, T., ... & Hankeln, T. (2011). Old proteins–new locations: myoglobin, haemoglobin, neuroglobin and cytoglobin in solid tumours and cancer cells. *Acta physiologica*, *202*(3), 563-581.

Green, D. R., & Kroemer, G. (2004). The pathophysiology of mitochondrial cell death.*Science*, *305*(5684), 626-629.
Green, D. R., & Kroemer, G. (2004). The pathophysiology of mitochondrial cell death.*Science*, *305*(5684), 626-629.
Gruber, C. J., Gruber, D. M., Gruber, I. M., Wieser, F., & Huber, J. C. (2004). Anatomy of the estrogen response element. *Trends in endocrinology & metabolism*, *15*(2), 73-78.

Haga, N., Fujita, N., & Tsuruo, T. (2003). Mitochondrial aggregation precedes cytochrome c release from mitochondria during apoptosis. *Oncogene*, *22*(36), 5579.

Haines, B., Demaria, M., Mao, X., Xie, L., Campisi, J., Jin, K., & Greenberg, D. A. (2012). Hypoxia-inducible factor-1 and neuroglobin expression.*Neuroscience letters*, *514*(2), 137-140.

Hales, K. G. (2010). Mitochondrial fusion and division. *Nature Education*, *3*(9), 12.

Hall, J. M., & Korach, K. S. (2002). Analysis of the molecular mechanisms of human estrogen receptors α and β reveals differential specificity in target promoter regulation by xenoestrogens.*Journal of Biological Chemistry*, *277*(46), 44455-44461.

Hall, J. M., & McDonnell, D. P. (1999). The estrogen receptor β-isoform (ERβ) of the human estrogen receptor modulates ERα transcriptional activity and is a key regulator of the cellular response to estrogens and antiestrogens. *Endocrinology*, *140*(12), 5566-5578.

Hall, J. M., McDonnell, D. P., & Korach, K. S. (2002). Allosteric regulation of estrogen receptor structure, function, and coactivator recruitment by different estrogen response elements. *Molecular endocrinology*, *16*(3), 469-486.

Hamdane, D., Kiger, L., Dewilde, S., Green, B. N., Pesce, A., Uzan, J., ... & Marden, M. C. (2003). The redox state of the cell regulates the ligand binding affinity of human neuroglobin and cytoglobin. *Journal of Biological Chemistry*, *278*(51), 51713-51721.

Hankeln, T., Ebner, B., Fuchs, C., Gerlach, F., Haberkamp, M., Laufs, T. L., ... & Saaler-Reinhardt, S. (2005). Neuroglobin and cytoglobin in search of their role in the vertebrate globin family. *Journal of inorganic biochemistry*, *99*(1), 110-119.

Hankeln, T., Wystub, S., Laufs, T., Schmidt, M., Gerlach, F., Saaler-Reinhardt, S., ... & Burmester, T. (2004). The Cellular and Subcellular Localization of Neuroglobin and Cytoglobin-A Clue to Their Function?. *IUBMB life*, *56*(11-12), 671-679.

Hayyan, M., Hashim, M. A., & AlNashef, I. M. (2016). Superoxide ion: Generation and chemical implications. *Chemical reviews*, *116*(5), 3029-3085.

Hegele-Hartung, C., Siebel, P., Peters, O., Kosemund, D., Müller, G., Hillisch, A., ... & Fritzemeier, K. H. (2004). Impact of isotype-selective estrogen receptor agonists on ovarian function. *Proceedings of the National Academy of Sciences of the United States of America*, *101*(14), 5129-5134.

Herold, S., Fago, A., Weber, R. E., Dewilde, S., & Moens, L. (2004). Reactivity studies of the Fe (III) and Fe (II) NO forms of human neuroglobin reveal a potential role against oxidative stress. *Journal of Biological Chemistry*, *279*(22), 22841-22847.

Hollenbeck, P. J., & Saxton, W. M. (2005). The axonal transport of mitochondria. *Journal of cell science*, *118*(23), 5411-5419.

Hota, K. B., Hota, S. K., Srivastava, R. B., & Singh, S. B. (2012). Neuroglobin regulates hypoxic response of neuronal cells through Hif-1α-and Nrf2-mediated mechanism. *Journal of Cerebral Blood Flow & Metabolism*, *32*(6), 1046-1060.

Hundahl, C. A., Allen, G. C., Hannibal, J., Kjaer, K., Rehfeld, J. F., Dewilde, S., ... & Hay-Schmidt, A. (2010). Anatomical characterization of cytoglobin and neuroglobin mRNA and protein expression in the mouse brain. *Brain research*, *1331*, 58-73.

Hundahl, C. A., Hannibal, J., Fahrenkrug, J., Dewilde, S., & Hay-Schmidt, A. (2010). Neuroglobin expression in the rat suprachiasmatic nucleus: colocalization, innervation, and response to light. *Journal of Comparative Neurology*, *518*(9), 1556-1569.

Hundahl, C. A., Luuk, H., Ilmjärv, S., Falktoft, B., Raida, Z., Vikesaa, J., ... & Hay-Schmidt, A. (2011). Neuroglobin-deficiency exacerbates Hif1A and c-FOS response, but does not affect neuronal survival during severe hypoxia in vivo.

Hundahl, C., Kelsen, J., Kjær, K., Rønn, L. C. B., Weber, R. E., Geuens, E., ... & Nyengaard, J. R. (2006). Does neuroglobin protect neurons from ischemic insult? A quantitative investigation of neuroglobin expression following transient MCAo in spontaneously hypertensive rats. *Brain research*, *1085*(1), 19-27.

Iverson, S. L., & Orrenius, S. (2004). The cardiolipin–cytochrome c interaction and the mitochondrial regulation of apoptosis. *Archives of biochemistry and biophysics*, *423*(1), 37-46.

Jariel-Encontre, I., Bossis, G., & Piechaczyk, M. (2008). Ubiquitin-independent degradation of proteins by the proteasome. *Biochimica et Biophysica Acta (BBA)-Reviews on Cancer*, *1786*(2), 153-177.

Jayaraman, T., Tejero, J., Chen, B. B., Blood, A. B., Frizzell, S., Shapiro, C., ... & Conrads, T. P. (2011). 14-3-3 binding and phosphorylation of neuroglobin during hypoxia modulate six-to-five heme pocket coordination and rate of nitrite reduction to nitric oxide. *Journal of Biological Chemistry*, *286*(49), 42679-42689.

Jia, M., Dahlman-Wright, K., & Gustafsson, J. Å. (2015). Estrogen receptor alpha and beta in health and disease. *Best Practice & Research Clinical Endocrinology & Metabolism*, *29*(4), 557-568.

Jin, K., Mao, X. O., Xie, L., Khan, A. A., & Greenberg, D. A. (2008). Neuroglobin protects against nitric oxide toxicity. *Neuroscience letters*,*430*(2), 135-137.

Jin, K., Mao, X., Xie, L., & Greenberg, D. A. (2011). Neuroglobin expression in human arteriovenous malformation and intracerebral hemorrhage. In*Intracerebral Hemorrhage Research* (pp. 315-319). Springer Vienna.

Jin, K., Mao, Y., Mao, X., Xie, L., & Greenberg, D. A. (2010). Neuroglobin expression in ischemic stroke. *Stroke; a journal of cerebral circulation*,*41*(3), 557.

Jover-Mengual, T., Miyawaki, T., Latuszek, A., Alborch, E., Zukin, R. S., & Etgen, A. M. (2010). Acute estradiol protects CA1 neurons from ischemia-induced apoptotic cell death via the PI3K/Akt pathway. *Brain research*, *1321*, 1-12.

Ju, D., & Xie, Y. (2006). Identification of the preferential ubiquitination site and ubiquitin-dependent degradation signal of Rpn4. *Journal of Biological Chemistry*, *281*(16), 10657-10662.

Kagan, V. E., Tyurin, V. A., Jiang, J., Tyurina, Y. Y., Ritov, V. B., Amoscato, A. A., ... & Vlasova, I. I. (2005). Cytochrome c acts as a cardiolipin oxygenase required for release of proapoptotic factors. *Nature chemical biology*, *1*(4), 223-232.

Kanai, A. J., Pearce, L. L., Clemens, P. R., Birder, L. A., VanBibber, M. M., Choi, S. Y., ... & Peterson, J. (2001). Identification of a neuronal nitric oxide synthase in isolated cardiac mitochondria using electrochemical detection. *Proceedings of the National Academy of Sciences*, *98*(24), 14126-14131.

Kang, X., & Carey, J. (1999). Role of heme in structural organization of cytochrome c probed by semisynthesis. *Biochemistry*, *38*(48), 15944-15951.

Karbowski, M., & Youle, R. J. (2003). Dynamics of mitochondrial morphology in healthy cells and during apoptosis. *Cell death and differentiation*, *10*(8), 870.

Karbowski, M., Arnoult, D., Chen, H., Chan, D. C., Smith, C. L., & Youle, R. J. (2004). Quantitation of mitochondrial dynamics by photolabeling of individual organelles shows that mitochondrial fusion is blocked during the Bax activation phase of apoptosis. *J Cell Biol*, *164*(4), 493-499.

Karihtala, P., & Soini, Y. (2007). Reactive oxygen species and antioxidant mechanisms in human tissues and their relation to malignancies. *Apmis*,*115*(2), 81-103.

Katzenellenbogen, B. S. (1996). Estrogen receptors: bioactivities and interactions with cell signaling pathways. *Biology of Reproduction*,*54*(2), 287-293.

Kehrer, J. P., Jones, D. P., Lemasters, J. J., Farber, J. L., & Jaeschke, H. (1990). Mechanisms of hypoxic cell injury: Summary of the Symposium Presented at the 1990 Annual Meeting of the Society of Toxicology. *Toxicology and applied pharmacology*, *106*(2), 165-178.

Kelsen, J., Hundahl, C. A., & Hay-Schmidt, A. (2008). Neuroglobin: endogenous neuroprotectant or maintenance of homeostasis?. *Stroke*, *39*(11), e177-e178.

Khan, A. A., Mao, X. O., Banwait, S., DerMardirossian, C. M., Bokoch, G. M., Jin, K., & Greenberg, D. A. (2008). Regulation of hypoxic neuronal death signaling by neuroglobin. *The FASEB Journal*, *22*(6), 1737-1747.

Khan, A. A., Mao, X. O., Banwait, S., DerMardirossian, C. M., Bokoch, G. M., Jin, K., & Greenberg, D. A. (2008). Regulation of hypoxic neuronal death signaling by neuroglobin. *The FASEB Journal*, *22*(6), 1737-1747.

Khan, A. A., Mao, X. O., Banwait, S., Jin, K., & Greenberg, D. A. (2007). Neuroglobin attenuates β-amyloid neurotoxicity in vitro and transgenic Alzheimer phenotype in vivo. *Proceedings of the National Academy of Sciences*, *104*(48), 19114-19119.

Khan, A. A., Wang, Y., Sun, Y., Mao, X. O., Xie, L., Miles, E., ... & Greenberg, D. A. (2006). Neuroglobin-overexpressing transgenic mice are resistant to cerebral and myocardial ischemia. *Proceedings of the National Academy of Sciences*, *103*(47), 17944-17948.

Kim, J. A., Wei, Y., & Sowers, J. R. (2008). Role of mitochondrial dysfunction in insulin resistance.*Circulation research*, *102*(4), 401-414.

Kluck, R. M., Ellerby, L. M., Ellerby, H. M., Naiem, S., Yaffe, M. P., Margoliash, E., ... & Newmeyer, D. D. (2000). Determinants of cytochrome c pro-apoptotic activity The role of lysine 72 trimethylation. *Journal of Biological Chemistry*,*275*(21), 16127-16133.

Kluck, R. M., Ellerby, L. M., Ellerby, H. M., Naiem, S., Yaffe, M. P., Margoliash, E., ... & Newmeyer, D. D. (2000). Determinants of cytochrome c pro-apoptotic activity The role of lysine 72 trimethylation. *Journal of Biological Chemistry*, *275*(21), 16127-16133.

Knott, A. B., & Bossy-Wetzel, E. (2008). Impairing the mitochondrial fission and fusion balance: a new mechanism of neurodegeneration. *Annals of the New York Academy of Sciences*, *1147*(1), 283-292.

Kroemer, G., & Reed, J. C. (2000). Mitochondrial control of cell death. *Nature medicine*, *6*(5).

Kroemer, G., Dallaporta, B., & Resche-Rigon, M. (1998). The mitochondrial death/life regulator in apoptosis and necrosis. *Annual review of physiology*, *60*(1), 619-642.

Kuhl, H. (2005). Pharmacology of estrogens and progestogens: influence of different routes of administration. *Climacteric*, *8*(sup1), 3-63.

Kuiper, G. G., Carlsson, B. O., Grandien, K. A. J., Enmark, E., Häggblad, J., Nilsson, S., & Gustafsson, J. A. (1997). Comparison of the ligand binding specificity and transcript tissue distribution of estrogen receptors α and β. *Endocrinology*, *138*(3), 863-870.

Kuiper, G. G., Enmark, E., Pelto-Huikko, M., Nilsson, S., & Gustafsson, J. A. (1996). Cloning of a novel receptor expressed in rat prostate and ovary. *Proceedings of the National Academy of Sciences*, *93*(12), 5925-5930.

Kuwana, T., Mackey, M. R., Perkins, G., Ellisman, M. H., Latterich, M., Schneiter, R., ... & Newmeyer, D. D. (2002). Bid, Bax, and lipids cooperate to form supramolecular openings in the outer mitochondrial membrane. *Cell*, *111*(3), 331-342.

Lechauve, C., Augustin, S., Cwerman-Thibault, H., Bouaita, A., Forster, V., Célier, C., ... & Corral-Debrinski, M. (2012). Neuroglobin involvement in respiratory chain function and retinal ganglion cell integrity. *Biochimica et Biophysica Acta (BBA)-Molecular Cell Research*, *1823*(12), 2261-2273.

Lechauve, C., Augustin, S., Cwerman-Thibault, H., Bouaita, A., Forster, V., Célier, C., ... & Corral-Debrinski, M. (2012). Neuroglobin involvement in respiratory chain function and retinal

ganglion cell integrity. *Biochimica et Biophysica Acta (BBA)-Molecular Cell Research*, *1823*(12), 2261-2273.

Lecker, S. H., Goldberg, A. L., & Mitch, W. E. (2006). Protein degradation by the ubiquitin–proteasome pathway in normal and disease states. *Journal of the American Society of Nephrology*, *17*(7), 1807-1819.

Leitman, D. C., Paruthiyil, S., Yuan, C., Herber, C. B., Olshansky, M., Tagliaferri, M., ... & Speed, T. P. (2012, January). Tissue-specific regulation of genes by estrogen receptors. In *Seminars in reproductive medicine* (Vol. 30, No. 01, pp. 14-22). Thieme Medical Publishers.

Lenaz, G., & Genova, M. L. (2010). Structure and organization of mitochondrial respiratory complexes: a new understanding of an old subject. *Antioxidants & redox signaling*, *12*(8), 961-1008.

Levin, E. R. (2000). Cell localization, physiology, and nongenomic actions of estradiol receptors. *J Appl Physiol*, *91*, 1860-1867.

Levin, E. R. (2009). Plasma membrane estrogen receptors. *Trends in Endocrinology & Metabolism*,*20*(10), 477-482.

Li, A., Zhang, S., Li, J., Liu, K., Huang, F., & Liu, B. (2016). Metformin and resveratrol inhibit Drp1-mediated mitochondrial fission and prevent ER stress-associated NLRP3 inflammasome activation in the adipose tissue of diabetic mice. *Molecular and cellular endocrinology*, *434*, 36-47.

Li, D., Chen, X. Q., Li, W. J., Yang, Y. H., Wang, J. Z., & Yu, A. C. H. (2007). Cytoglobin up-regulated by hydrogen peroxide plays a protective role in oxidative stress. *Neurochemical research*, *32*(8), 1375-1380.

Li, R. C., Guo, S. Z., Lee, S. K., & Gozal, D. (2010). Neuroglobin protects neurons against oxidative stress in global ischemia. *Journal of Cerebral Blood Flow & Metabolism*, *30*(11), 1874-1882.

Li, R. C., Morris, M. W., Lee, S. K., Pouranfar, F., Wang, Y., & Gozal, D. (2008). Neuroglobin protects PC12 cells against oxidative stress. *Brain research*, *1190*, 159-166.

Li, R. C., Morris, M. W., Lee, S. K., Pouranfar, F., Wang, Y., & Gozal, D. (2008). Neuroglobin protects PC12 cells against oxidative stress. *Brain research*, *1190*, 159-166.

Li, R. C., Pouranfar, F., Lee, S. K., Morris, M. W., Wang, Y., & Gozal, D. (2008). Neuroglobin protects PC12 cells against β-amyloid-induced cell injury.*Neurobiology of aging*, *29*(12), 1815-1822.

Li, W., Wu, Y., Ren, C., Lu, Y., Gao, Y., Zheng, X., & Zhang, C. (2011). The activity of recombinant human neuroglobin as an antioxidant and free radical scavenger. *Proteins: Structure, Function, and Bioinformatics*, *79*(1), 115-125.

Li, X., Fang, P., Mai, J., Choi, E. T., Wang, H., & Yang, X. F. (2013). Targeting mitochondrial reactive oxygen species as novel therapy for inflammatory diseases and cancers. *Journal of hematology & oncology*, *6*(1), 19.

Li, X., Lu, Y., Jin, W., Liang, K., Mills, G. B., & Fan, Z. (2006). Autophosphorylation of Akt at Threonine 72 and Serine 246 A potential mechanism of regulation of Akt kinase activity. *Journal of Biological Chemistry*, *281*(19), 13837-13843.

Li, X., Zhao, X., Fang, Y., Jiang, X., Duong, T., Fan, C., ... & Kain, S. R. (1998). Generation of destabilized green fluorescent protein as a transcription reporter. *Journal of Biological Chemistry*, *273*(52), 34970-34975.

Liang, J., Xie, Q., Li, P., Zhong, X., & Chen, Y. (2015). Mitochondrial estrogen receptor β inhibits cell apoptosis via interaction with Bad in a ligand-independent manner. *Molecular and cellular biochemistry*, *401*(1-2), 71-86.

Lin, C. Y., Ström, A., Kong, S. L., Kietz, S., Thomsen, J. S., Tee, J. B., ... & Gustafsson, J. Å. (2007). Inhibitory effects of estrogen receptor beta on specific hormone-responsive gene expression and association with disease outcome in primary breast cancer. *Breast Cancer Research*, *9*(2), R25.

Lin, Y., Fang, L., Xue, X. H., Murong, S. X., Wang, N., & Wu, Z. Y. (2008). Association between Ngb polymorphisms and ischemic stroke in the Southern Chinese Han population. *BMC medical genetics*, *9*(1), 1.

Lindberg, M. K., Movérare, S., Skrtic, S., Gao, H., Dahlman-Wright, K., Gustafsson, J. A., & Ohlsson, C. (2003). Estrogen receptor (ER)-β reduces ERα-regulated gene transcription, supporting a "Ying Yang" relationship between ERα and ERβ in mice.*Molecular endocrinology*, *17*(2), 203-208.

Lipton, P. (1999). Ischemic cell death in brain neurons. *Physiological reviews*, *79*(4), 1431-1568.

Liu, J., Yu, Z., Guo, S., Lee, S. R., Xing, C., Zhang, C., ... & Wang, X. (2009). Effects of neuroglobin overexpression on mitochondrial function and oxidative stress following hypoxia/reoxygenation in cultured neurons. *Journal of neuroscience research*, *87*(1), 164-170.

Liu, J., Yu, Z., Guo, S., Lee, S. R., Xing, C., Zhang, C., ... & Wang, X. (2009). Effects of neuroglobin overexpression on mitochondrial function and oxidative stress following hypoxia/reoxygenation in cultured neurons. *Journal of neuroscience research*, *87*(1), 164-170.

Lobenhofer, E. K., Bennett, L., Cable, P. L., Li, L., Bushel, P. R., & Afshari, C. A. (2002). Regulation of DNA replication fork genes by 17β-estradiol. *Molecular Endocrinology*, *16*(6), 1215-1229.

Loetscher, P., Pratt, G., & Rechsteiner, M. (1991). The C terminus of mouse ornithine decarboxylase confers rapid degradation on dihydrofolate reductase. Support for the pest hypothesis. *Journal of Biological Chemistry*, *266*(17), 11213-11220.

Logue, S. E., & Martin, S. J. (2008). Caspase activation cascades in apoptosis. *Biochemical Society Transactions*, *36*(1), 1-9.

Lösel, R., & Wehling, M. (2003). Nongenomic actions of steroid hormones. *Nature Reviews Molecular Cell Biology*, *4*(1), 46-55.

Lutter, M., Fang, M., Luo, X., Nishijima, M., Xie, X. S., & Wang, X. (2000). Cardiolipin provides specificity for targeting of tBid to mitochondria.*Nature cell biology*, *2*(10), 754-761.

MacAskill, A. F., & Kittler, J. T. (2010). Control of mitochondrial transport and localization in neurons.*Trends in cell biology*, *20*(2), 102-112.

Mammen, P. P., Shelton, J. M., Goetsch, S. C., Williams, S. C., Richardson, J. A., Garry, M. G., & Garry, D. J. (2002). Neuroglobin, a novel member of the globin family, is expressed in focal regions of the brain. *Journal of Histochemistry & Cytochemistry*, *50*(12), 1591-1598.

Marc, P., Margeot, A., Devaux, F., Blugeon, C., Corral-Debrinski, M., & Jacq, C. (2002). Genome-wide analysis of mRNAs targeted to yeast mitochondria. *EMBO reports*, *3*(2), 159-164.

Margolis, S. S., Walsh, S., Weiser, D. C., Yoshida, M., Shenolikar, S., & Kornbluth, S. (2003). PP1 control of M phase entry exerted through 14-3-3-regulated Cdc25 dephosphorylation. *The EMBO journal*, *22*(21), 5734-5745.

Marinis, E., Acaz-Fonseca, E., Arevalo, M. A., Ascenzi, P., Fiocchetti, M., Marino, M., & Garcia-Segura, L. M. (2013). 17β-Oestradiol Anti-Inflammatory Effects in Primary Astrocytes Require Oestrogen Receptor β-Mediated Neuroglobin Up-Regulation. *Journal of neuroendocrinology*, *25*(3), 260-270.

Marino, M., Galluzzo, P., & Ascenzi, P. (2006). Estrogen signaling multiple pathways to impact gene transcription. *Current genomics*, *7*(8), 497-508.

Marino, M., Galluzzo, P., Leone, S., Acconcia, F., & Ascenzi, P. (2006). Nitric oxide impairs the 17β-estradiol-induced apoptosis in human colon adenocarcinoma cells. *Endocrine-related cancer*,*13*(2), 559-569.

Martin, C., Ross, M., Chapman, K. E., Andrew, R., Bollina, P., Seckl, J. R., & Habib, F. K. (2004). CYP7B generates a selective estrogen receptor β agonist in human prostate. *The Journal of Clinical Endocrinology & Metabolism*, *89*(6), 2928-2935.

Matsuzaki, S., Szweda, L. I., & Humphries, K. M. (2009). Mitochondrial superoxide production and respiratory activity: biphasic response to ischemic duration. *Archives of biochemistry and biophysics*,*484*(1), 87-93.

Mattson, M. P., Gleichmann, M., & Cheng, A. (2008). Mitochondria in neuroplasticity and neurological disorders. *Neuron*, *60*(5), 748-766.

McGlynn, L. M., Tovey, S., Bartlett, J. M., Doughty, J., Cooke, T. G., & Edwards, J. (2013). Interactions between MAP kinase and oestrogen receptor in human breast cancer. *European Journal of Cancer*, *49*(6), 1176-1186.

Micevych, P. E., & Kelly, M. J. (2012). Membrane estrogen receptor regulation of hypothalamic function. *Neuroendocrinology*, *96*(2), 103-110.

Miller, T. W., Balko, J. M., Fox, E. M., Ghazoui, Z., Dunbier, A., Anderson, H., ... & Manning, H. C. (2011). ERα-dependent E2F transcription can mediate resistance to estrogen deprivation in human breast cancer. *Cancer discovery*, *1*(4), 338-351.

Min, L., & Jian-xing, X. (2007). Detoxifying function of cytochrome c against oxygen toxicity. *Mitochondrion*, *7*(1), 13-16.

Minet, E., Arnould, T., Michel, G., Roland, I., Mottet, D., Raes, M., ... & Michiels, C. (2000). ERK activation upon hypoxia: involvement in HIF-1 activation. *FEBS letters*, *468*(1), 53-58.

Miro, A. M., Sastre-Serra, J., Pons, D. G., Valle, A., Roca, P., & Oliver, J. (2011). 17β-Estradiol regulates oxidative stress in prostate cancer cell lines according to ERalpha/ERbeta ratio. *The Journal of steroid biochemistry and molecular biology*, *123*(3), 133-139.

Mishra, P., & Chan, D. C. (2016). Metabolic regulation of mitochondrial dynamics. *J Cell Biol*, jcb-201511036.

Monroe, D. G., Getz, B. J., Johnsen, S. A., Riggs, B. L., Khosla, S., & Spelsberg, T. C. (2003). Estrogen receptor isoform-specific regulation of endogenous gene expression in human osteoblastic cell lines expressing either ERα or ERβ. *Journal of cellular biochemistry*, *90*(2), 315-326.

Mooney, C., Wang, Y. H., & Pollastri, G. (2011). SCLpred: protein subcellular localization prediction by N-to-1 neural networks. *Bioinformatics*, *27*(20), 2812-2819.

Nakagawa, T., Shimizu, S., Watanabe, T., Yamaguchi, O., Otsu, K., Yamagata, H., ... & Tsujimoto, Y. (2005). Cyclophilin D-dependent mitochondrial permeability transition regulates some necrotic but not apoptotic cell death. *Nature*,*434*(7033), 652-658.

Nakagawa, Y. (2004). Initiation of apoptotic signal by the peroxidation of cardiolipin of mitochondria.*Annals of the New York Academy of Sciences*,*1011*(1), 177-184.

Nantes, I. L., Zucchi, M. R., Nascimento, O. R., & Faljoni-Alario, A. (2001). Effect of heme iron valence state on the conformation of cytochrome c and its association with membrane interfaces A CD and EPR investigation. *Journal of Biological Chemistry*, *276*(1), 153-158.

Nayak, G. H., Prentice, H. M., & Milton, S. L. (2011). Neuroprotective signaling pathways are modulated by adenosine in the anoxia tolerant turtle. *Journal of Cerebral Blood Flow & Metabolism*, *31*(2), 467-475.

Neupert, W. (1997). Protein import into mitochondria. *Annual review of biochemistry*, *66*(1), 863-917.

Nicolson, G. L. (2007). Metabolic syndrome and mitochondrial function: molecular replacement and antioxidant supplements to prevent membrane peroxidation and restore mitochondrial function.*Journal of cellular biochemistry*, *100*(6), 1352-1369.

Nilsen, J., & Brinton, R. D. (2003). Mechanism of estrogen-mediated neuroprotection: regulation of mitochondrial calcium and Bcl-2 expression. *Proceedings of the National Academy of Sciences*,*100*(5), 2842-2847.

Nussey, S. S., & Whitehead, S. A. (2013). *Endocrinology: an integrated approach*. CRC Press.

Olefsky, J. M. (2001). Nuclear receptor minireview series. *Journal of Biological Chemistry*, *276*(40), 36863-36864.

Oleksiewicz, U., Daskoulidou, N., Liloglou, T., Tasopoulou, K., Bryan, J., Gosney, J. R., ... & Xinarianos, G. (2011). Neuroglobin and myoglobin in non-small cell lung cancer: expression, regulation and prognosis. *Lung Cancer*, *74*(3), 411-418.

Orr, A. L., Ashok, D., Sarantos, M. R., Shi, T., Hughes, R. E., & Brand, M. D. (2013). Inhibitors of ROS production by the ubiquinone-binding site of mitochondrial complex I identified by chemical screening. *Free Radical Biology and Medicine*, *65*, 1047-1059.

Orrenius, S., & Zhivotovsky, B. (2005). Cardiolipin oxidation sets cytochrome c free. *Nature chemical biology*, *1*(4), 188-189.

Ott, M., Robertson, J. D., Gogvadze, V., Zhivotovsky, B., & Orrenius, S. (2002). Cytochrome c release from mitochondria proceeds by a two-step process. *Proceedings of the National Academy of Sciences*, *99*(3), 1259-1263.
Ott, M., Robertson, J. D., Gogvadze, V., Zhivotovsky, B., & Orrenius, S. (2002). Cytochrome c release from mitochondria proceeds by a two-step process. *Proceedings of the National Academy of Sciences*, *99*(3), 1259-1263.
Ott, M., Zhivotovsky, B., & Orrenius, S. (2007). Role of cardiolipin in cytochrome c release from mitochondria. *Cell death and differentiation*, *14*(7), 1243.

Ow, Y. L. P., Green, D. R., Hao, Z., & Mak, T. W. (2008). Cytochrome c: functions beyond respiration.*Nature Reviews Molecular Cell Biology*, *9*(7), 532-542.

Paige, L. A., Christensen, D. J., Grøn, H., Norris, J. D., Gottlin, E. B., Padilla, K. M., ... & Fowlkes, D. M. (1999). Estrogen receptor (ER) modulators each induce distinct conformational changes in ER α and ER β. *Proceedings of the National Academy of Sciences*, *96*(7), 3999-4004.

Palma, P. N., Krippahl, L., Wampler, J. E., & Moura, J. J. (2000). BiGGER: a new (soft) docking algorithm for predicting protein interactions. *Proteins: Structure, Function, and Bioinformatics*, *39*(4), 372-384.

Pan, Z., Voehringer, D. W., & Meyn, R. E. (1999). Analysis of redox regulation of cytochrome c-induced apoptosis in a cell-free system. *Cell Death & Differentiation*, *6*(7).

Paradies, G., Petrosillo, G., Paradies, V., & Ruggiero, F. M. (2009). Role of cardiolipin peroxidation and Ca 2+ in mitochondrial dysfunction and disease. *Cell calcium*, *45*(6), 643-650.

Parone, P. A., & Martinou, J. C. (2006). Mitochondrial fission and apoptosis: an ongoing trial. *Biochimica et Biophysica Acta (BBA)-Molecular Cell Research*, *1763*(5), 522-530.

Pedram, A., Razandi, M., Wallace, D. C., & Levin, E. R. (2006). Functional estrogen receptors in the mitochondria of breast cancer cells. *Molecular biology of the cell*, *17*(5), 2125-2137.

Peng, K., Tao, Y., Zhang, J., Wang, J., Ye, F., Dan, G., ... & Zou, Z. (2015). Resveratrol regulates mitochondrial biogenesis and fission/fusion to attenuate rotenone-induced neurotoxicity. *Oxidative medicine and cellular longevity*, *2016*.

Pesce, A., Bolognesi, M., Bocedi, A., Ascenzi, P., Dewilde, S., Moens, L., ... & Burmester, T. (2002). Neuroglobin and cytoglobin. *EMBO reports*, *3*(12), 1146-1151.

Pesce, A., Dewilde, S., Nardini, M., Moens, L., Ascenzi, P., Hankeln, T., ... & Bolognesi, M. (2003). Human brain neuroglobin structure reveals a distinct mode of controlling oxygen affinity.*Structure*, *11*(9), 1087-1095.

Peters, O., Back, T., Lindauer, U., Busch, C., Megow, D., Dreier, J., & Dirnagl, U. (1998). Increased formation of reactive oxygen species after permanent and reversible middle cerebral artery occlusion in the rat. *Journal of Cerebral Blood Flow & Metabolism*, *18*(2), 196-205.

Petrosillo, G., Ruggiero, F. M., Pistolese, M., & Paradies, G. (2001). Reactive oxygen species generated from the mitochondrial electron transport chain induce cytochrome c dissociation from beef-heart submitochondrial particles via cardiolipin peroxidation. Possible role in the apoptosis. *FEBS letters*, *509*(3), 435-438.

Pfanner, N., & Geissler, A. (2001). Versatility of the mitochondrial protein import machinery. *Nature Reviews Molecular Cell Biology*, *2*(5), 339-349.

Pike, A. C., Brzozowski, A. M., Hubbard, R. E., Bonn, T., Thorsell, A. G., Engström, O., ... & Carlquist, M. (1999). Structure of the ligand-binding domain of oestrogen receptor beta in the presence of a partial agonist and a full antagonist.*The EMBO journal*, *18*(17), 4608-4618.

Planchon, T. A., Gao, L., Milkie, D. E., Davidson, M. W., Galbraith, J. A., Galbraith, C. G., & Betzig, E. (2011). Rapid three-dimensional isotropic imaging of living cells using Bessel beam plane illumination. *Nature methods*, *8*(5), 417.

Potter, V. R., & DuBois, K. P. (1942). The quantitative determination of cytochrome c. *Journal of Biological Chemistry*, *142*(1), 417-426.

Prossnitz, E. R., Arterburn, J. B., & Sklar, L. A. (2007). GPR30: AG protein-coupled receptor for estrogen. *Molecular and cellular endocrinology*, *265*, 138-142.

Purring-Koch, C., & McLendon, G. (2000). Cytochrome c binding to Apaf-1: the effects of dATP and ionic strength. *Proceedings of the National Academy of Sciences*, *97*(22), 11928-11931.

Raha, S., & Robinson, B. H. (2001). Mitochondria, oxygen free radicals, and apoptosis. *American journal of medical genetics*, *106*(1), 62-70.

Raida, Z., Hundahl, C. A., Kelsen, J., Nyengaard, J. R., & Hay-Schmidt, A. (2012). Reduced infarct size in neuroglobin-null mice after experimental stroke in vivo. *Experimental & translational stroke medicine*, *4*(1), 15.

Rains, J. L., & Jain, S. K. (2011). Oxidative stress, insulin signaling, and diabetes. *Free Radical Biology and Medicine*, *50*(5), 567-575.

Ratajczak, T. (2001). Protein coregulators that mediate estrogen receptor function. *Reproduction, Fertility and Development*, *13*(4), 221-229.

Ravid, T., & Hochstrasser, M. (2008). Degradation signal diversity in the ubiquitin-proteasome system. *Nature reviews. Molecular cell biology*, *9*(9), 679.

Raychaudhuri, S., Skommer, J., Henty, K., Birch, N., & Brittain, T. (2010). Neuroglobin protects nerve cells from apoptosis by inhibiting the intrinsic pathway of cell death. *Apoptosis*, *15*(4), 401-411.
Raychaudhuri, S., Skommer, J., Henty, K., Birch, N., & Brittain, T. (2010). Neuroglobin protects nerve cells from apoptosis by inhibiting the intrinsic pathway of cell death. *Apoptosis*, *15*(4), 401-411.
Rettberg, J. R., Yao, J., & Brinton, R. D. (2014). Estrogen: a master regulator of bioenergetic systems in the brain and body. *Frontiers in neuroendocrinology*, *35*(1), 8-30.

Reuss, S., Saaler-Reinhardt, S., Weich, B., Wystub, S., Reuss, M. H., Burmester, T., & Hankeln, T. (2002). Expression analysis of neuroglobin mRNA in rodent tissues. *Neuroscience*, *115*(3), 645-656.

Richardson, T. E., Yang, S. H., Wen, Y., & Simpkins, J. W. (2011). Estrogen protection in Friedreich's ataxia skin fibroblasts. *Endocrinology*, *152*(7), 2742-2749.

Riemer, J., Fischer, M., & Herrmann, J. M. (2011). Oxidation-driven protein import into mitochondria: Insights and blind spots. *Biochimica et Biophysica Acta (BBA)-Biomembranes*, *1808*(3), 981-989.

Riggio, M., Polo, M. L., Blaustein, M., Colman-Lerner, A., Lüthy, I., Lanari, C., & Novaro, V. (2011). PI3K/AKT pathway regulates phosphorylation of steroid receptors, hormone independence and tumor differentiation in breast cancer. *Carcinogenesis*, *33*(3), 509-518.

Ripple, M. O., Abajian, M., & Springett, R. (2010). Cytochrome c is rapidly reduced in the cytosol after mitochondrial outer membrane permeabilization. *Apoptosis*, *15*(5), 563-573.

Robb, E. L., & Stuart, J. A. (2011). Resveratrol interacts with estrogen receptor-β to inhibit cell replicative growth and enhance stress resistance by upregulating mitochondrial superoxide dismutase.*Free Radical Biology and Medicine*, *50*(7), 821-831.

Robb, E. L., & Stuart, J. A. (2014). The stilbenes resveratrol, pterostilbene and piceid affect growth and stress resistance in mammalian cells via a mechanism requiring estrogen receptor beta and the induction of Mn-superoxide dismutase.*Phytochemistry*, *98*, 164-173.

Ryan, K. J. (1982). Biochemistry of aromatase: significance to female reproductive physiology. *Cancer research*, *42*(8 Supplement), 3342s-3344s.

Sanchez, E. R. (2012). Chaperoning steroidal physiology: lessons from mouse genetic models of Hsp90 and its cochaperones. *Biochimica et Biophysica Acta (BBA)-Molecular Cell Research*, *1823*(3), 722-729.

Sanchis-Gomar, F., Luis Garcia-Gimenez, J., Carmen Gomez-Cabrera, M., & V Pallardo, F. (2014). Mitochondrial biogenesis in health and disease. Molecular and therapeutic approaches. *Current pharmaceutical design*, *20*(35), 5619-5633.

Santel, A., & Frank, S. (2008). Shaping mitochondria: the complex posttranslational regulation of the mitochondrial fission protein DRP1. *IUBMB life*,*60*(7), 448-455.

Santucci, R., Sinibaldi, F., Patriarca, A., Santucci, D., & Fiorucci, L. (2010). Misfolded proteins and neurodegeneration: role of non-native cytochrome c in cell death. *Expert review of proteomics*, *7*(4), 507-517.

Sarkar, S. N., Huang, R. Q., Logan, S. M., Yi, K. D., Dillon, G. H., & Simpkins, J. W. (2008). Estrogens directly potentiate neuronal L-type Ca2+ channels.*Proceedings of the National Academy of Sciences*,*105*(39), 15148-15153.

Sastre-Serra, J., Nadal-Serrano, M., Pons, D. G., Valle, A., Oliver, J., & Roca, P. (2012). The effects of 17β-estradiol on mitochondrial biogenesis and function in breast cancer cell lines are dependent on the ERα/ERβ ratio. *Cellular Physiology and Biochemistry*, *29*(1-2), 261-268.

Sastre-Serra, J., Valle, A., Company, M. M., Garau, I., Oliver, J., & Roca, P. (2010). Estrogen down-regulates uncoupling proteins and increases oxidative stress in breast cancer. *Free Radical Biology and Medicine*, *48*(4), 506-512.

Saurin, A. T., Martin, J. L., Heads, R. J., Foley, C., Mockridge, J. W., Wright, M. J., ... & Marber, M. S. (2000). The role of differential activation of p38-mitogen-activated protein kinase in preconditioned ventricular myocytes. *The FASEB Journal*, *14*(14), 2237-2246.

Schatz, G., & Dobberstein, B. (1996). Common principles of protein translocation across membranes. *Science*, *271*(5255), 1519.

Schmidt, M., Gerlach, F., Avivi, A., Laufs, T., Wystub, S., Simpson, J. C., ... & Burmester, T. (2004). Cytoglobin is a respiratory protein in connective tissue and neurons, which is up-regulated by hypoxia. *Journal of Biological Chemistry*, *279*(9), 8063-8069.

Schmidt, M., Giessl, A., Laufs, T., Hankeln, T., Wolfrum, U., & Burmester, T. (2003). How does the eye breathe? Evidence for neuroglobin-mediated oxygen supply in the mammalian retina. *Journal of Biological Chemistry*, *278*(3), 1932-1935.

Schrader, C., Schielke, A., Ellerbroek, L., & Johne, R. (2012). PCR inhibitors–occurrence, properties and removal. *Journal of applied microbiology*, *113*(5), 1014-1026.

Schrader, E. K., Harstad, K. G., & Matouschek, A. (2009). Targeting proteins for degradation. *Nature chemical biology*, *5*(11), 815-822.

Schwindinger, W. F., & Robishaw, J. D. (2001). Heterotrimeric G-protein bg-dimers in growth and differentiation. *Oncogene*, *20*(13), 1653-1660.

Sena, L. A., & Chandel, N. S. (2012). Physiological roles of mitochondrial reactive oxygen species. *Molecular cell*, *48*(2), 158-167.

Sharef, S. W., Al-Senaidi, K., & Joshi, S. N. (2013). Successful treatment of cardiomyopathy due to very long-chain acyl-CoA dehydrogenase deficiency: first case report from Oman with literature review. *Oman medical journal*, *28*(5), 354.

Shi, Y., Chen, J., Weng, C., Chen, R., Zheng, Y., Chen, Q., & Tang, H. (2003). Identification of the protein–protein contact site and interaction mode of human VDAC1 with Bcl-2 family proteins.*Biochemical and biophysical research communications*, *305*(4), 989-996.

Simoncini, T., Mannella, P., Fornari, L., Caruso, A., Varone, G., & Genazzani, A. R. (2004). Genomic and non-genomic effects of estrogens on endothelial cells. *Steroids*, *69*(8), 537-542.

Simpkins, J. W., & Dykens, J. A. (2008). Mitochondrial mechanisms of estrogen neuroprotection. *Brain research reviews*, *57*(2), 421-430.

Simpkins, J. W., Yi, K. D., Yang, S. H., & Dykens, J. A. (2010). Mitochondrial mechanisms of estrogen neuroprotection. *Biochimica et Biophysica Acta (BBA)-General Subjects*, *1800*(10), 1113-1120.

Sivitz, W. I., & Yorek, M. A. (2010). Mitochondrial dysfunction in diabetes: from molecular mechanisms to functional significance and therapeutic opportunities. *Antioxidants & redox signaling*, *12*(4), 537-577.

Skommer, J., Wlodkowic, D., & Deptala, A. (2007). Larger than life: mitochondria and the Bcl-2 family.*Leukemia research*, *31*(3), 277-286.

Smagghe, B. J., Trent III, J. T., & Hargrove, M. S. (2008). NO dioxygenase activity in hemoglobins is ubiquitous in vitro, but limited by reduction in vivo.*PloS one*, *3*(4), e2039.

Smith, C. L., & O'Malley, B. W. (2004). Coregulator function: a key to understanding tissue specificity of selective receptor modulators. *Endocrine reviews*, *25*(1), 45-71.

Soltysik, K., & Czekaj, P. (2013). Membrane estrogen receptors-is it an alternative way of estrogen action. *J Physiol Pharmacol*, *64*(2), 129-142.

Stanton, R. C., Seifter, J. L., Boxer, D. C., Zimmerman, E., & Cantley, L. C. (1991). Rapid release of bound glucose-6-phosphate dehydrogenase by growth factors. Correlation with increased enzymatic activity. *Journal of Biological Chemistry*, *266*(19), 12442-12448.

Stellwagen, E. (1968). Carboxymethylation of horse heart ferricytochrome c and cyanferricytochrome c. *Biochemistry*, *7*(7), 2496-2501.

Stossi, F., Barnett, D. H., Frasor, J., Komm, B., Lyttle, C. R., & Katzenellenbogen, B. S. (2004). Transcriptional profiling of estrogen-regulated gene expression via estrogen receptor (ER) α or ERβ in human osteosarcoma cells: distinct and common target genes for these receptors. *Endocrinology*,*145*(7), 3473-3486.

Suen, D. F., Norris, K. L., & Youle, R. J. (2008). Mitochondrial dynamics and apoptosis. *Genes & development*, *22*(12), 1577-1590.

Sun, Y., Jin, K., Mao, X. O., Zhu, Y., & Greenberg, D. A. (2001). Neuroglobin is up-regulated by and protects neurons from hypoxic-ischemic injury. *Proceedings of the National Academy of Sciences*,*98*(26), 15306-15311.

Sun, Y., Jin, K., Peel, A., Mao, X. O., Xie, L., & Greenberg, D. A. (2003). Neuroglobin protects the brain from experimental stroke in vivo. *Proceedings of the National Academy of Sciences*, *100*(6), 3497-3500.

Sun, Y., Jin, K., Peel, A., Mao, X. O., Xie, L., & Greenberg, D. A. (2003). Neuroglobin protects the brain from experimental stroke in vivo.*Proceedings of the National Academy of Sciences*,*100*(6), 3497-3500.

Sur, K., McFall, S. M., Yeh, E. T., Jangam, S. R., Hayden, M. A., Stroupe, S. D., & Kelso, D. M. (2010). Immiscible phase nucleic acid purification eliminates PCR inhibitors with a single pass of paramagnetic particles through a hydrophobic liquid. *The Journal of Molecular Diagnostics*, *12*(5), 620-628.

Suslov, O., & Steindler, D. A. (2005). PCR inhibition by reverse transcriptase leads to an overestimation of amplification efficiency. *Nucleic acids research*, *33*(20), e181-e181.

Suto, D., Sato, K., Ohba, Y., Yoshimura, T., & Fujii, J. (2005). Suppression of the pro-apoptotic function of cytochrome c by singlet oxygen via a haem redox state-independent mechanism. *Biochemical Journal*, *392*(2), 399-406.

Szeto, H. H. (2006). Mitochondria-targeted peptide antioxidants: novel neuroprotective agents. *The AAPS journal*, *8*(3), E521-E531.

Szymanski, M., Wang, R., Fallin, M. D., Bassett, S. S., & Avramopoulos, D. (2010). Neuroglobin and Alzheimer's dementia: Genetic association and gene expression changes. *Neurobiology of aging*,*31*(11), 1835-1842.

Tapodi, A., Debreceni, B., Hanto, K., Bognar, Z., Wittmann, I., Gallyas, F., ... & Sumegi, B. (2005). Pivotal role of Akt activation in mitochondrial protection and cell survival by poly (ADP-ribose) polymerase-1 inhibition in oxidative stress. *Journal of Biological Chemistry*, *280*(42), 35767-35775.

Taylor, R. C., Cullen, S. P., & Martin, S. J. (2008). Apoptosis: controlled demolition at the cellular level. *Nature reviews Molecular cell biology*, *9*(3), 231-241.

Thomas, C., & Gustafsson, J. Å. (2011). The different roles of ER subtypes in cancer biology and therapy. *Nature Reviews Cancer*, *11*(8), 597-608.

Tondera, D., Grandemange, S., Jourdain, A., Karbowski, M., Mattenberger, Y., Herzig, S., ... & Ehses, S. (2009). SLP-2 is required for stress-induced mitochondrial hyperfusion. *The EMBO journal*, *28*(11), 1589-1600.

Toshiyuki, M., & Reed, J. C. (1995). Tumor suppressor p53 is a direct transcriptional activator of the human bax gene. *Cell*, *80*(2), 293-299.

Totta, P., Pesiri, V., Marino, M., & Acconcia, F. (2014). Lysosomal function is involved in 17β-estradiol-induced estrogen receptor α degradation and cell proliferation. *PloS one*, *9*(4), e94880.

Trent, J. T., & Hargrove, M. S. (2002). A ubiquitously expressed human hexacoordinate hemoglobin.*Journal of Biological Chemistry*, *277*(22), 19538-19545.

Truscott, K. N., Brandner, K., & Pfanner, N. (2003). Mechanisms of protein import into mitochondria.*Current Biology*, *13*(8), R326-R337.

Tuominen, E. K., Wallace, C. J., & Kinnunen, P. K. (2002). Phospholipid-cytochrome c interaction evidence for the extended lipid anchorage. *Journal of Biological Chemistry*, *277*(11), 8822-8826.

Ungvari, Z., Sonntag, W. E., De Cabo, R., Baur, J. A., & Csiszar, A. (2011). Mitochondrial protection by resveratrol. *Exercise and sport sciences reviews*, *39*(3), 128.

Valente, A. J., Maddalena, L. A., Robb, E. L., Moradi, F., & Stuart, J. A. (2017). A simple ImageJ macro tool for analyzing mitochondrial network morphology in mammalian cell culture. *Acta Histochemica*, *119*(3), 315-326.

Valero, T. (2014). Editorial (Thematic Issue: Mitochondrial Biogenesis: Pharmacological Approaches). *Current pharmaceutical design*, *20*(35), 5507-5509.

Vallone, B., Nienhaus, K., Brunori, M., & Nienhaus, G. U. (2004). The structure of murine neuroglobin: novel pathways for ligand migration and binding.*Proteins: Structure, Function, and Bioinformatics*,*56*(1), 85-92.

van Beek-Harmsen, B. J., & van der Laarse, W. J. (2005). Immunohistochemical determination of cytosolic cytochrome C concentration in cardiomyocytes. *Journal of Histochemistry & Cytochemistry*, *53*(7), 803-807.

Varshavsky, A. (1996). The N-end rule: functions, mysteries, uses. *Proceedings of the National Academy of Sciences*, *93*(22), 12142-12149.

Veitch, N. C. (2004). Horseradish peroxidase: a modern view of a classic enzyme. *Phytochemistry*, *65*(3), 249-259.

Ventura-Clapier, R., Garnier, A., & Veksler, V. (2008). Transcriptional control of mitochondrial biogenesis: the central role of PGC-1α. *Cardiovascular research*, *79*(2), 208-217.

Vosler, P. S., Graham, S. H., Wechsler, L. R., & Chen, J. (2009). Mitochondrial targets for stroke focusing basic science research toward development of clinically translatable therapeutics. *Stroke*, *40*(9), 3149-3155.

Wakasugi, K., & Morishima, I. (2005). Preparation and characterization of a chimeric zebrafish-human neuroglobin engineered by module substitution. *Biochemical and biophysical research communications*, *330*(2), 591-597.

Wakasugi, K., Kitatsuji, C., & Morishima, I. (2005). Possible neuroprotective mechanism of human neuroglobin. *Annals of the New York Academy of Sciences*, *1053*(1), 220-230.

Wakasugi, K., Nakano, T., & Morishima, I. (2003). Oxidized human neuroglobin acts as a heterotrimeric Gα protein guanine nucleotide dissociation inhibitor. *Journal of Biological Chemistry*, *278*(38), 36505-36512.

Wang, I. H., Chen, H. Y., Wang, Y. H., Chang, K. W., Chen, Y. C., & Chang, C. R. (2014). Resveratrol modulates mitochondria dynamics in replicative senescent yeast cells. *PloS one*, *9*(8), e104345.

Wang, L. M., Wang, Y. J., Cui, M., Luo, W. J., Wang, X. J., Barber, P. A., & Chen, Z. Y. (2013). A dietary polyphenol resveratrol acts to provide neuroprotection in recurrent stroke models by regulating AMPK and SIRT1 signaling, thereby reducing energy requirements during ischemia.*European Journal of Neuroscience*, *37*(10), 1669-1681.

Wang, X. (2013). Mitochondrial mechanisms of neuroglobin's neuroprotection. *Oxidative medicine and cellular longevity*, *2013*.

Wang, X., Grammatikakis, N., Siganou, A., Stevenson, M. A., & Calderwood, S. K. (2004). Interactions between Extracellular Signal-regulated Protein Kinase 1, 14-3-3ϵ, and Heat Shock Factor 1 during Stress. *Journal of Biological Chemistry*, *279*(47), 49460-49469.

Wang, X., Liu, J., Zhu, H., Tejima, E., Tsuji, K., Murata, Y., ... & Lo, E. H. (2008). Effects of neuroglobin overexpression on acute brain injury and long-term outcomes after focal cerebral ischemia. *Stroke*, *39*(6), 1869-1874.

Watanabe, S., & Wakasugi, K. (2008). Neuroprotective function of human neuroglobin is correlated with its guanine nucleotide dissociation inhibitor activity. *Biochemical and biophysical research communications*, *369*(2), 695-700.

Watanabe, S., Takahashi, N., Uchida, H., & Wakasugi, K. (2012). Human neuroglobin functions as an oxidative stress-responsive sensor for neuroprotection. *Journal of Biological Chemistry*, *287*(36), 30128-30138.

Weigel, N. L., & Zhang, Y. (1998). Ligand-independent activation of steroid hormone receptors. *Journal of molecular medicine*, *76*(7), 469-479.

Weiland, T. R., Kundu, S., Trent, J. T., Hoy, J. A., & Hargrove, M. S. (2004). Bis-histidyl hexacoordination in hemoglobins facilitates heme reduction kinetics. *Journal of the American Chemical Society*, *126*(38), 11930-11935.

Whitten, P. L., & Naftolin, F. (1998). 8Reproductive actions of phytoestrogens. *Bailliere's clinical endocrinology and metabolism*, *12*(4), 667-690.

Whitten, P. L., & Patisaul, H. B. (2001). Cross-species and interassay comparisons of phytoestrogen action. *Environmental health perspectives*, *109*(Suppl 1), 5.

Wu, E. H., & Wong, Y. H. (2006). Activation of muscarinic M 4 receptor augments NGF-induced pro-survival Akt signaling in PC12 cells. *Cellular signalling*, *18*(3), 285-293.

Wystub, S., Laufs, T., Schmidt, M., Burmester, T., Maas, U., Saaler-Reinhardt, S., ... & Reuss, S. (2003). Localization of neuroglobin protein in the mouse brain. *Neuroscience letters*, *346*(1), 114-116.

Xu, J., Wu, R. C., & O'Malley, B. W. (2009). Normal and cancer-related functions of the p160 steroid receptor coactivator (SRC) family. *Nature reviews. Cancer*, *9*(9), 615.

Yang, S. H., Liu, R., Perez, E. J., Wen, Y., Stevens, S. M., Valencia, T., ... & Simpkins, J. W. (2004). Mitochondrial localization of estrogen receptor β.*Proceedings of the National Academy of Sciences*,*101*(12), 4130-4135.

Yao, J., & Brinton, R. D. (2012). Estrogen regulation of mitochondrial bioenergetics: implications for prevention of Alzheimer's disease. *Advances in pharmacology (San Diego, Calif.), 64*, 327.

Ye, S. Q., Zhou, X. Y., Lai, X. J., Zheng, L., & Chen, X. Q. (2009). Silencing neuroglobin enhances neuronal vulnerability to oxidative injury by down-regulating 14-3-3γ. *Acta pharmacologica Sinica*, *30*(7), 913-918.

Yong-ling, P. O., Green, D. R., Hao, Z., & Mak, T. W. (2008). Cytochrome c: functions beyond respiration. *Nature reviews. Molecular cell biology*, *9*(7), 532.

Yoshikawa, T., Furukawa, Y., Wakamatsu, Y., Takemura, S., Tanaka, H., & Kondo, M. (1982). Experimental hypoxia and lipid peroxide in rats. *Biochemical medicine*, *27*(2), 207-213.

Youle, R. J., & Van Der Bliek, A. M. (2012). Mitochondrial fission, fusion, and stress. *Science*, *337*(6098), 1062-1065.

Yu, S. W., Andrabi, S. A., Wang, H., Kim, N. S., Poirier, G. G., Dawson, T. M., & Dawson, V. L. (2006). Apoptosis-inducing factor mediates poly (ADP-ribose)(PAR) polymer-induced cell death.*Proceedings of the National Academy of Sciences*,*103*(48), 18314-18319.

Yu, T., Wang, X., Purring-Koch, C., Wei, Y., & McLendon, G. L. (2001). A mutational epitope for cytochrome C binding to the apoptosis protease activation factor-1. *Journal of Biological Chemistry*,*276*(16), 13034-13038.

Yu, T., Wang, X., Purring-Koch, C., Wei, Y., & McLendon, G. L. (2001). A mutational epitope for cytochrome C binding to the apoptosis protease activation factor-1. *Journal of Biological Chemistry*, *276*(16), 13034-13038.

Yu, Z., Liu, J., Guo, S., Xing, C., Fan, X., Ning, M., ... & Wang, X. (2009). Neuroglobin-overexpression alters hypoxic response gene expression in primary neuron culture following oxygen glucose deprivation. *Neuroscience*, *162*(2), 396-403.

Yu, Z., Liu, N., Li, Y., Xu, J., & Wang, X. (2013). Neuroglobin overexpression inhibits oxygen–glucose deprivation-induced mitochondrial permeability transition pore opening in primary cultured mouse cortical neurons. *Neurobiology of disease*, *56*, 95-103.

Yu, Z., Liu, N., Liu, J., Yang, K., & Wang, X. (2012). Neuroglobin, a novel target for endogenous neuroprotection against stroke and neurodegenerative disorders. *International journal of molecular sciences*, *13*(6), 6995-7014.

Yu, Z., Xu, J., Liu, N., Wang, Y., Li, X., Pallast, S., ... & Wang, X. (2012). Mitochondrial distribution of neuroglobin and its response to oxygen–glucose deprivation in primary-cultured mouse cortical neurons. *Neuroscience*, *218*, 235-242.

Zhang, C., Wang, C., Deng, M., Li, L., Wang, H., Fan, M., ... & He, F. (2002). Full-length cDNA cloning of human neuroglobin and tissue expression of rat neuroglobin. *Biochemical and biophysical research communications*, *290*(5), 1411-1419.

Zhang, J., Lan, S. J., Liu, Q. R., Liu, J. M., & Chen, X. Q. (2013). Neuroglobin, a novel intracellular hexa-coordinated globin, functions as a tumor suppressor in hepatocellular carcinoma via Raf/MAPK/Erk. *Molecular pharmacology*, *83*(5), 1109-1119.

Zhao, H., Shimohata, T., Wang, J. Q., Sun, G., Schaal, D. W., Sapolsky, R. M., & Steinberg, G. K. (2005). PI-3/AKT kinase pathway contributes to neuroprotective effect of hypothermia against cerebral ischemia in rats. *Journal of Cerebral Blood Flow & Metabolism*, *25*, S472-S472.

Zhao, Y., Wang, Z. B., & Xu, J. X. (2003). Effect of Cytochrome c on the Generation and Elimination of O and H2O2 in Mitochondria. *Journal of Biological Chemistry*, *278*(4), 2356-2360.

Zhou, M., Diwu, Z., Panchuk-Voloshina, N., & Haugland, R. P. (1997). A stable nonfluorescent derivative of resorufin for the fluorometric determination of trace hydrogen peroxide: applications in detecting the activity of phagocyte NADPH oxidase and other oxidases. *Analytical biochemistry*, *253*(2), 162-168.

Zhu, C., Wang, X., Qiu, L., Peeters-Scholte, C., Hagberg, H., & Blomgren, K. (2004). Nitrosylation precedes caspase-3 activation and translocation of apoptosis-inducing factor in neonatal rat cerebral hypoxia-ischaemia. *Journal of neurochemistry*,*90*(2), 462-471.

Zhu, Y., Li, M., Wang, X., Jin, H., Liu, S., Xu, J., & Chen, Q. (2012). Caspase cleavage of cytochrome c1 disrupts mitochondrial function and enhances cytochrome c release. *Cell research*, *22*(1), 127-141.

Zhu, Y., Sun, Y., Jin, K., & Greenberg, D. A. (2002). Hemin induces neuroglobin expression in neural cells. *Blood*, *100*(7), 2494-2498.

Zucchi, M. R., Nascimento, O. R., Faljoni-Alario, A., Prieto, T., & Iseli, L. (2003). Modulation of cytochrome c spin states by lipid acyl chains: a continuous-wave electron paramagnetic resonance (CW-EPR) study of haem iron.*Biochemical Journal*, *370*(2), 671-678.

7.0 Appendix

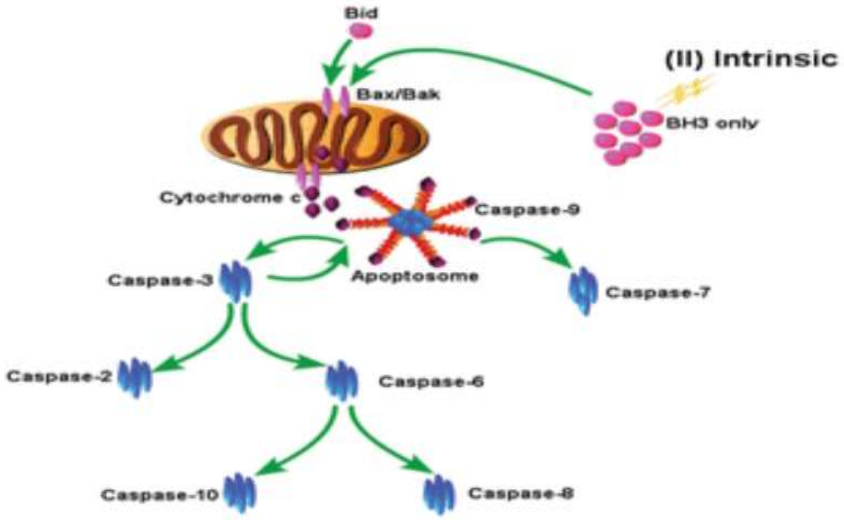

Figure 1.1 Intrinsic Apoptotic Pathway

The figure depicts the intrinsic apoptotic pathway. The release of cytochrome c from the mitochondrion into the cytosol, leads to the formation of the apoptosome. The apoptosome activates procaspase-9 into caspase-9 that activates the caspase cascade, inexorably leading to apoptosis. The image was obtained from Logue and Martin, 2008.

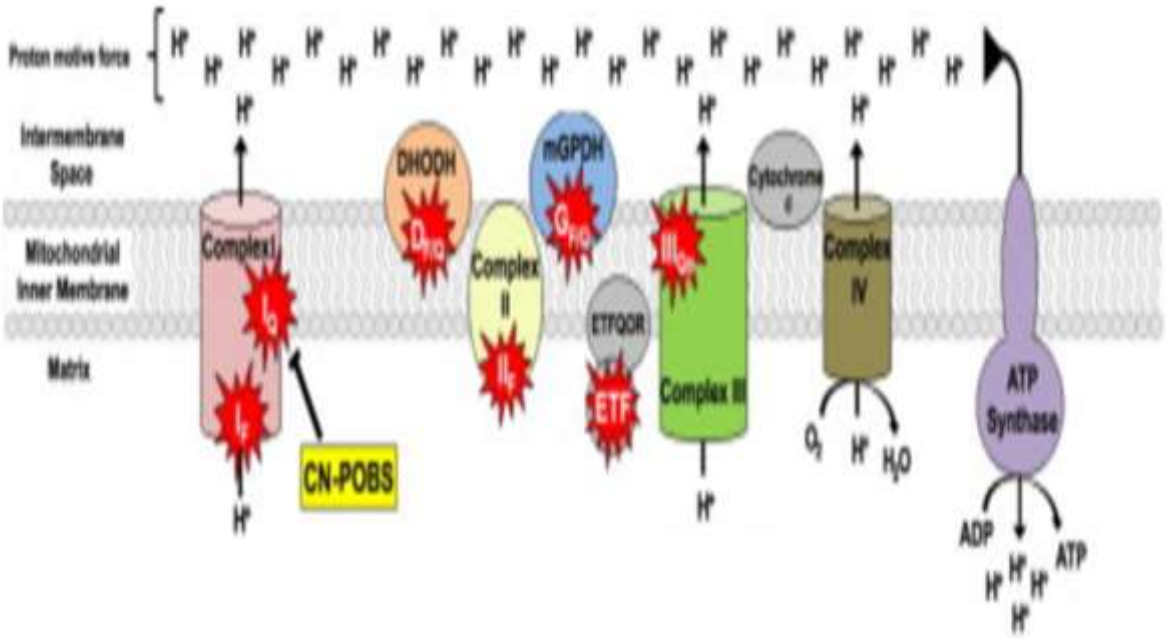

Figure 1.2 Electron Transport Chain in the Inner Mitochondrial Membrane

The figure depicts the complexes embedded within the inner mitochondrial membrane that are responsible for transport of electrons. The sites at which ROS are produced is portrayed as the red shapes. The image was obtained from Orr et al., 2013.

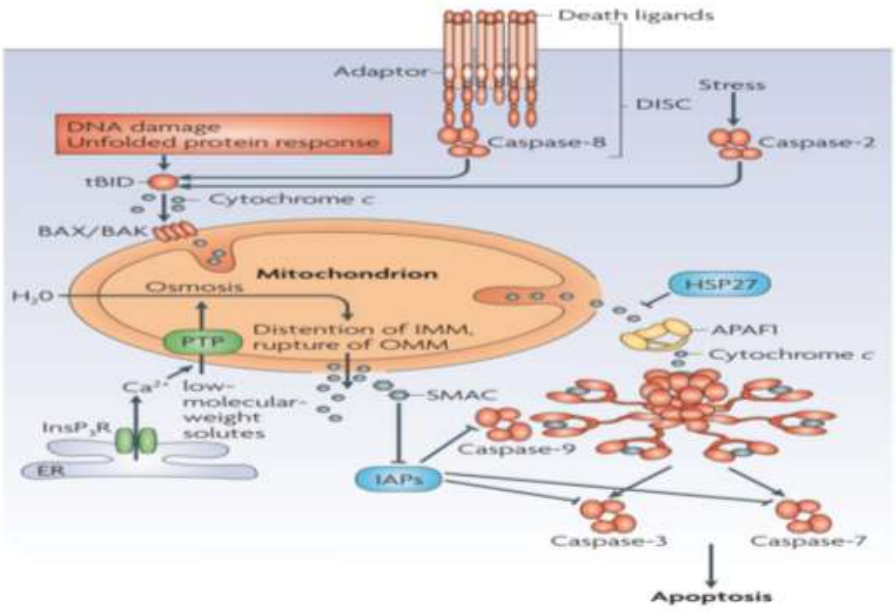

Figure 1.3 Apoptotic Signalling Pathway

The figure depicts both the extrinsic and the intrinsic apoptotic pathway. The bottom left corner of the figure shows the release of cytochrome c from the mitochondrion into the cytosol, forming the apoptosome. The apoptosome activates procaspase-9 into caspase-9 that will eventually lead to apoptosis. The image was obtained from Yong-ling et al., 2008.

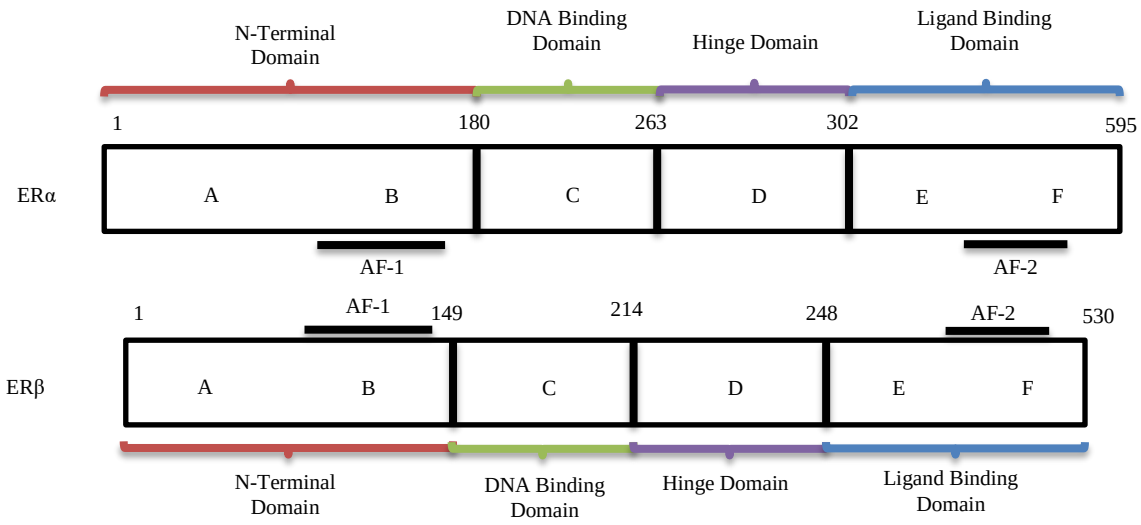

Figure 1.4 Estrogen Receptor Structure

The figure depicts the structural overview of the estrogen receptors. The top structure portrays the ERα and the bottom structure pertains to ERβ. The numbers on the structures represent the amino acid sequences, and the domains are labeled from A to F; domains A and B form the N-Terminal Domain, and E and F form the Ligand Binding Domain. AF: Activation Function

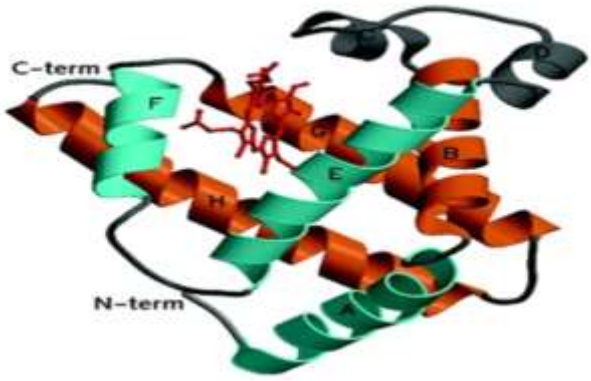

Figure 1.5 Three "Over" Three Globin Fold Structure Overview

The figure depicts the globin fold of Ngb, comprised of 8 α-helical segments labeled from A to H. The three over three fold involves 3 helices B, G and H "over" the 3 helices A, E and F. The haem group is "sandwiched" within the fold. The image was obtained from Pesce et al., 2002.

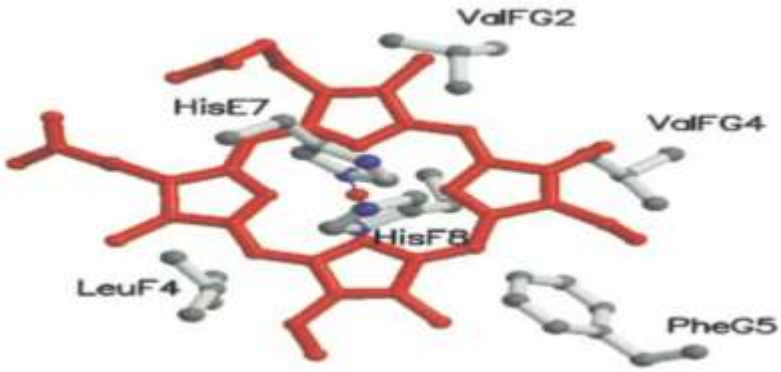

Figure 1.6 Stereo View of the Hexacoordinate Haem
The residues HisE7 (distal), HisF8, LeuF4, ValFG2, ValFG4, and PheG5 (proximal) are depicted. The HisE7 and HisF8 residues assume an orthogonal orientation. The image was obtained from Pesce et al., 2003.

Ngb

MERPEPELIRQSWRAVSRSPLEHGTVLFARLFALEPDLLPLFQYNCRQFSSPEDCLSSPEFLDHIRKVMLVID
AAVTNVEDLSSLEEYLASLGRKHRAVGVKLSSFSTVGESLLYMLEKCLGPAFTPATRAAWSQLYGAVVQA
MSRGWDGE

Figure 1.7 Primary Structure of Ngb with ERK and 14-3-3 Binding Sites
The residues HisE7 and HisF8 that coordinate the haem group are highlighted in yellow, the residues comprising the 14-3-3 binding sites are highlighted in green and the pink highlight represents the ERK docking site. The letters in dark represent the phosphorylation of PKA and ERK.

Mb

MGLSDGEWQLVLNVWGKVEADIPGHGQEVLIRLFKGHPETLEKFDKFKHLKSEDEMKASEDLKKHGATV
LTALGGILKKKGHHEAEIKPLAQSHATKHKIPVKYLEFISECIIQVLQSKHPGDFGADAQGAMNKALELFRK
DMASNYKELGFQG

Hbα

MVLSPADKTNVKAAWGKVGAHAGEYGAEALERMFLSFPTTKTYFPHFDLSHGSAQVKGHGKKVADALT
NAVAHVDDMPNALSALSDLHAHKLRVDPVNFKLLSHCLLVTLAAHLPAEFTPAVHASLDKFLASVSTVLT
SKYR

Hbβ

MVHLTPEEKSAVTALWGKVNVDEVGGEALGRLLVVYPWTQRFFESFGDLSTPDAVMGNPKVKAHGKKV
LGAFSDGLAHLDNLKGTFATLSELHCDKLHVDPENFRLLGNVLVCVLAHHFGKEFTPPVQAAYQKVVAG
VANALAHKYH

Ngb

MERPEPELIRQSWRAVSRSPLEHGTVLFAR***L***FALEPDLLPL***F***Q***Y***NCRQFSSPEDCLSSPEFLD***H***IR***K******V***ML***V***ID
AAVTNVEDLSSLEEYLAS***L***GRK***H***RAVGVKLSS***F***ST***V***GESLLYMLEKCLGPAFTPATRAAWSQLYGAVVQA
MSRGWDGE

Figure 1.8 Primary Structures of the Globins Ngb, Mb and Hb
The top amino acid sequence represents myoglobin, the second and third amino acid sequences represent haemoglobin (α and β respectively) and the bottom line represents neuroglobin. The residues HisE7 and HisF8 that coordinate the haem group are highlighted in yellow on the Ngb sequence. The residues that come into contact with the haem group are italicized, underlined and in bold.

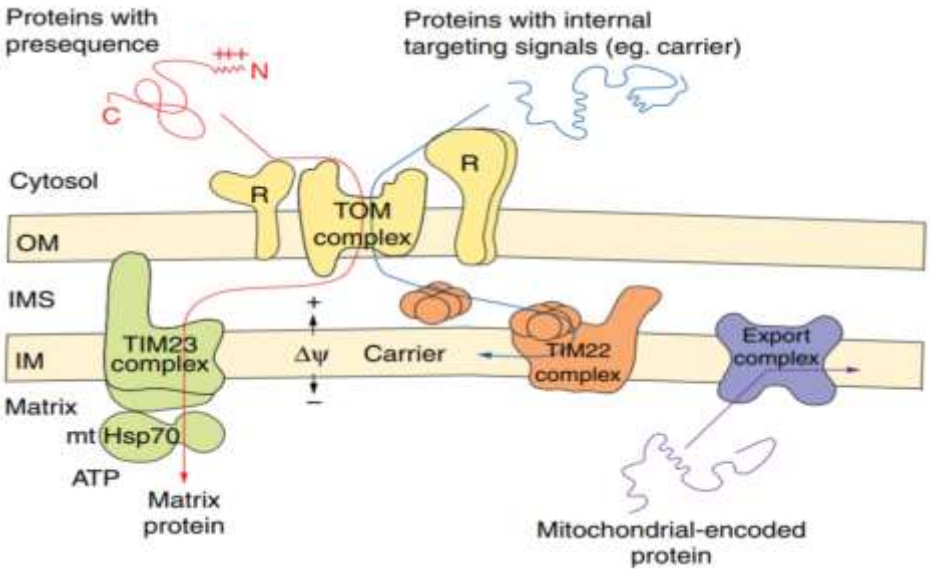

Figure 1.9 Protein Import into Mitochondrion
The complexes TOM, TIM23 and TIM22 are responsible for importing proteins destined to the internal compartments, while the Export complex is responsible for exporting proteins from the matrix and into the inner membrane. The specific receptor (R) is the site of binding for proteins with the N-terminal sequence or internal signals, which then directs the protein through the general import pore (GIP) of the translocase of the outer membrane (TOM). The proteins with the N-terminal presequence are imported across the inner membrane via the TIM23 complex and into the matrix. The proteins with the internal targeting sequences are destined for the inner membrane, and are directed by the Tim factors to the TIM22. Membrane insertion at the TIM22 complex is dependent on the membrane potential. The export complex export proteins that are encoded in the mitochondria and some imported proteins to the inner membrane. IM: inner membrane; IMS: intermembrane space; OM: outer membrane. The image was obtained from Truscott et al., 2003.

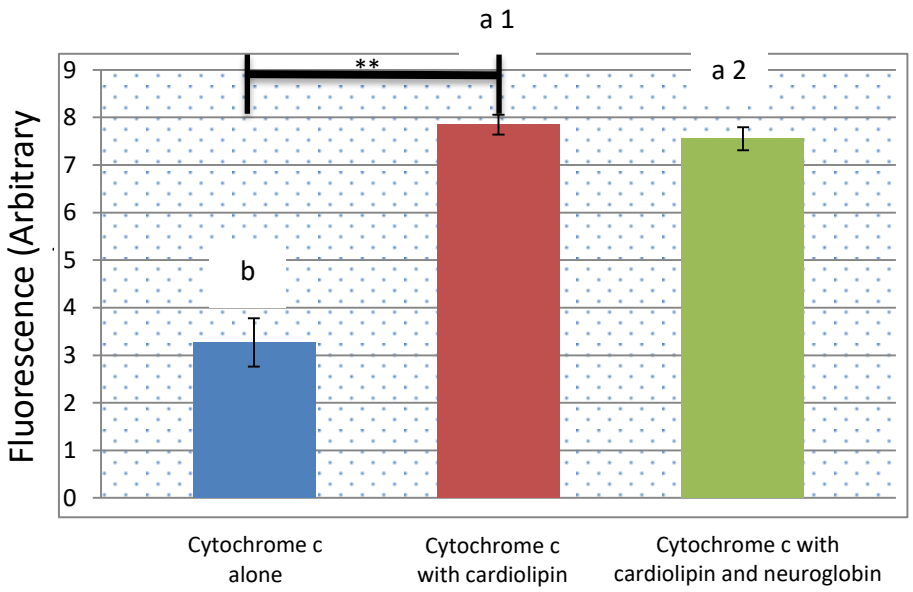

Figure 2.1: Neuroglobin does not inhibit Cytochrome c Peroxidase Activity

The bar chart shows the three different experimental conditions: cytochrome c alone (negative control), cytochrome c with cardiolipin (positive control) and cytochrome c with cardiolipin and neuroglobin. The bars represent means ± SEM from triplicates for each condition. The statistical analysis between the positive control (a1) and the experimental condition (a2) were analyzed with the independent T-test (p-value = 0.24). ** indicates a p-value less than 0.001.

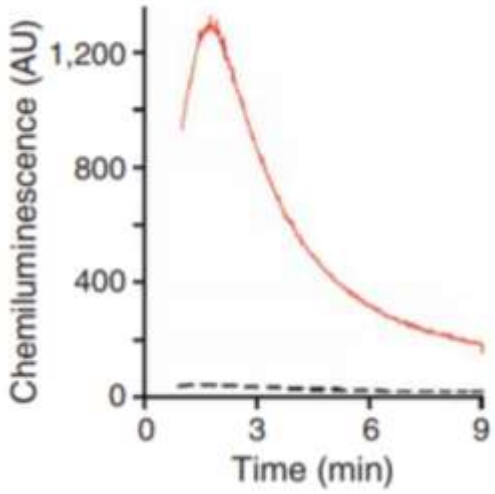

Figure 2.2 H_2O_2-Induced oxidation chemiluminescence response

The figure depicts the oxidation of luminol via H_2O_2 in a manner similar to the Amplex Red reagent. The red curve shows cyt c with cardiolipin, while the black dotted curve shows cyt c without cardiolipin.

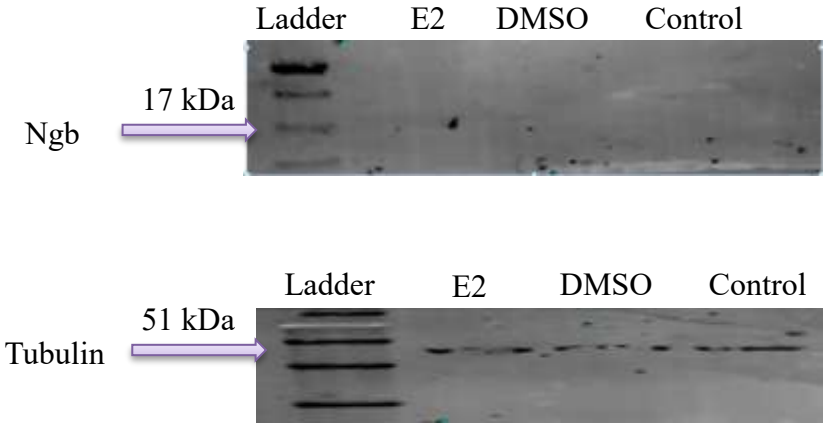

Figure 3.1 Western Blot Visualization of Ngb

The images of the membranes show the attempted detection of Ngb after treatment with 10 nM E2, vehicle and negative controls for 24 hours. The top image shows Ngb detection and the bottom image shows tubulin loading control.

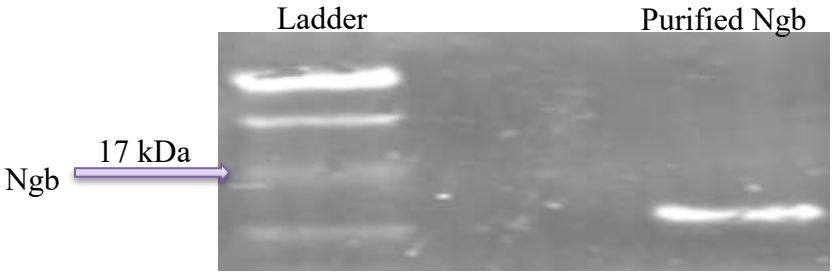

Figure 3.2 Western Blot Visualization of Purified Ngb

The images of the membrane show the detection of 2 µg of purified Ngb.

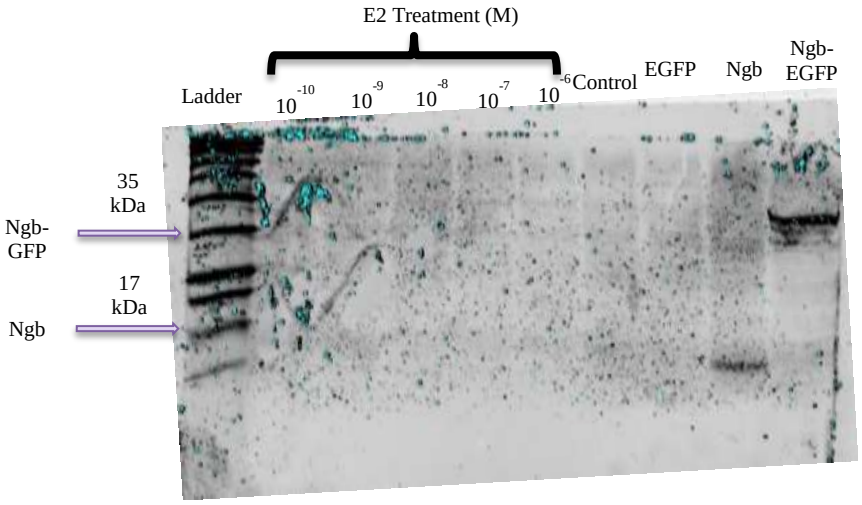

Figure 3.3 Western Blot Visualization of Ngb with Different E2 Concentrations and Plasmid Variant Transfections

The image of the membrane shows the detection of Ngb after treatment of different E2 concentrations and negative control for 24 hours. The last three lanes show the attempted detection of Ngb bands after SH-SY5Y transient transfection; the Ngb bands

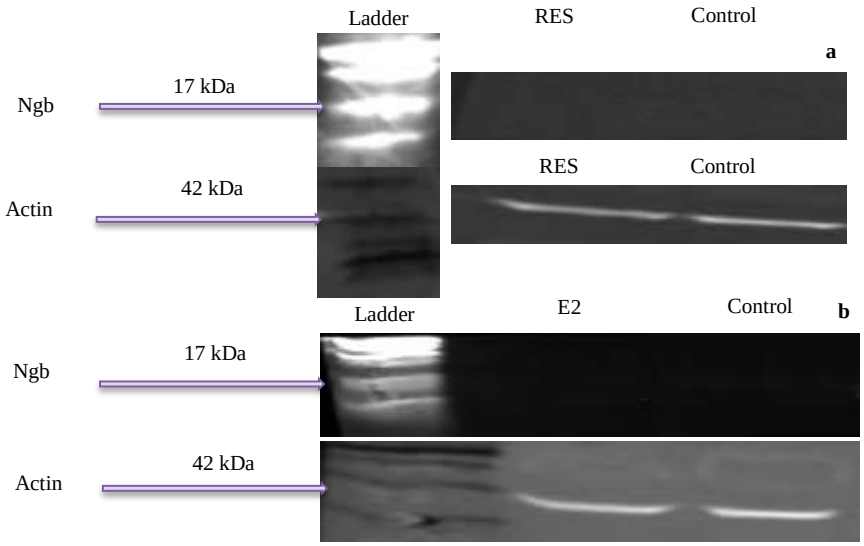

Figure 3.4 Western Blot Visualization of Ngb after Treatment with 10 µM E2 or RES for 24 hours

The top half images of the membranes show the detection of Ngb after treatment of a) E2 and b) RES. The bottom half images of a) and b) show the actin loading control.

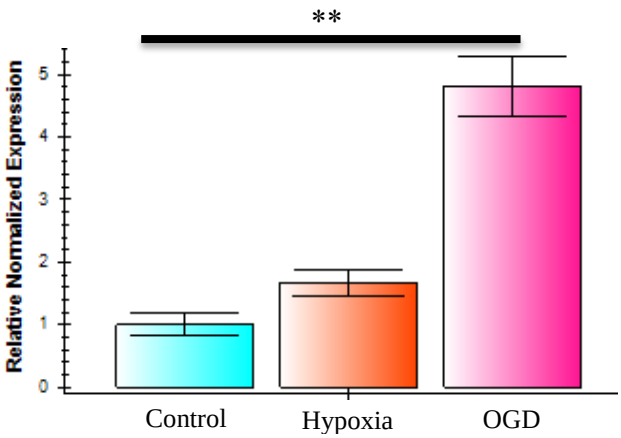

Figure 3.5 Ngb mRNA Transcript Levels in SH-SY5Y with OGD and Hypoxia

The hypoxia and OGD PCR was used as a positive control for the success of the technique. The mRNA level is greatly upregulated in OGD, but is not significant in hypoxia. The housekeeping gene used here is GAPD.

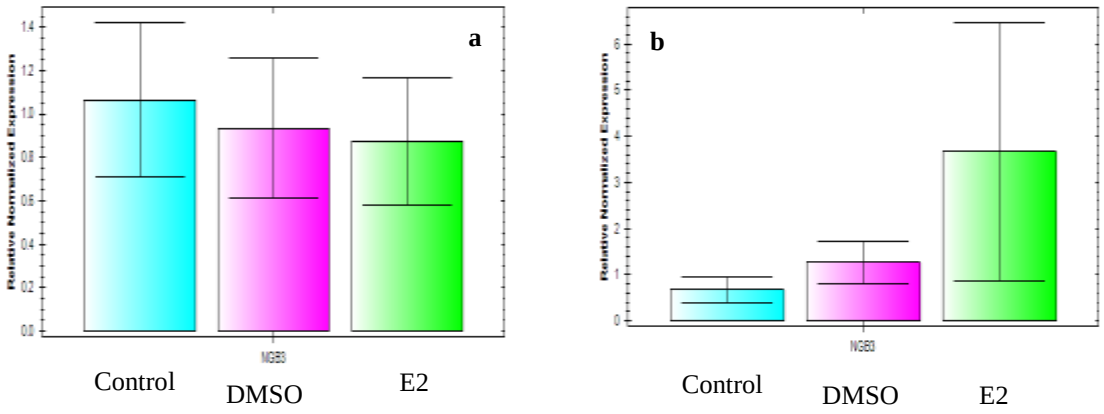

Figure 3.6 Ngb mRNA Transcript Levels in MCF-7 and DLD-1 cells after 10 nM E2 stimulation for 24 hours

The figure depicts the levels of Ngb mRNA transcripts after 24 hour stimulation with 10 nM E2. a) Shows the mRNA transcript expression level in MCF-7 and b) shows the mRNA transcript expression level in DLD-1. The housekeeping genes used here are GAPD and PPIA.

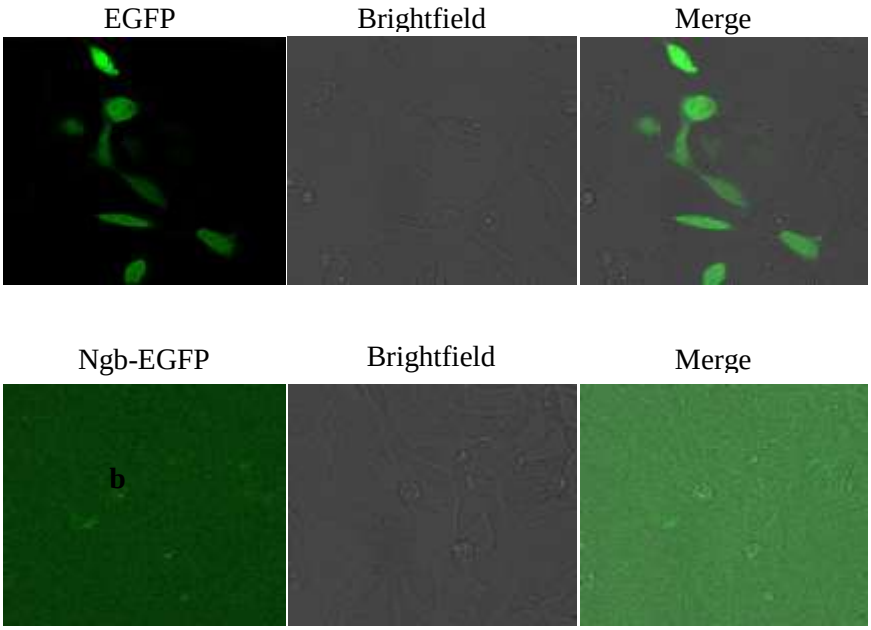

Figure 3.7 Confocal Microscope Live Images of EGFP Alone Protein and the Ngb-EGFP Fusion Protein

The images depict the images of SHY-SY5Y cells after the transfection of EGFP alone plasmid construct and the Ngb-EGFP fusion plasmid construct. a) Shows the fluorescence of the EGFP, with the brightfield channel being used to create contrast to view both transfected and non-transfected cells. These images were captured at 350 ms exposure time. b) Shows the fluorescence of the Ngb-EGFP fusion protein, with the brightfield channel being used to create contrast to view both transfected and non-transfected cells. These images were captured at 1500 ms exposure time.

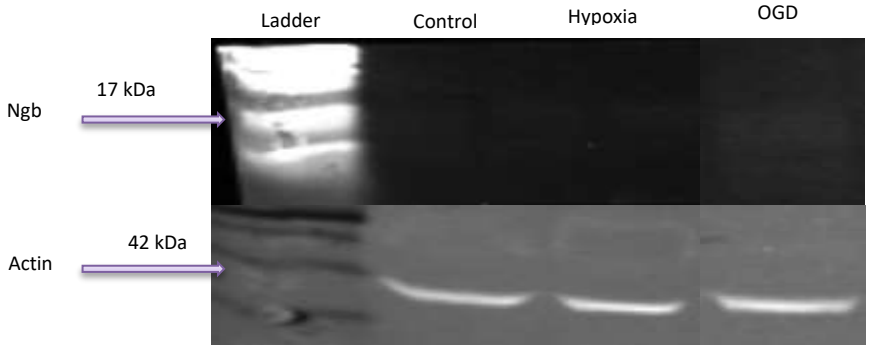

Figure 3.8 Western blot of SH-SY5Y cells underwent Hypoxic and OGD insult

The images depict the visualization of Ngb bands in SH-SY5Y cells that underwent hypoxic and OGD insults to confirm the difference in Ngb expression obtained from the qRT-PCR. The top half depicts the western blot of the hypoxia experiment and the OGD experiment for the visualization of Ngb. The bottom half depicts the western blot of Actin, the loading control.

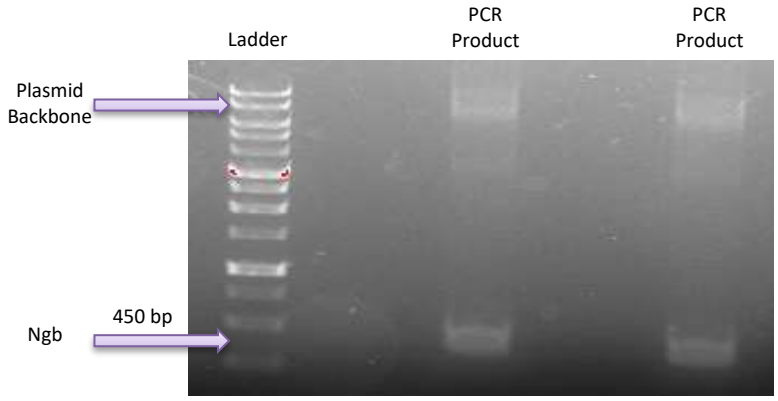

Figure 3.9 Gel electrophoresis after PCR amplification of Ngb

The image depicts the amplification of Ngb bands from the pCMV3-GFPSpark-Ngb obtained from Sino Biological Inc.

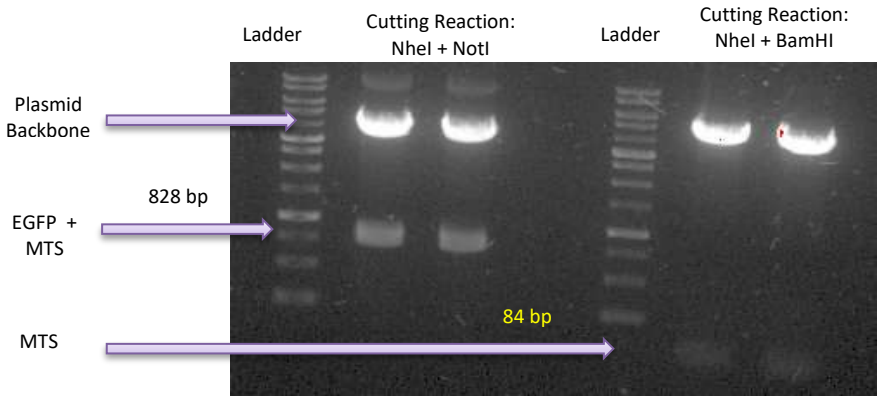

Figure 3.10 Gel electrophoresis after restriction enzyme cutting reactions of mEmerald Mito-7 plasmid

The image depicts the separation of EGFP and the mitochondrial targeting sequence (MTS) after the cutting reaction using restriction enzymes. The left half of the image shows the cutting reaction with the enzymes NheI and NotI to separate EGFP and MTS from the plasmid backbone. The second half of the image shows the cutting reaction with the enzymes NheI and BamHI to separate MTS only.

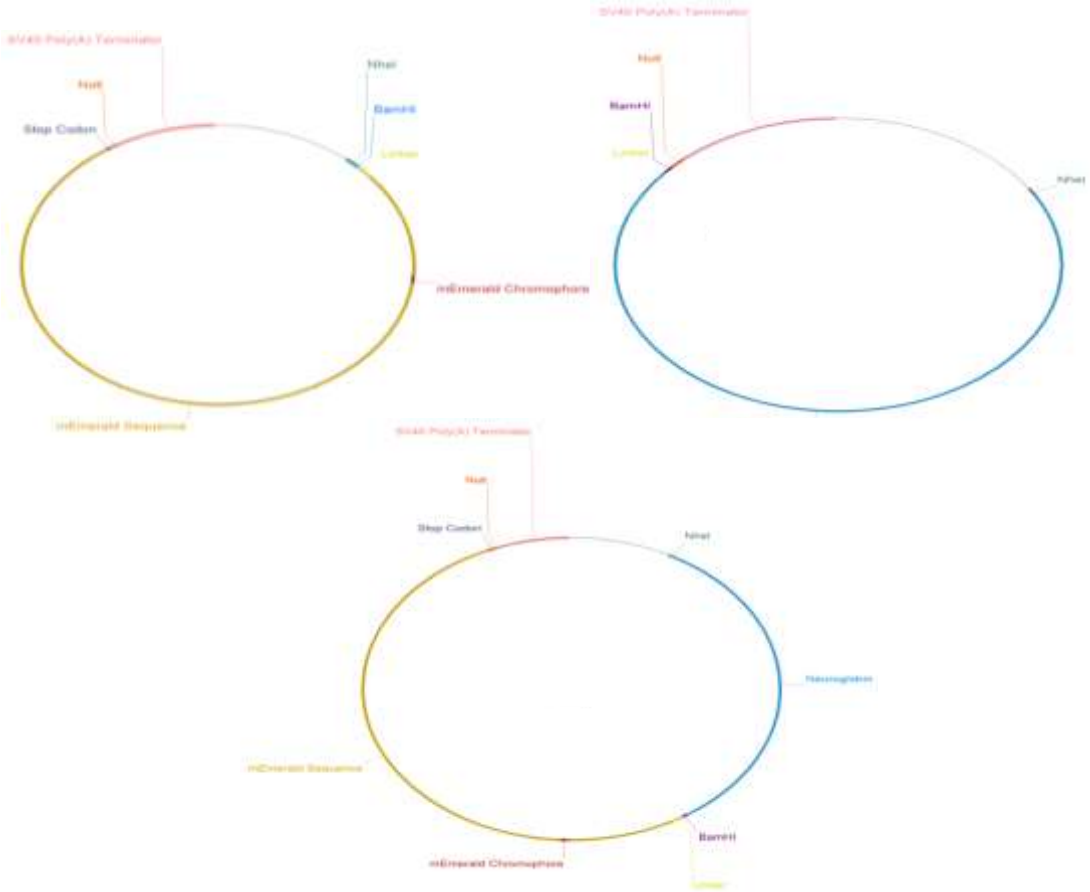

Figure 3.11 Diagrams depicting the construct of the plasmids for the transfection experiments

The images depict the graphic mapping of the plasmids with Ngb-EGFP fusion, Ngb alone and EGFP alone after Gibson Assembly. The maps were obtained by using A plasmid Editor (ApE), a program developed by M. Wayne Davis. from the plasmid backbone. The different sequences are highlighted by different colours.

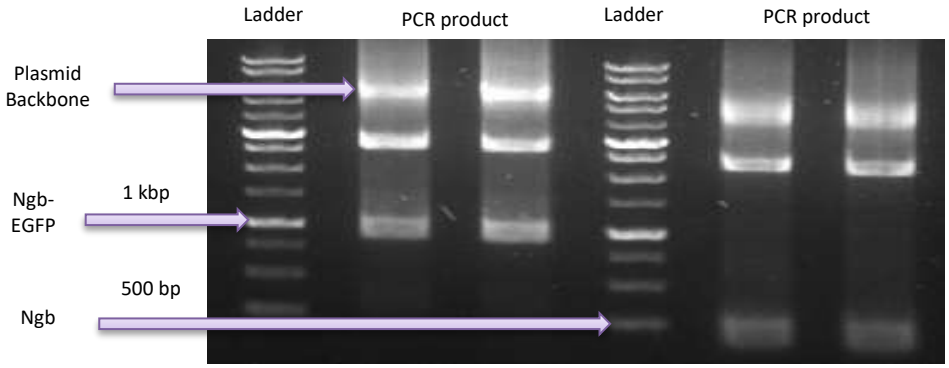

Figure 3.12 Gel electrophoresis of colony PCR to assess proper insertion at the seams after Gibson Assembly

The image depicts the separation of the Ngb-EGFP fusion and Ngb alone after colony PCR. The Ngb alone band lies at the correct size, and the Ngb-EGFP fusion sequence lies at the approximate correct size, indicating the success of the Gibson Assembly. The plasmids were sent to the Sickkids Lab to confirm the correct sequences, and the results have confirmed that sequences are in alignment.

Table 3.1 Cq levels for the Ngb mRNA transcripts in MCF-7 cells treated with E2, vehicle and negative control for 24 hours

The tables show the Cq levels for the Ngb mRNA transcripts in MCF-7 cells. The table on the left depicts the Cq levels for the MCF-7 cells treated with 10 nM E2 for 24 hours alongside the NRT Cq levels. The table in the middle depicts the Cq levels for the MCF-7 cells treated with the vehicle for 24 hours alongside the NRT Cq levels. The table on the right depicts the Cq levels for the MCF-7 cells without any treatment alongside the NRT Cq levels.

Sample	Cq
E2 Replicate	29.11
E2 Replicate	28.77
E2 Replicate	28.47
E2 Replicate	28.31
E2 Replicate	28.25
E2 Replicate	28.25
E2 Replicate	28.44
E2 Replicate	28.52
E2 Replicate	28.28
E2 NRT	28.5
E2 NRT	28.05
E2 NRT	28.42

Sample	Cq
DMSO Replicate	27.96
DMSO Replicate	27.33
DMSO Replicate	27.05
DMSO Replicate	26.9
DMSO Replicate	27.14
DMSO Replicate	27.16
DMSO Replicate	27.56
DMSO Replicate	27.47
DMSO Replicate	27.48
DMSO NRT	26.48
DMSO NRT	26.86
DMSO NRT	28.11

Sample	Cq
Control Replicate	28.13
Control Replicate	27.88
Control Replicate	27.3
Control Replicate	27.33
Control Replicate	27.4
Control Replicate	27.42
Control Replicate	26.9
Control Replicate	26.91
Control Replicate	26.83
Control NRT	27.12
Control NRT	26.93
Control NRT	27.38

Table 3.2 Cq levels for the Ngb mRNA transcripts in MCF-7 cells treated with E2 for 4 hours or 24 hours

The tables show the Cq levels for the Ngb mRNA transcripts in MCF-7 cells. The table on the left depicts the Cq levels for the MCF-7 cells treated with 10 nM E2 for 24 hours alongside the NRT Cq levels. The table in the middle depicts the Cq levels for the MCF-7 cells treated with 10 nM E2 for 24 hours and then treated with DNAse alongside the NRT Cq levels. The table on the right depicts the Cq levels for the MCF-7 cells treated with 10 nM E2 for 4 hours alongside NRT Cq levels.

Sample	Cq
E2 Replicate	32.4
E2 Replicate	31.7
E2 Replicate	31.4
E2 NRT	31.1

Sample	Cq
E2 + DNAse Replicate	33.9
E2 + DNAse Replicate	38.8
E2 + DNAse Replicate	33.5
E2 + DNAse NRT	34.2

Sample	Cq
E2 Replicate	31.7
E2 Replicate	31.3
E2 Replicate	31.1
E2 NRT	31.2

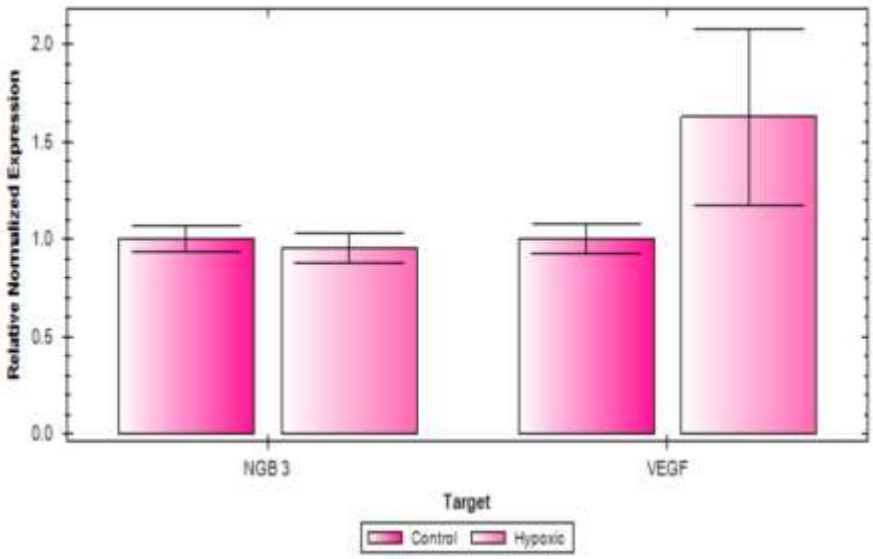

Figure 3.13 Expression levels of Ngb and VEGF in normoxia and hypoxia

The image depicts the expression levels of Ngb and VEGF mRNA transcripts under normoxic and hypoxic conditions. VEGF mRNA level upregulation in hypoxia was used as a positive control for the hypoxic experiments.

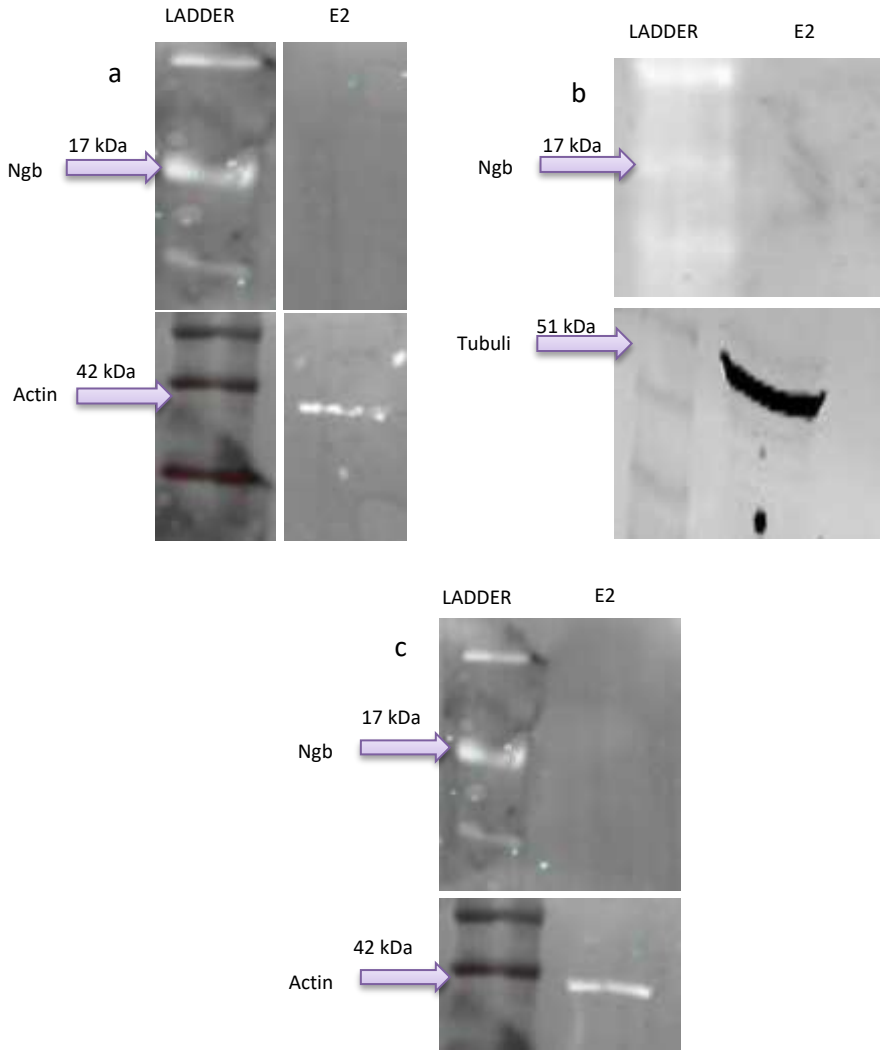

Figure 3.14 Western blots images for different transfer times and voltages for semi-dry transfer

The images show the detection of neuroglobin bands in the top halves and show the loading controls in the bottom halves. a) depicts the visualization attempt at the transfer settings: 15V under 15 minutes and b) 15V under 30 minutes. c) portrays the visualization attempt at the transfer settings: 25V under 15 minutes.

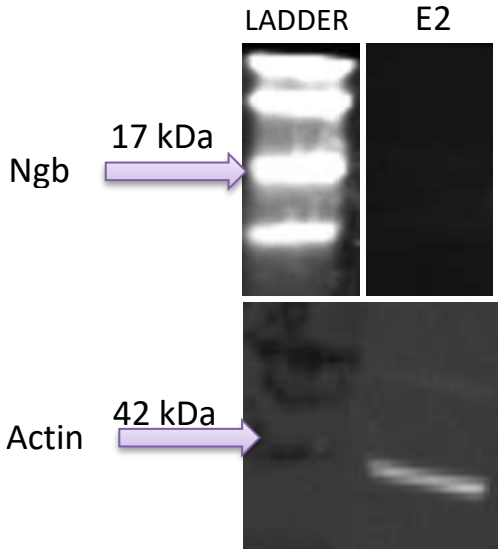

Figure 3.15 Western blots images for different transfer buffer for semi-dry transfer

The image shows the detection of neuroglobin band in the top half and shows the loading control in the bottom half. The transfer was done using a different transfer buffer (Bjerrum Schaefer-Nielson Buffer).

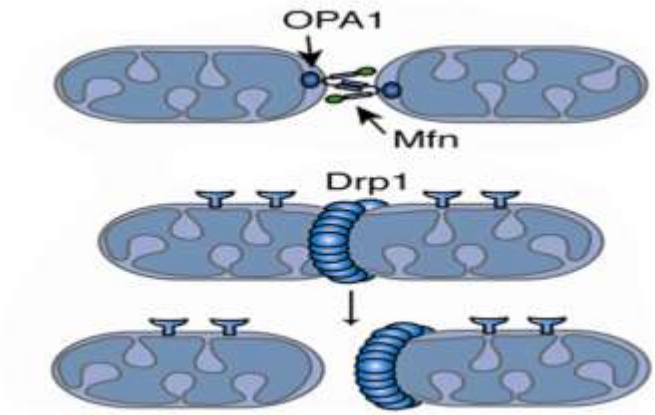

Figure 4.1 Mitochondrial fusion and fission

The figure depicts the GTPases that control fusion and fission and the process that they undertake. a) portrays OPA1 and Mfn and the process of mitochondrial fusion. b) portrays Drp1 and the process of mitochondrial fission.

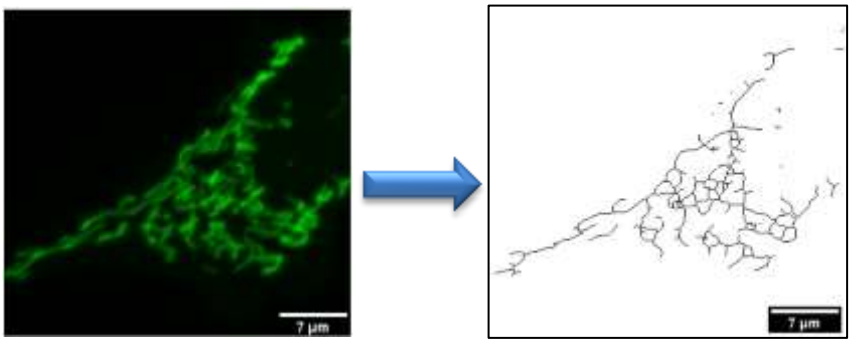

Figure 4.2 Skeletonizing Mitochondrial Network of Stable-Transfected SH-SY5Y

The image on the left shows an image from Carl Zeiss microscope, with the mitochondrial network coloured green. The image on the right depicts MiNA skeletonization for quantification.

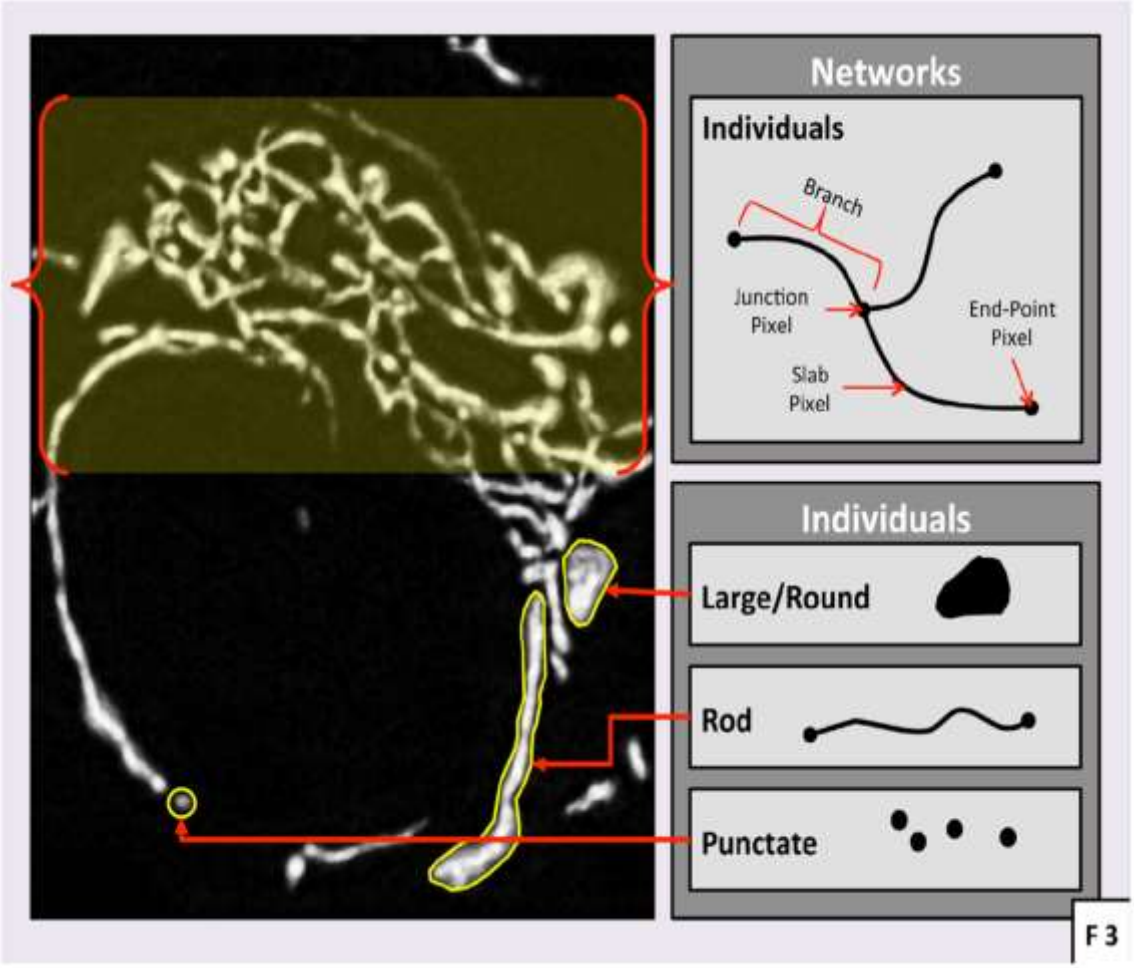

Figure 4.3 Quantification of Mitochondria based on Different Shapes

The image on the left depicts mitochondrial networks, with different mitochondrial shapes being highlighted in yellow. The diagrams on the right portray the different shapes that assess fusion or fission, with networks indicating fusion and individuals indicating fission. The image was obtained from Valente et al., 2017.

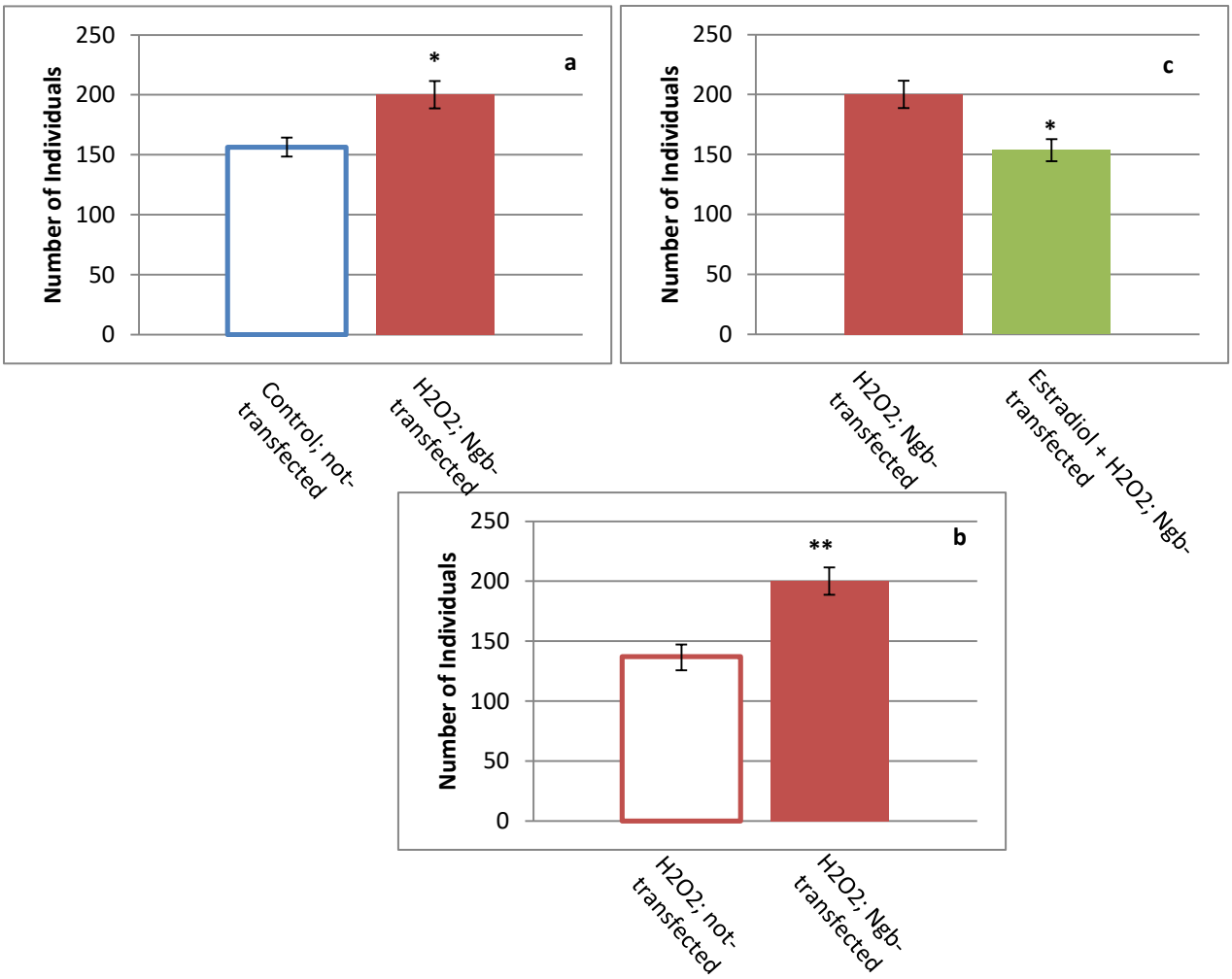

Figure 4.4 Quantification of Mitochondrial Individuals after Estradiol Pretreatment under Hydrogen Peroxide Stress

The figures portray the differences in the number of mitochondrial individuals. (a) shows the comparison between the non-transfected SH-SY5Y cells of the control group with the Ngb-transfected SH-SY5Y cells under H2O2 stress. (b) shows the comparison between the non-transfected SH-SY5Y cells under H2O2 stress with the Ngb-transfected SH-SY5Y cells under H2O2 stress. (c) shows the comparison between the Ngb-transfected SH-SY5Y cells under H2O2 stress and Ngb-transfected SH-SY5Y cells under H2O2 stress after estradiol pretreatment. Data is represented as mean ± SEM.

*: indicates p-value <0.05

**: indicates p-value <0.01

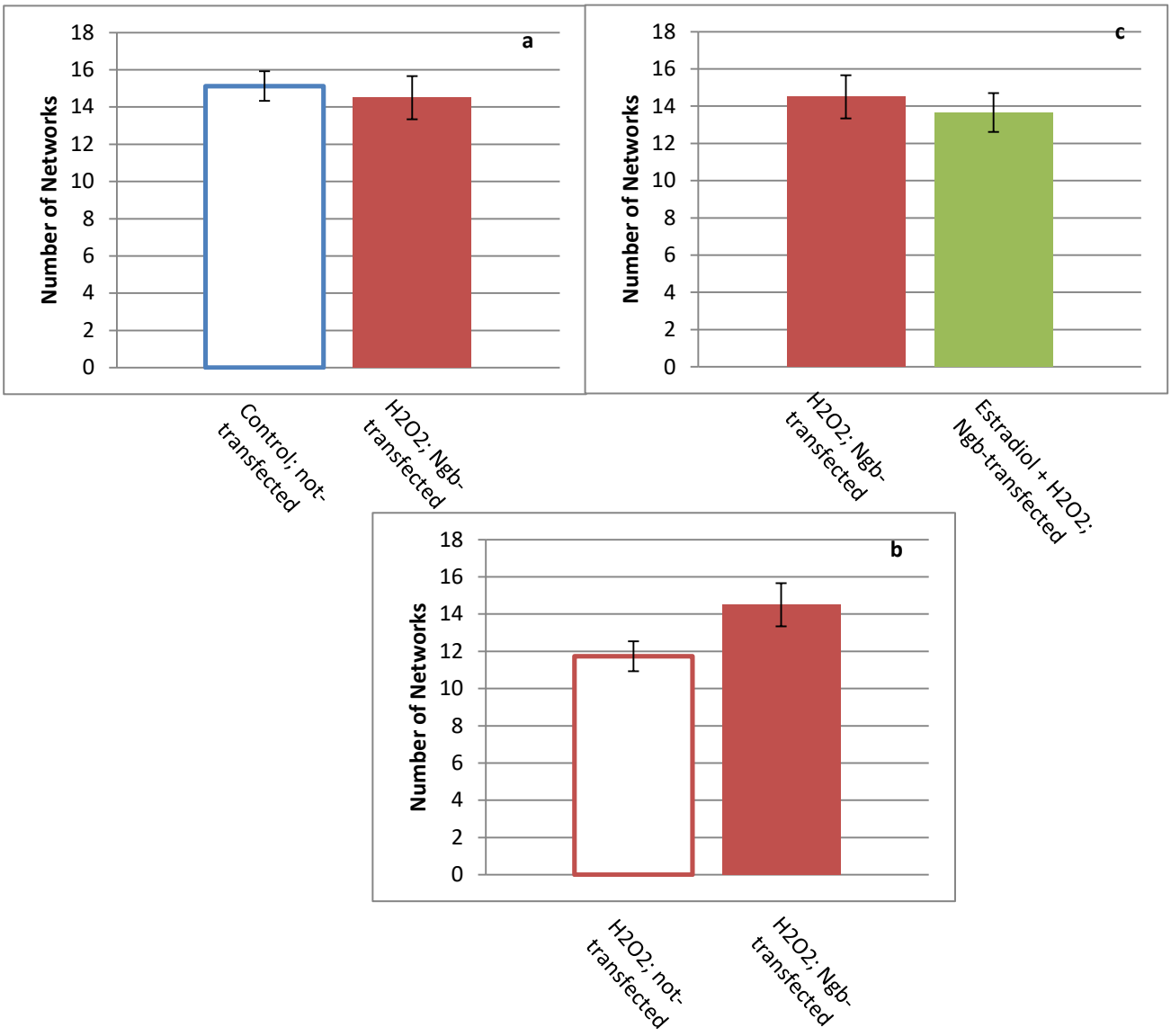

Figure 4.5 Quantification of Mitochondrial Networks after Estradiol Pretreatment under Hydrogen Peroxide Stress

The figures portray the differences in the number of mitochondrial networks. (a) shows the comparison between the non-transfected SH-SY5Y cells of the control group with the Ngb-transfected SH-SY5Y cells under H2O2 stress. (b) shows the comparison between the non-transfected SH-SY5Y cells under H2O2 stress with the Ngb-transfected SH-SY5Y cells under H2O2 stress. (c) shows the comparison between the Ngb-transfected SH-SY5Y cells under H2O2 stress and Ngb-transfected SH-SY5Y cells under H2O2 stress after estradiol pretreatment. Data is represented as mean ± SEM.

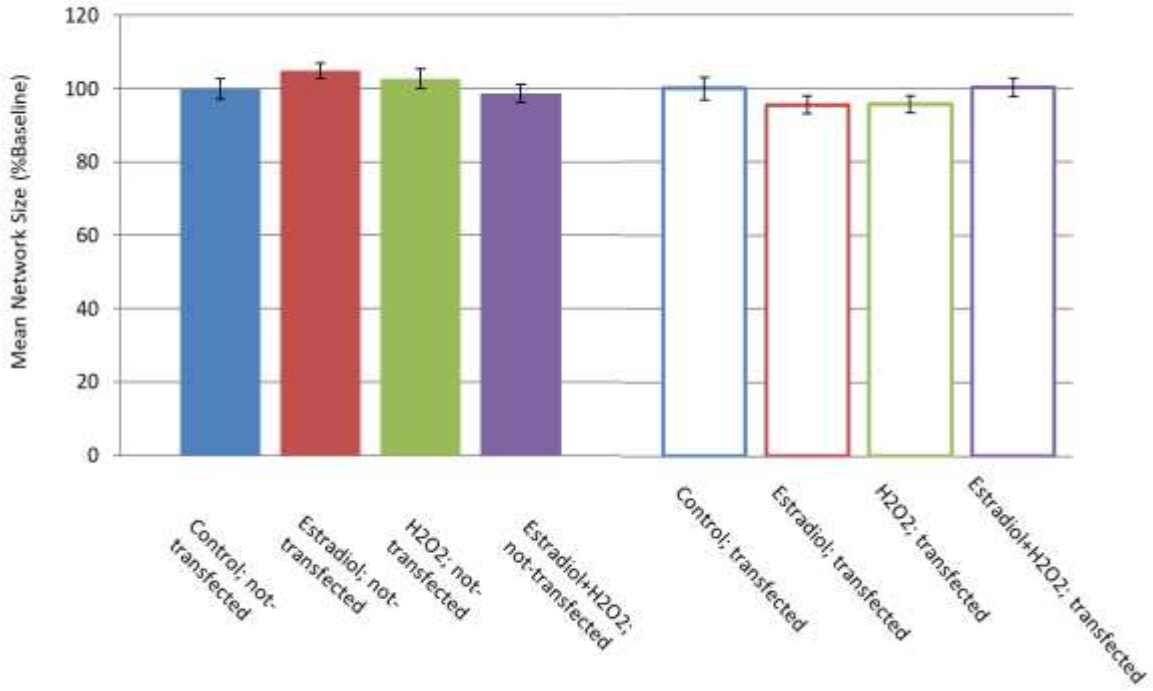

Figure 4.6 Quantification of Mitochondrial Mean Network Sizes after Estradiol Pretreatment under Hydrogen Peroxide Stress

T
T
c
S
c

The figure portrays the differences in the number of mitochondrial branches per network. The left side of the figure depicts the non-transfected SH-SY5Y cells under various conditions of treatments, while the right side of the figure depicts the Ngb-transfected SH-SY5Y cells under the same conditions of treatment. Data has been normalized to the controls of each form of transfection and is represented as mean ± SEM.

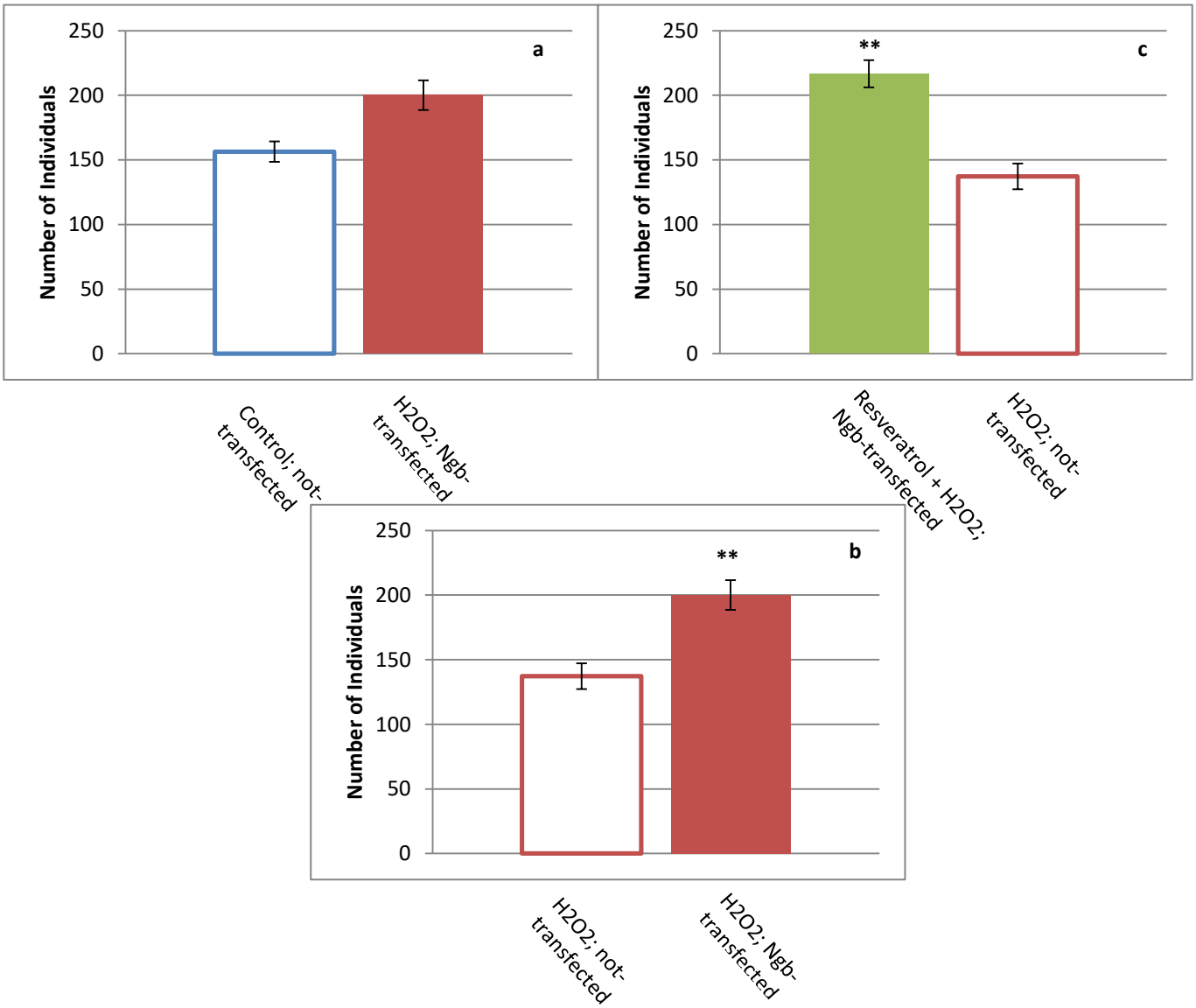

Figure 4.7 Quantification of Mitochondrial Individuals after Resveratrol Pretreatment under Hydrogen Peroxide Stress

The figures portray the differences in the number of mitochondrial individuals. (a) shows the comparison between the non-transfected SH-SY5Y cells of the control group with the Ngb-transfected SH-SY5Y cells under H2O2 stress. (b) shows the comparison between the non-transfected SH-SY5Y cells under H2O2 stress with the Ngb-transfected SH-SY5Y cells under H2O2 stress. (c) shows the comparison between the non-transfected SH-SY5Y cells under H2O2 stress and Ngb-transfected SH-SY5Y cells under H2O2 stress after resveratrol pretreatment. Data is represented as mean ± SEM.

**: indicates p-value <0.01

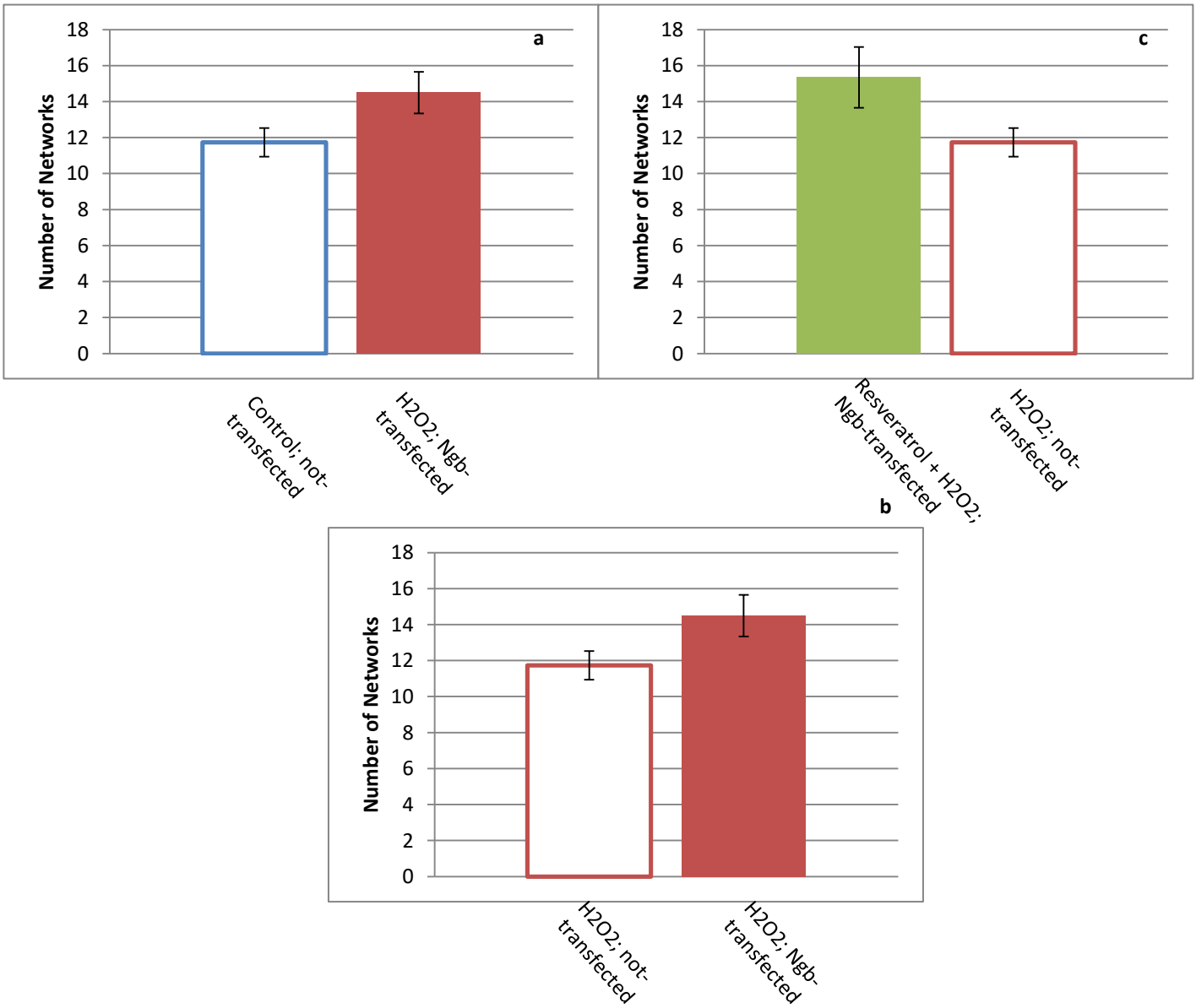

Figure 4.8 Quantification of Mitochondrial Networks after Resveratrol Pretreatment under Hydrogen Peroxide Stress

The figures portray the differences in the number of mitochondrial networks. (a) shows the comparison between the non-transfected SH-SY5Y cells of the control group with the Ngb-transfected SH-SY5Y cells under H2O2 stress. (b) shows the comparison between the non-transfected SH-SY5Y cells under H2O2 stress with the Ngb-transfected SH-SY5Y cells under H2O2 stress. (c) shows the comparison between the non-transfected SH-SY5Y cells under H2O2 stress and Ngb-transfected SH-SY5Y cells under H2O2 stress after resveratrol pretreatment. Data is represented as mean ± SEM.

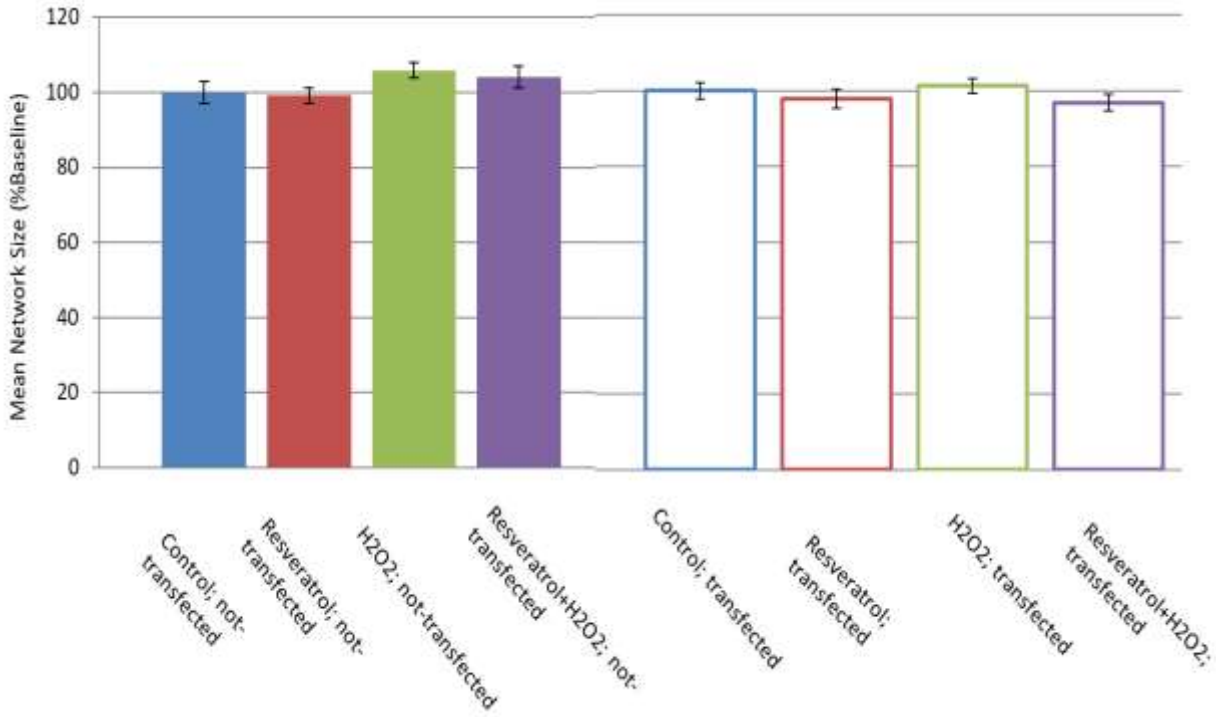

Figure 4.9 Quantification of Mitochondrial Mean Network Sizes after Resveratrol Pretreatment under Hydrogen Peroxide Stress

The figure portrays the differences in the number of mitochondrial branches per network. The left side of the figure depicts the non-transfected SH-SY5Y cells under various conditions of treatments, while the right side of the figure depicts the Ngb-transfected SH-SY5Y cells under the same conditions of treatment. Data has been normalized to the controls of each form of transfection and is represented as mean ± SEM.

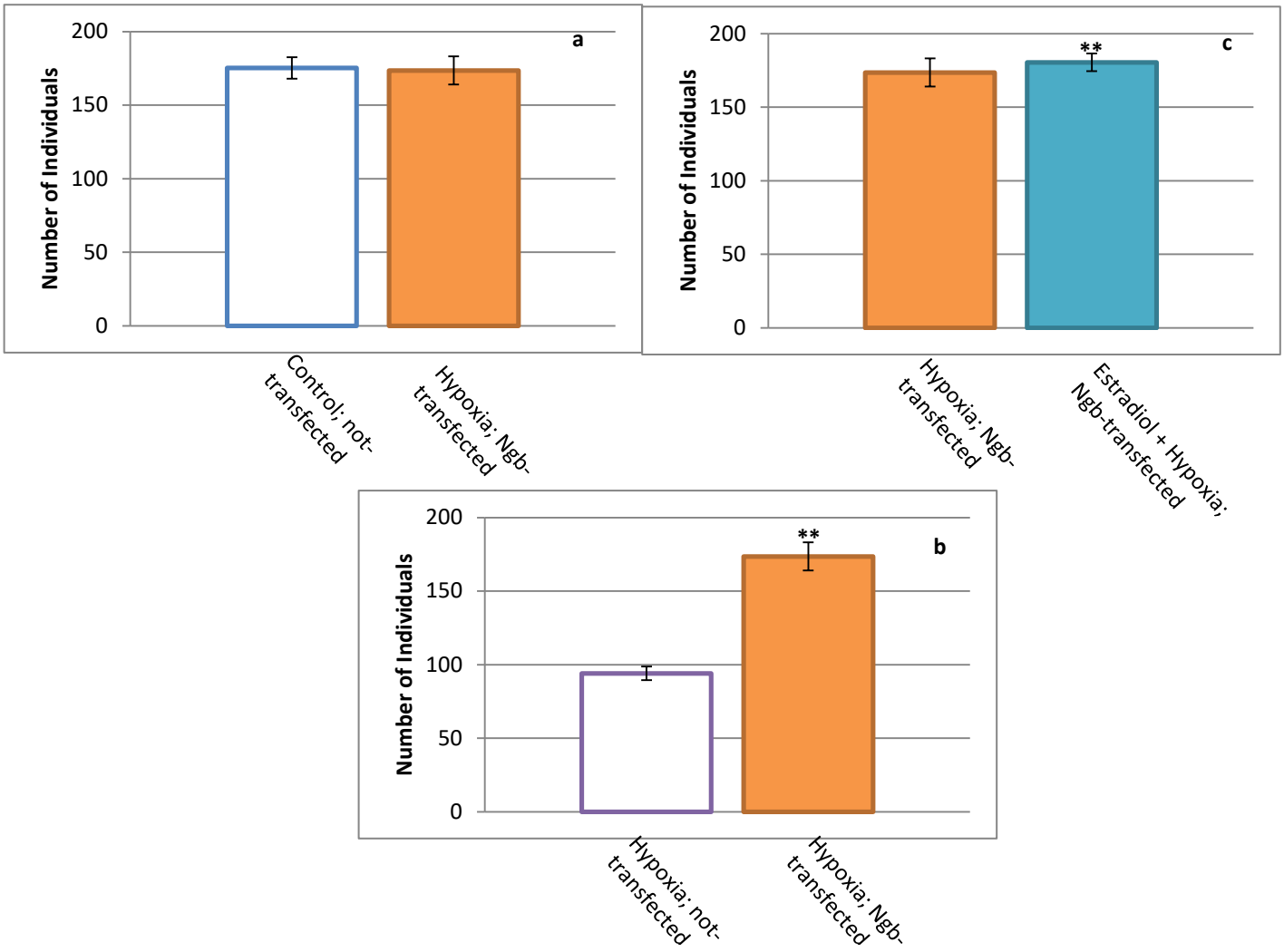

Figure 4.10 Quantification of Mitochondrial Individuals after Estradiol Pretreatment under Hypoxic Stress

The figures portray the differences in the number of mitochondrial individuals. (a) shows the comparison between the non-transfected SH-SY5Y cells of the control group with the Ngb-transfected SH-SY5Y cells under hypoxic stress. (b) shows the comparison between the non-transfected SH-SY5Y cells under hypoxic stress with the Ngb-transfected SH-SY5Y cells under hypoxic stress. (c) shows the comparison between the Ngb-transfected SH-SY5Y cells under hypoxic stress and Ngb-transfected SH-SY5Y cells under hypoxic stress after estradiol pretreatment. Data is represented as mean ± SEM.

**: indicates p-value <0.01

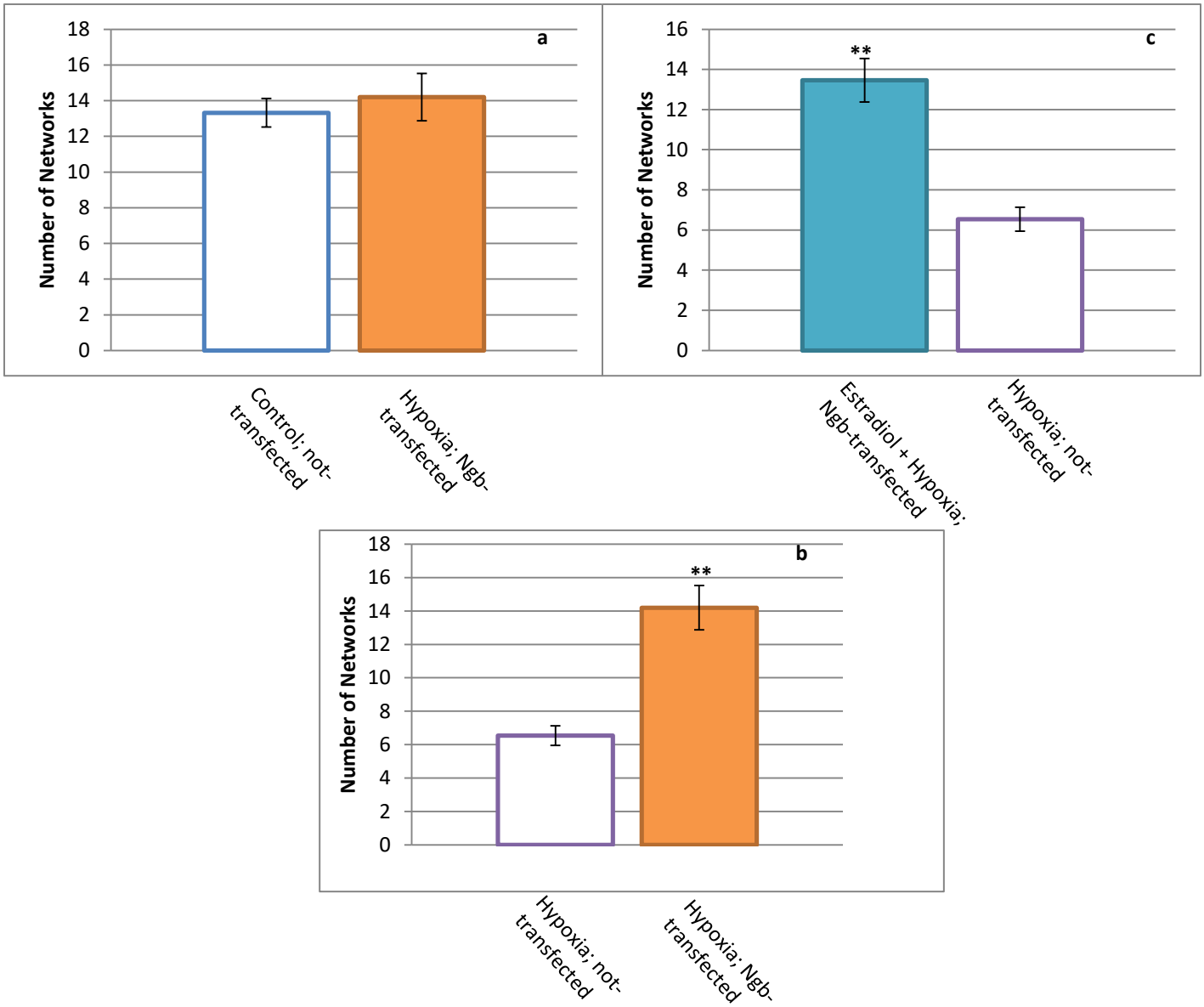

Figure 4.11 Quantification of Mitochondrial Networks after Estradiol Pretreatment under Hypoxic Stress

The figures portray the differences in the number of mitochondrial networks. (a) shows the comparison between the non-transfected SH-SY5Y cells of the control group with the Ngb-transfected SH-SY5Y cells under hypoxic stress. (b) shows the comparison between the non-transfected SH-SY5Y cells under hypoxic stress with the Ngb-transfected SH-SY5Y cells under hypoxic stress. (c) shows the comparison between the non-transfected SH-SY5Y cells under hypoxic stress and Ngb-transfected SH-SY5Y cells under hypoxic stress after estradiol pretreatment. Data is represented as mean ± SEM.

**: indicates p-value < 0.01

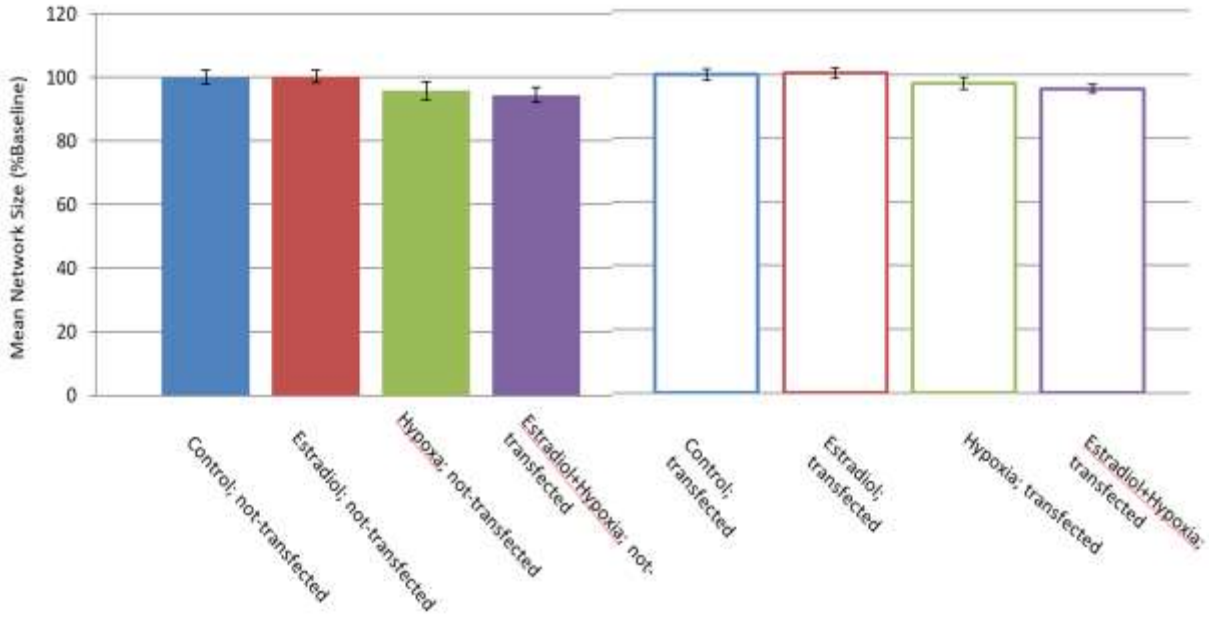

Figure 4.12 Quantification of Mitochondrial Mean Network Sizes after Estradiol Pretreatment under Hypoxic Stress

The figure portrays the differences in the number of mitochondrial branches per network. The left side of the figure depicts the non-transfected SH-SY5Y cells under various conditions of treatments, while the right side of the figure depicts the Ngb-transfected SH-SY5Y cells under the same conditions of treatment. Data has been normalized to the controls of each form of transfection and is represented as mean ± SEM.

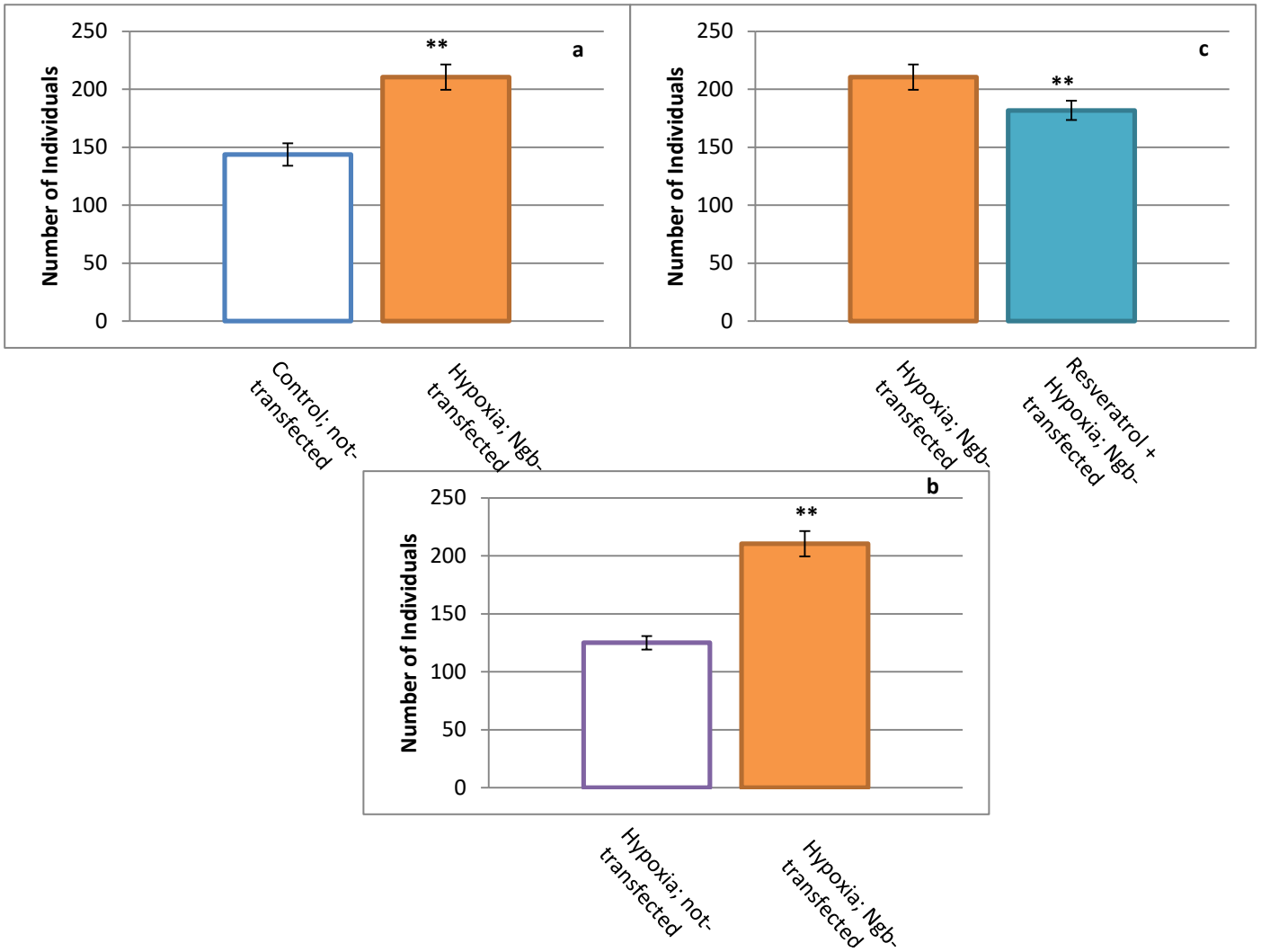

Figure 4.13 Quantification of Mitochondrial Individuals after Resveratrol Pretreatment under Hypoxic Stress

The figures portray the differences in the number of mitochondrial individuals. (a) shows the comparison between the non-transfected SH-SY5Y cells of the control group with the Ngb-transfected SH-SY5Y cells under hypoxic stress. (b) shows the comparison between the non-transfected SH-SY5Y cells under hypoxic stress with the Ngb-transfected SH-SY5Y cells under hypoxic stress. (c) shows the comparison between the Ngb-transfected SH-SY5Y cells under hypoxic stress and Ngb-transfected SH-SY5Y cells under hypoxic stress after estradiol pretreatment. Data is represented as mean ± SEM.

**: indicates p-value <0.01

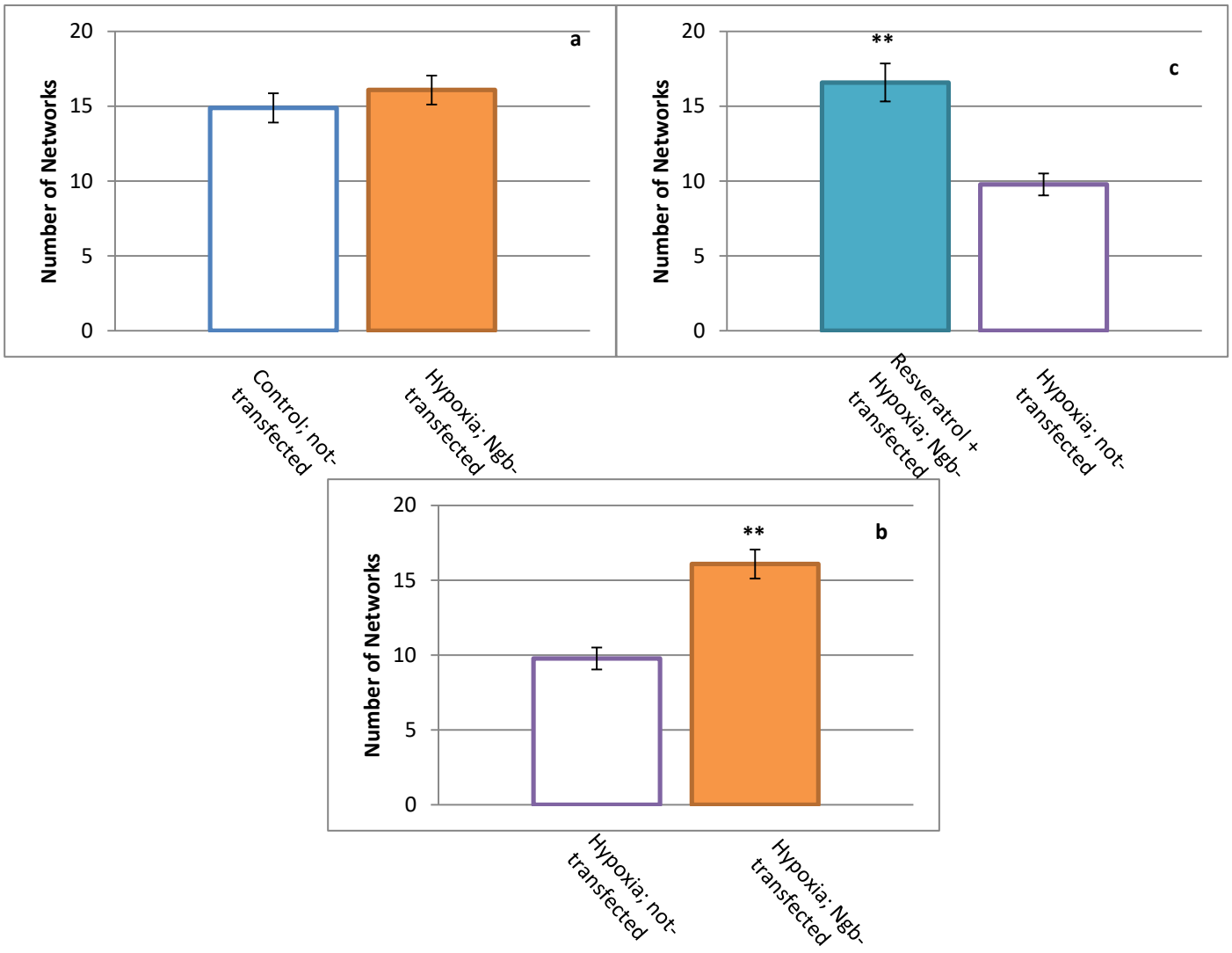

Figure 4.14 Quantification of Mitochondrial Networks after Resveratrol Pretreatment under Hypoxic Stress

The figures portray the differences in the number of mitochondrial networks. (a) shows the comparison between the non-transfected SH-SY5Y cells of the control group with the Ngb-transfected SH-SY5Y cells under hypoxic stress. (b) shows the comparison between the non-transfected SH-SY5Y cells under hypoxic stress with the Ngb-transfected SH-SY5Y cells under hypoxic stress. (c) shows the comparison between the non-transfected SH-SY5Y cells under hypoxic stress and Ngb-transfected SH-SY5Y cells under hypoxic stress after estradiol pretreatment. Data is represented as mean ± SEM.

**: indicates p-value < 0.01

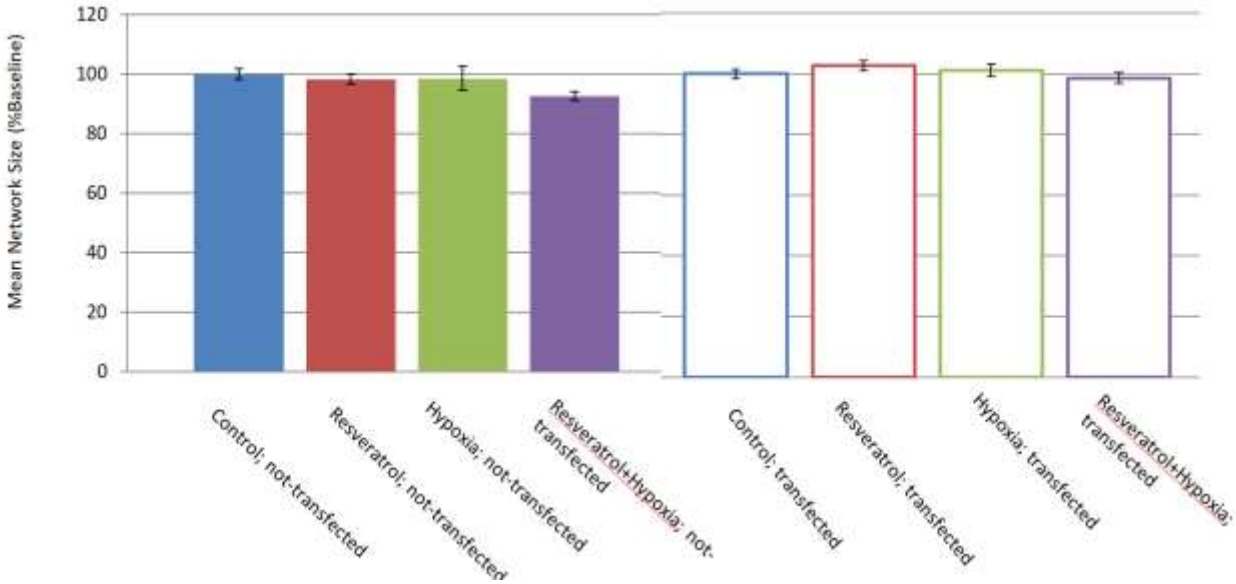

Figure 4.15 Quantification of Mitochondrial Mean Network Sizes after Resveratrol Pretreatment under Hypoxic Stress

The figure portrays the differences in the number of mitochondrial branches per network. The left side of the figure depicts the non-transfected SH-SY5Y cells under various conditions of treatments, while the right side of the figure depicts the Ngb-transfected SH-SY5Y cells under the same conditions of treatment. Data has been normalized to the controls of each form of transfection and is represented as mean ± SEM.

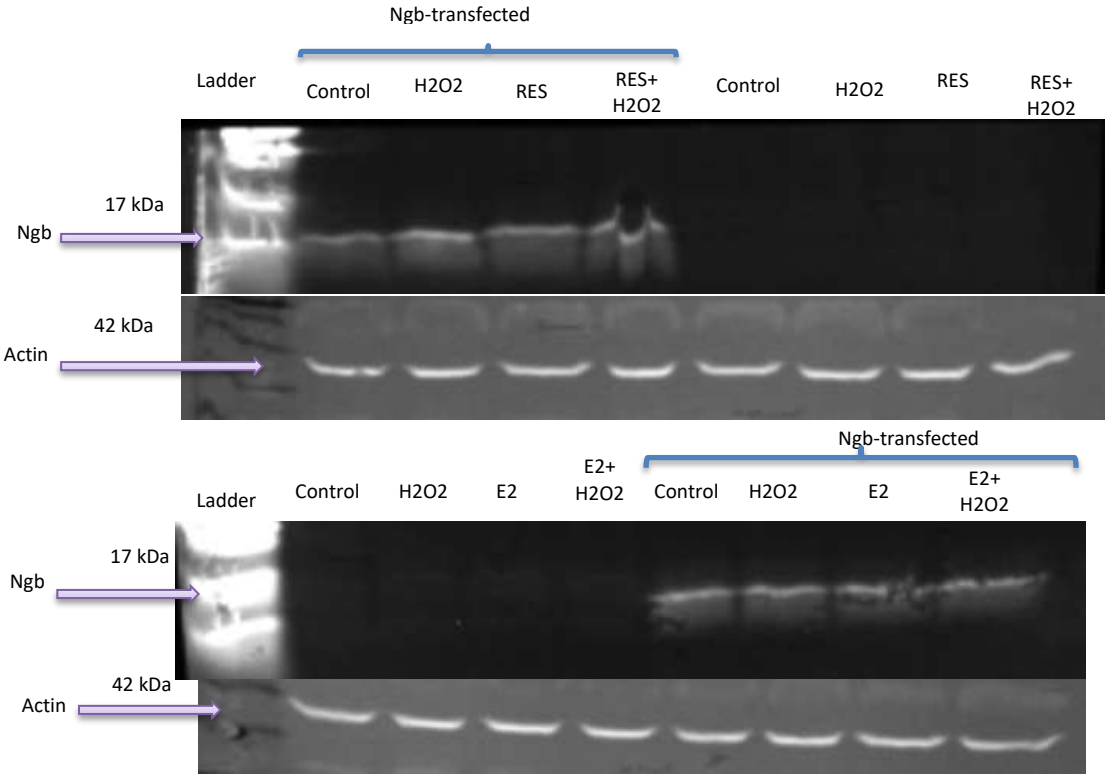

Figure 4.7 Western blot of SH-SY5Y cells that were pretreated with E2 or RES during H_2O_2 insult to confirm successful transfection

The images depict the visualization of Ngb bands in SH-SY5Y cells that were pretreated with E2 or RES during H_2O_2 insult to confirm the success of transfection. The top half depicts the western blot of Ngb and the loading control actin after the pretreatment of RES during H_2O_2 insult. The bottom half depicts the western blot of Ngb and the loading control actin after the pretreatment of E2 during H_2O_2 insult.

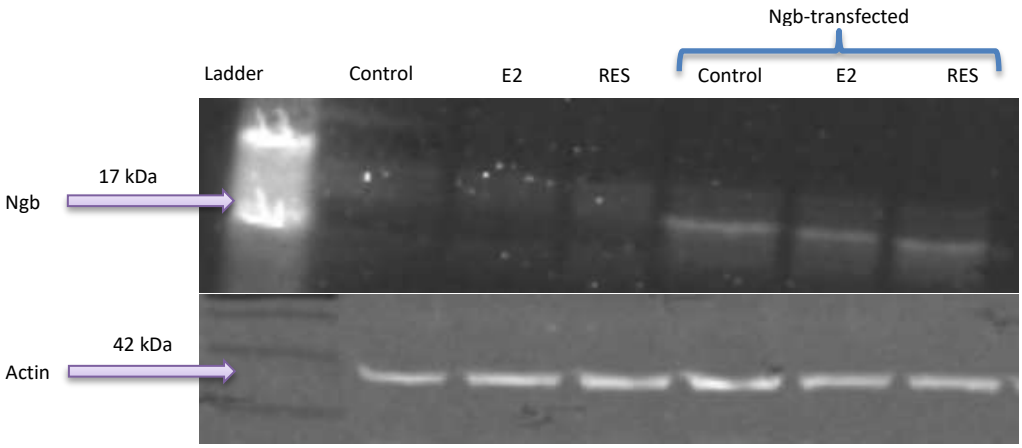

Figure 4.8 Western blot of SH-SY5Y cells that were pretreated with E2 or RES without any stress to confirm successful transfection

The images depict the visualization of Ngb bands in SH-SY5Y cells that were pretreated with E2 or RES without any stress or insult to confirm the success of transfection. The top half depicts the western blot of Ngb after the pretreatment with E2 or RES. The bottom half depicts the western blot of the loading control Actin.

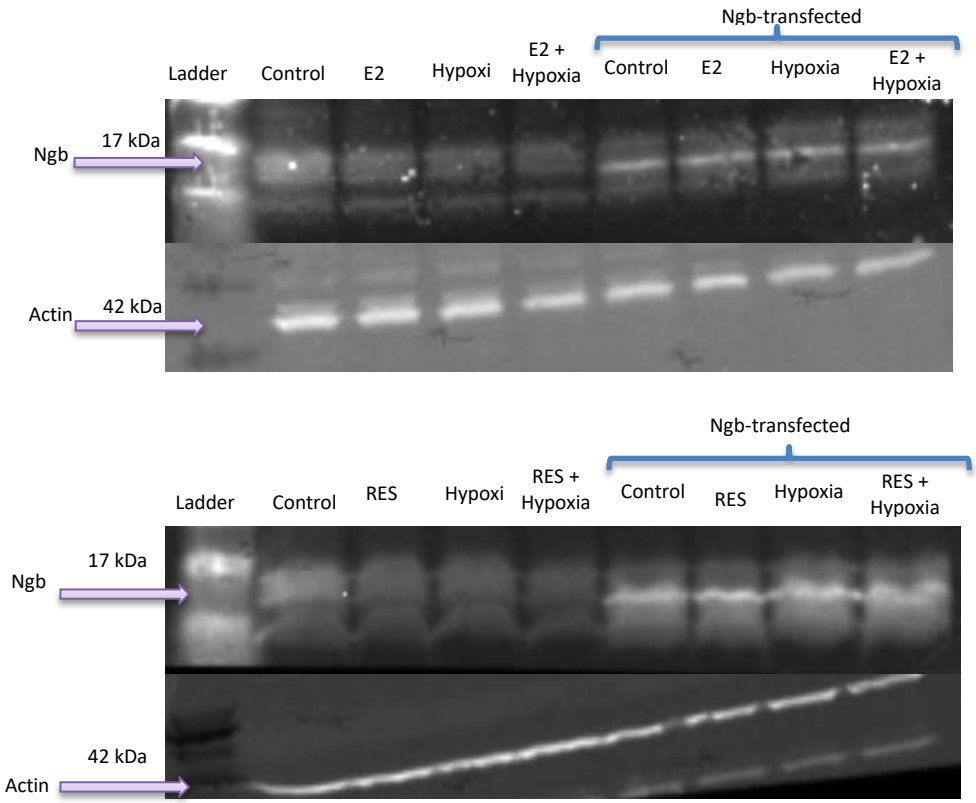

Figure 4.9 Western blot of SH-SY5Y cells that were pretreated with E2 or RES under hypoxic insult to confirm successful transfection

The images depict the visualization of Ngb bands in SH-SY5Y cells that were pretreated with E2 or RES under hypoxic insult to confirm the success of transfection. The top half depicts the western blot of Ngb and the loading control actin after the pretreatment with E2 under hypoxic insult. The bottom half depicts the western blot of Ngb and actin after the pretreatment with RES under hypoxic insult.

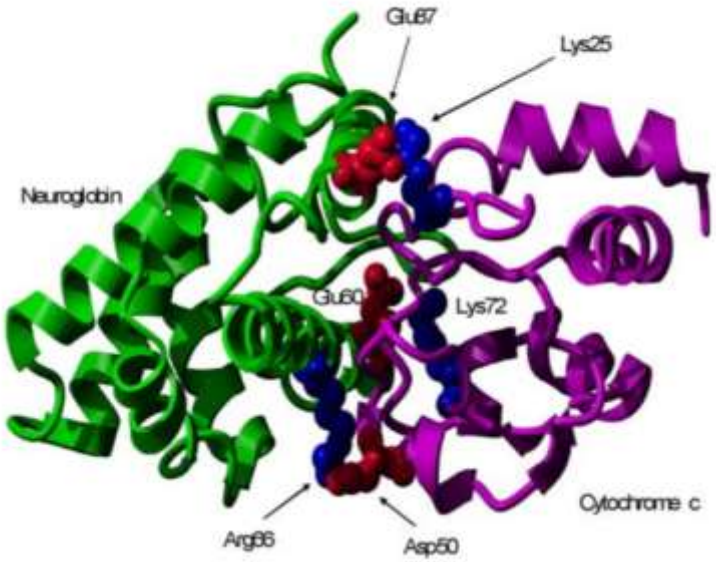

Figure 5.1 Docking Structure of Ngb-Cytochrome c Complex

The figure depicts a physical interaction between cyt c and Ngb, where the Lys25 and Lys72 on cyt c bind with Gluc67 and Glu60 on Ngb. This structure was calculated using BIGGER (Palma et al., 2000) and rendered using YASARA. This image was obtained from Raychaudhuri et al., 2010.